DOE/ID/12781-1
(DE92002444)

DEVELOPMENT OF A PROCESS CONTROL SENSOR FOR THE GLASS INDUSTRY

Phase I: Development Report

By
Matthew Gardner
Auston Candee
John Kramlich
Richard Koppang

May 1991

Work Performed Under Contract No. FC07-89ID12781

For
U.S. Department of Energy
Office of Industrial Technologies
Washington, D.C.

By
Energy and Environmental Research Corporation
Irvine, California

DISCLAIMER

This report was prepared as an account of work sponsored by an agency of the United States Government. Neither the United States Government nor any agency thereof, nor any of their employees, makes any warranty, express or implied, or assumes any legal liability or responsibility for the accuracy, completeness, or usefulness of any information, apparatus, product, or process disclosed, or represents that its use would not infringe privately owned rights. Reference herein to any specific commercial product, process, or service by trade name, trademark, manufacturer, or otherwise does not necessarily constitute or imply its endorsement, recommendation, or favoring by the United States Government or any agency thereof. The views and opinions of authors expressed herein do not necessarily state or reflect those of the United States Government or any agency thereof.

This report has been reproduced directly from the best available copy.

Available to DOE and DOE contractors from the Office of Scientific and Technical Information, P.O. Box 62, Oak Ridge, TN 37831; prices available from (615)576-8401, FTS 626-8401.

Available to the public from the National Technical Information Service, U. S. Department of Commerce, 5285 Port Royal Rd., Springfield, VA 22161.

Printed in the United States of America. Office of Scientific and Technical Information. Oak Ridge. Tennessee

DOE/ID/12781--1

DE92 002444

DEVELOPMENT OF A PROCESS CONTROL SENSOR FOR THE GLASS INDUSTRY

Phase I: Development Report

Prepared by:

Matthew Gardner
Auston Candee
John Kramlich
Richard Koppang

May 1991

Work Performed Under Contract DE-PS07-89ID12781

Prepared for
U. S. Department of Energy
Idaho Operations Office, Idaho Falls, ID
Sponsored by the Office of the Assistant Secretary
for Conservation and Renewable Energy
Office of Industrial Technologies
Washington D.C.

Prepared by
Energy and Environmental Research Corportation
18 Mason
Irvine, California 92718

TABLE OF CONTENTS

Section			Page
EXECUTIVE SUMMARY			E-1
1.0	INTRODUCTION AND OBJECTIVES		1-1
	1.1	Glass Manufacturing Needs	1-1
	1.2	Optical Approaches	1-3
	1.3	Technical Approach	1-4
2.0	ASSESSMENT AND APPLICATIONS		2-1
	2.1	Approach	2-1
	2.2	Industrial Assessment	2-4
		2.2.1 Industrial Energy Use Profiles	2-7
		2.2.2 Forehearth and Forming Applications	2-11
		2.2.3 Annealing and Tempering Lehrs	2-14
	2.3	Measurement Methods	2-14
	2.4	Market Assessment	2-20
		2.4.1 Applications	2-20
		2.4.2 Projected Market	2-27
3.0	PRELIMINARY DESIGN AND DEVELOPMENT		3-1
	3.1	Approach	3-1
	3.2	Preliminary Design	3-3
	3.3	Component Description	3-12
	3.4	Breadboard Tests	3-13
	3.5	Model Development	3-18
		3.5.1 Glass Radiative Transfer Model	3-18
		3.5.2 Theoretical Sensitivity Studies	3-21
		3.5.3 Calibration Methodology	3-24
		3.5.4 True Radiance Model	3-25
		3.5.5 Data Analysis	3-27
		3.5.6 Thermal Deconvolution	3-27

TABLE OF CONTENTS (Continued)

Section			Page
4.0	LABORATORY DESIGN, SENSOR TEST AND VERIFICATION		4-1
	4.1	Approach and Test Plan	4-2
	4.2	Pilot Furnace Design	4-5
		4.2.1 Data Acquisition System	4-5
		4.2.2 Furnace and Operating Instrumentation	4-5
		4.2.3 Sensor Calibration	4-9
	4.3	Parametric Studies	4-11
		4.3.1 Interference Sensitivities	4-14
		4.3.2 Optical Methods Assessment	4-17
		4.3.3 Glass Characterization	4-23
		4.3.4 Temperature Profile Deconvolution	4-29
		4.3.5 Bench Scale TAS Operating Characteristics	4-37
	4.4	Recommended Methods	4-42
5.0	PROVISIONAL ECONOMICS		5-1
	5.1	Approach	5-1
	5.2	Cost Savings	5-3
	5.3	Capital Costs and Payback	5-3
REFERENCES			R-1
APPENDIX A - COST ESTIMATES			A-1

EXECUTIVE SUMMARY

Introduction

This project was initiated to fill a need in the glass industry for a non-contact temperature sensor for glass melts. At present, the glass forming industry (*e.g.*, bottle manufacture) consumes significant amounts of energy. Careful control of temperature at the point the bottle is molded is necessary to prevent the bottle from being rejected as out-of-specification. In general, the entire glass melting and conditioning process is designed to minimize this rejection rate, maximize throughput and thus control energy and production costs.

This program focuses on the design, development and testing of an advanced optically based pyrometer for glass melts. The pyrometer operates simultaneously at four wavelengths; through analytical treatment of the signals, internal temperature profiles within the glass melt can be resolved. A novel multiplexer allows optical signals from a large number of fiber-optic sensors to be collected and resolved by a single detector at a location remote from the process. This results in a significant cost savings on a per measurement point basis.

The development program is divided into two phases. Phase I involves the construction of a breadboard version on the instrument and its testing on a pilot-scale furnace. In Phase II, a prototype analyzer will be constructed and tested on a commercial forehearth. This report covers the Phase I activities.

Glass Manufacturing Needs

The glass for bottle manufacture is first melted in the melter. Several streams of glass are extracted from the refiner section of the melter and delivered to the bottling machines through forehearths. The forehearths condition the glass, remove bubbles, and adjust the temperature. At the bottling machine a "gob" of glass is punched out of the melt and blown into a bottle mold. Although the melter consumes the most energy, its temperature control is not as critical as the later processes. Industry has clearly stated that the greatest

need is to provide precise, multipoint temperature profile instrumentation on the forehearths, the gob, and the mold surfaces. Higher quality measurements and improved process control are the most direct means of reducing rejection rates and improving energy efficiency. At present, the process is controlled by a combination of operator experience, temperature measurements in various parts of the furnace refractory structure, and through the use of submerged thermocouples. Although these submerged thermocouples provide the most direct measurements currently available, they are costly, are prone to drift, and they have short lifetimes. Thus, the critical needs identified by the glass industry are for improved temperature measurement in the forehearth, at the gob, and on the mold surface. Probably the most stringent requirement is sensor to sensor precision and sensor absolute precision (±1°F). Section 2.0 of the report details the industry survey that led to the selection of the targeted applications.

Summary of the Approach

The stringent accuracy requirements have identified a number of critical optical design issues needing resolution:

- the need for a high signal to noise ratio, multicolor pyrometer operating over a broad optical spectrum, 1 to 4-1/2 μm
- elimination of stray light (reradiated) which could bias optical measurements
- frequent, in situ calibrations against a precision, black body calibrator

Significant progress was made in resolving these issues, although the demonstrated accuracy of ±4°F was short of the ±1°F goal.

Glass melts are somewhat transparent at certain IR wavelengths. With a typical opaque material, narrow wavelength optical pyrometry will receive radiant emission only from the surface. With glass, the emission represents a sum from

various depths within the glass. At short wavelengths, most glasses tend to be more transparent, and the average signal originates from a greater depth. For longer wavelengths, the glass becomes opaque, and the signal represents the surface emission only. The mathematics for calculating the radiant emission from a glass with known properties and a given temperature profile were defined by Viskanta.[1] Thus, in theory, one can take emission measurements at several wavelengths, and through proper deconvolution, define the temperature profile within the glass. In the past, the difficulty has been the cost of obtaining the multicolor measurements in the required wavelength range. This we have addressed through the use of the optical multiplexer. The stray light issue was resolved through a series of experiments which evaluated normal and off normal (Brewster's Angle) sensor configurations and employing narrow acceptance angle optics. A number of black body calibration techniques were also evaluated.

System Design

The heart of the system is the optical multiplexer shown in Figure E-1. This system was originally developed as part of an IR moisture analyzer system, but was modified for the current application. The off process multiplexer is capable of accepting eight optical fibers, and exposing each to four narrow bandpass filters. The multiplexer accomplishes this through a rotating commutator. For each rotation of the commutator, light from each fiber is briefly focused through each filter and onto the detector. Thus, 32 distinct optical signals are received by the detector during each rotation. To accommodate the wavelengths needed for this application (1.6 - 4.5 μm), the fiber material was changed from high purity silica to a heavy metal fluoride composition. Several other components were also changed to expand the wavelength performance, and an extra lens was added to the optical multiplexer to reduce chromatic aberration over this larger wavelength range. The pulsed signal from the detector is

1 Viskanta, R. 1974. "Infrared Radiation Techniques for Glass Surface and Temperature Distribution Measurements." IEEE Ind. Appl. Soc., Annu. Meet., 9th, Conf. Rec., Pittsburgh, PA, Oct. 7-10 1974 pt 2, p 1045-1056. Publ. by IEEE (74 CHO 833-41A), New York, NY, 1974.

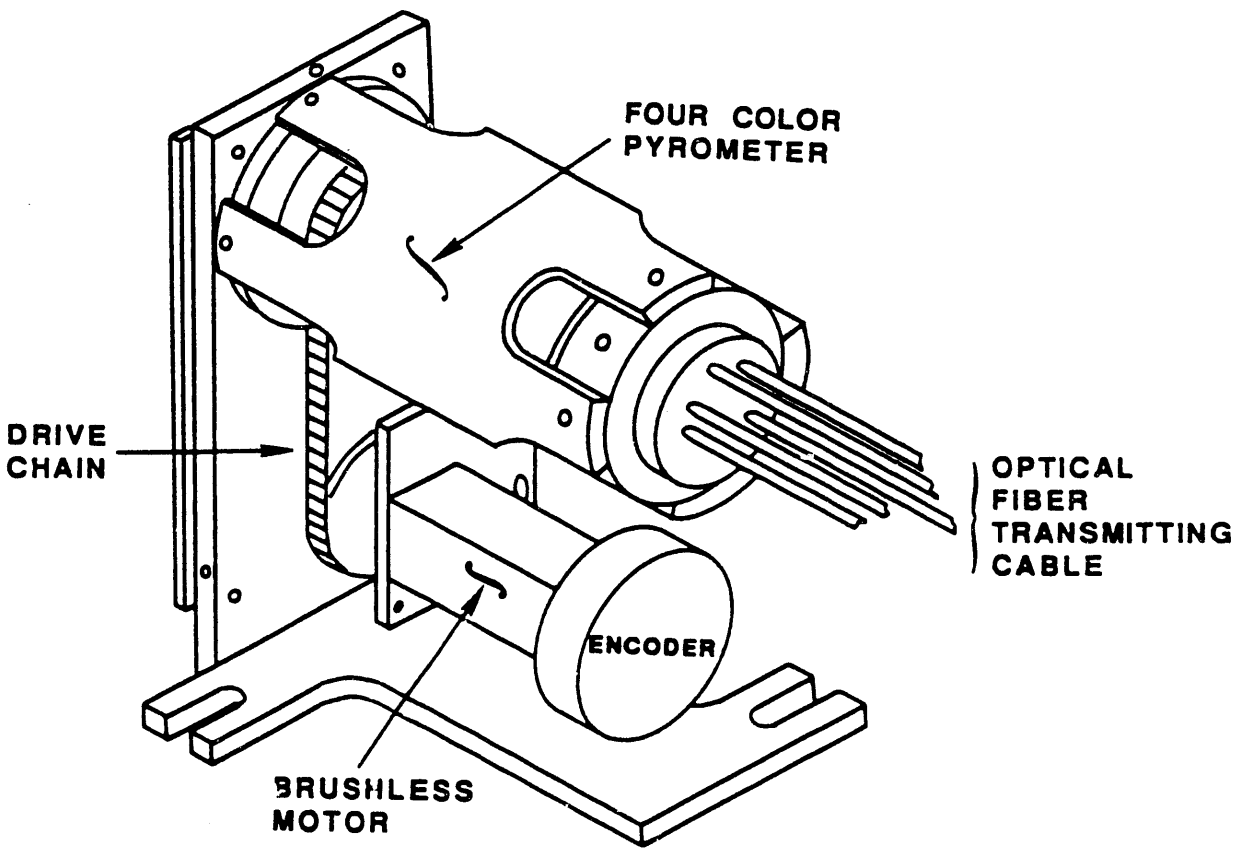

Figure E-1. EER optical multiplexer.

amplified and digitized by an optical bench interface card. The card communicates with an external computer via standard bus computer architecture for data acquisition and eventually for automatic process control.

The light collectors themselves are passive and simple, and are compatible with the harsh environments existing on the production line. The optical signal is collected by off-axis parabolic mirrors and focused onto the ends of the fibers. The entire assembly is contained within an metal cylinder, including the alignment hardware for the fiber pickup. The fibers are contained within flexible metal cladding, and lead to the multiplexer on the factory floor or in the control room.

A number of black body calibration techniques and configurations were conceived and evaluated including hot wires, commercial calibrators and miniaturized targets. An in-furnace, instrumented SiC target was found to be the most stable and accurate approach.

Pilot-Scale Furnace

Tests were conducted in a box furnace rigged to perform as a pilot-scale test system. The furnace, shown in Figure E-2, consists of a box cavity of dimensions 12" wide by 20" long by 12" high. Two crucibles placed in the furnace hold the melt (9" high by 6-3/4" diameter). These are instrumented with state of the art triplex submergible thermocouples. One crucible sits on a water-cooled plate. This is used to extract heat and establish a steady-state temperature gradient in the glass. A small catalytic combustor (platinum gauze) is mounted outside the oven, and is used to supply the oven with combustion gas for atmospheric interference tests. The maximum oven temperature is 2250°F.

Initially, the furnace and sensor were used to address a number of preliminary design issues. These included:

- Fiber Diameter. The amount of signal transmitted to the detector is proportional to the cross-sectional area of the fiber. Several fiber sizes were tested to select the minimum size that yielded acceptable signal. Both fiber flexibility and cost motivated the need for

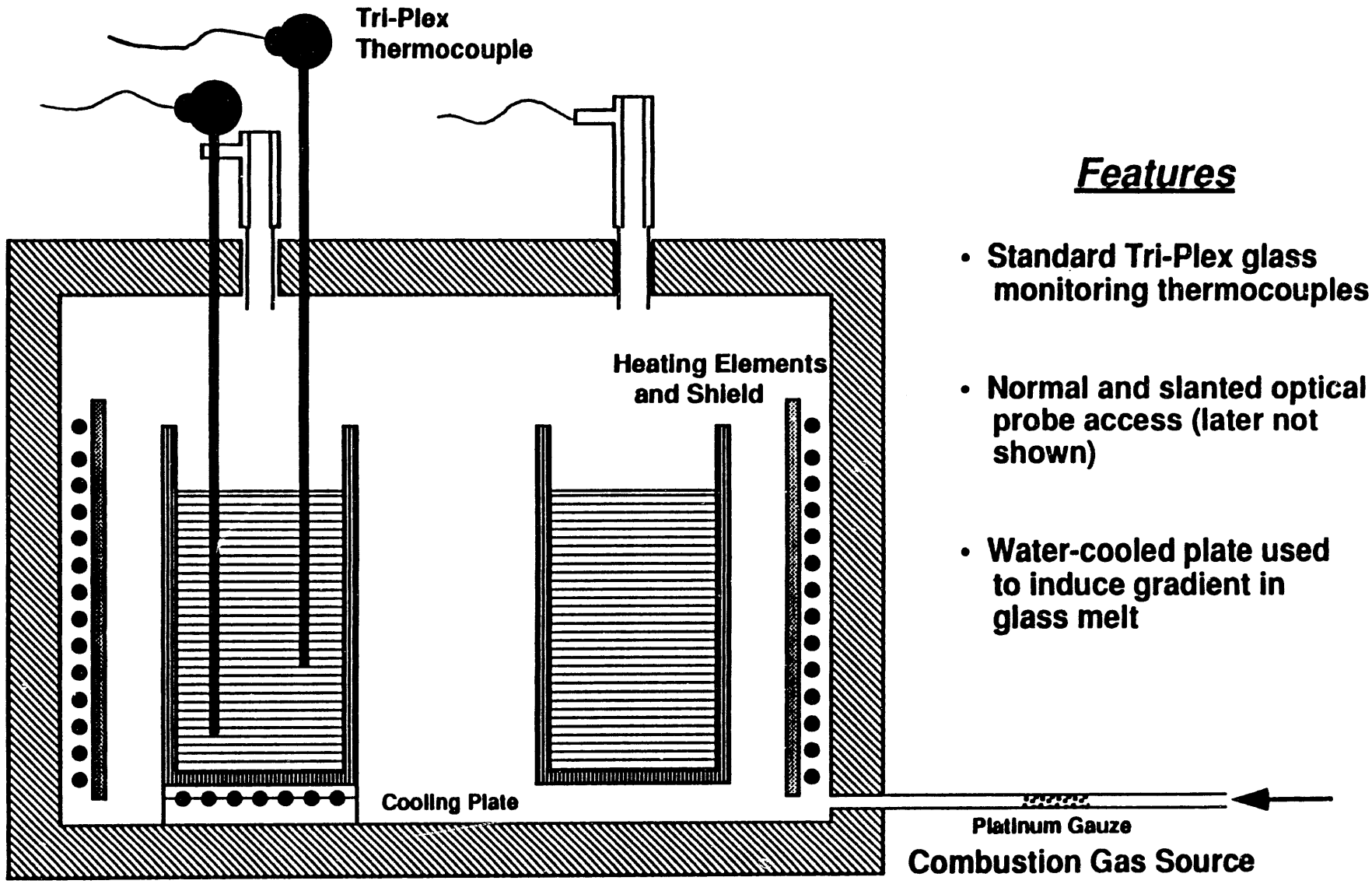

Figure E-2. Pilot scale glass furnace.

minimizing the fiber diameter. A diameter of 450 μm was selected for further work.

- Signal Recovery. Proper matching between source output, sensor aperture, optical throughput and detector responsivity are essential to achieving a usable signal. Errors in design and misalignment will also lead to unacceptable losses. A black-body cavity was used to inject a known radiance into the optical system. The signal recovered at the detector was analyzed to determine losses. The actual signal corresponded to 35% of the theoretical signal, with a signal to noise ratio of 30. The "order of magnitude" test showed that the optics were not overly sensitive to alignment and that the optical system was properly matched to the application. Wider band width narrow band pass filters were selected for subsequent tests to increase signal levels.

- Calibration. Several calibration sources were investigated. The final design was an instrumented, in-furnace notched silicon carbide block. The emissivity of the block exceeds 0.99, which introduces little error into the calibration relative to a full black body.

Optical Data Acquisition

Most of the testing focused on four wavelengths (2.4, 3.0, 3.5, and 4.0 μm). Two types of glass were used, a green glass and a flint glass.

The first test series examined the influence of the background gas on the signal. Testing normally used an air atmosphere. During the course of one isothermal test, the air flow to the furnace was replaced for 70 minutes by flue gas from the catalytic combustor. After this, the furnace was again purged with air. No significant change in signal was associated with the change in furnace atmosphere. This was expected, because each of the wavelengths had been selected to avoid water and CO_2 absorption bands that would be significant over the optical path in the furnace.

One of the most important problems faced in optical pyrometry within furnaces is avoiding contamination of the signal by background radiation. This is a particular problem in forehearth applications because the use of gas flames above the glass can heat the roof of the furnace to temperatures above that of the glass. Thus, the pyrometry signal can become affected by high energy

reflected radiation. Two approaches to this problem were investigated in this program: normal angle pyrometry and Brewster's angle pyrometry.

Normal angle pyrometry makes use of the fact that glass reflectivity is relatively low at a normal angle with the surface. In the theoretical limit, a sensor mounted over the glass would see only its own reflection, and reflected radiation originating on the hot walls would not find its way into the light path. In reality, the sensor has a small acceptance angle, which means that some thermal radiation from the walls near the sensor can be reflected off of the glass surface and into the light path. This was avoided by placing a small cooled collar around the sensor. The collar eliminated any hot walls from being visible as reflected images in the glass. This was tested by inserting an electrically heated coil into the cooled collar region. The test showed that the hot coil did not influence the glass signal except when the coil was inserted into the light path. For these tests the coil was heated to 2300°F, a temperature significantly above that of the glass. Thus, it was concluded that normal angle pyrometry provides a simple approach to meeting the needs of eliminating reflected radiation. Note that the collar does not have to be cooled to room temperature. All that is necessary is to cool it to the point where its thermal radiation becomes insignificant relative to that of the glass. Because glass emission is such a strong function of temperature, the collar only needs to be 400-500°F below the glass temperature. This means that air cooling is probably the preferred approach.

Brewster's angle pyrometry is based on the fact that light reflected from a dielectric surface (such as glass) is polarized into one plane at Brewster's angle. By monitoring the glass melt at this angle and using a polarizing filter, all of the reflected radiation can be removed. Initial tests with this approach did not meet expectations. Although the reasons for the poor performance were not fully assessed, it appeared the glass may have lost some of its dielectric properties at high temperatures. Also, Brewster's angle is wavelength specific. Thus, although one of the four wavelengths used in these tests may have been correctly aligned, the other three would not have been at their critical angles.

For the present, the Brewster's angle approach was abandoned in favor of the normal angle approach.

The measurement wavelengths are first calibrated against the in-furnace black body to relate detector photon count to temperature.

Glass emissivities were derived by comparing color pyrometry measurements from the optical bench with glass thermocouple measurements. The difference between the color measurements and the actual thermocouple readings was attributed to the emissivity, which was generally found to be of the order of 0.9. Emissivities were calculated in this way for each of the two glass types, and each of the four wavelengths over the full temperature range.

Glass absorption coefficients were found from the literature. These vary with glass type, wavelength and temperature. Under normal circumstances, these properties should be measured for each glass type under each application.

Temperature Profile Resolution

Two types of temperature gradients were investigated. The first is a time-unsteady gradient induced in the glass by a change in the furnace set point. Figure E-3 shows thermocouple profiles within the flint glass melt as the set point of the oven is increased. Due to the high thermal inertia of the glass, over 100 minutes is needed for equilibrium to be reestablished. Figure E-4 shows the uncorrected color measurements for each of the four wavelengths with time.

These were resolved into temperature profiles using the following simplified procedure. Using the radiation measurements, an equivalent isothermal temperature can be defined from Planck's equation for each wavelength which will give the same radiance as was measured. If a wide range of hypothetical temperature profiles are analyzed with the Viskanta equation, one finds that these calculated isothermal temperatures cross the non-isothermal profiles at nearly the same depth. This suggests the temperature profile can be developed by (1) measuring the radiant emission at each wavelength, (2) calculating the

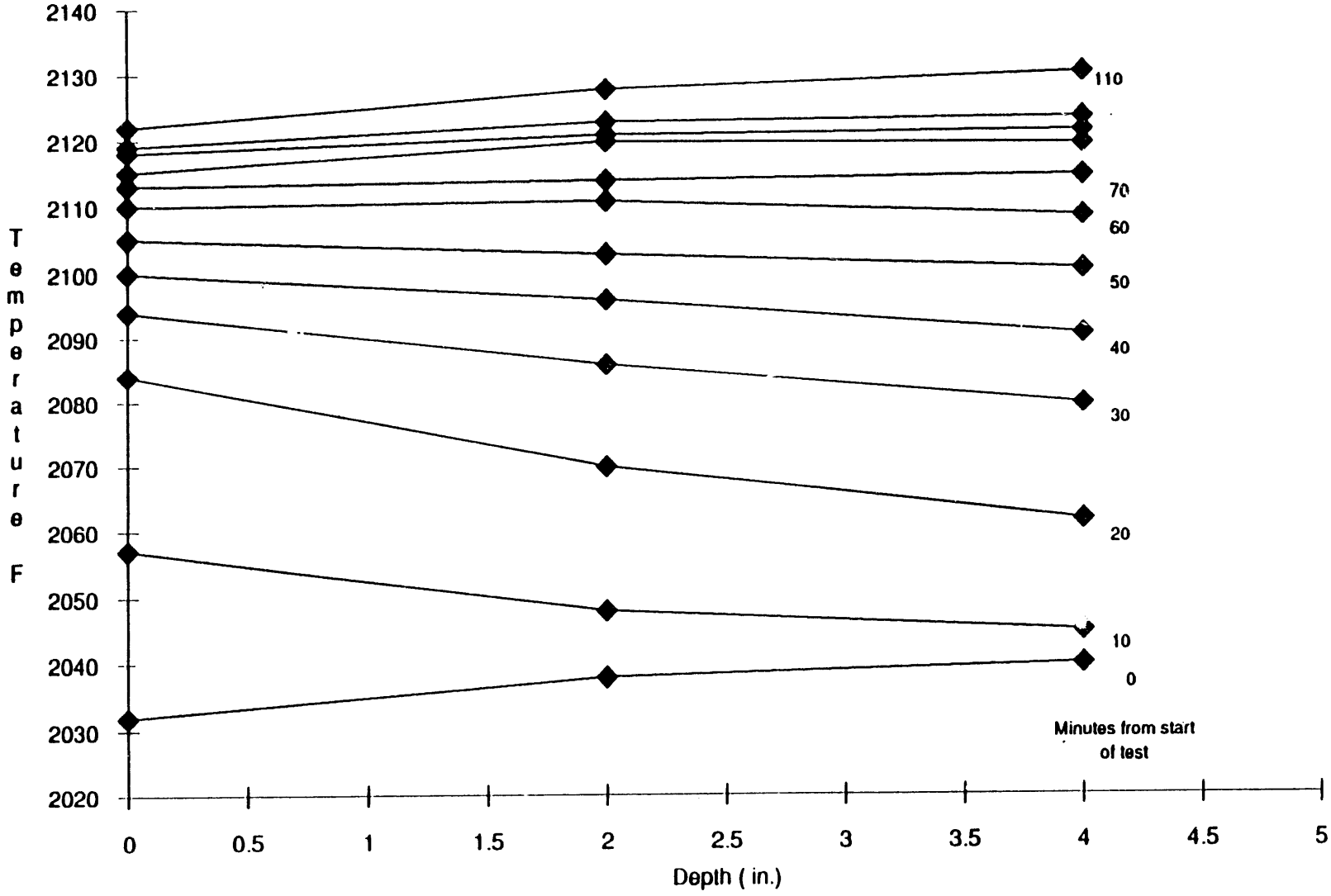

Figure E-3. Referee temperature profile vs. time.

- **Plot shows T.C. data and raw color temperature data.**
- **Optical pyrometer is clearly following the increasing temperature. Is the gradient resolvable?**

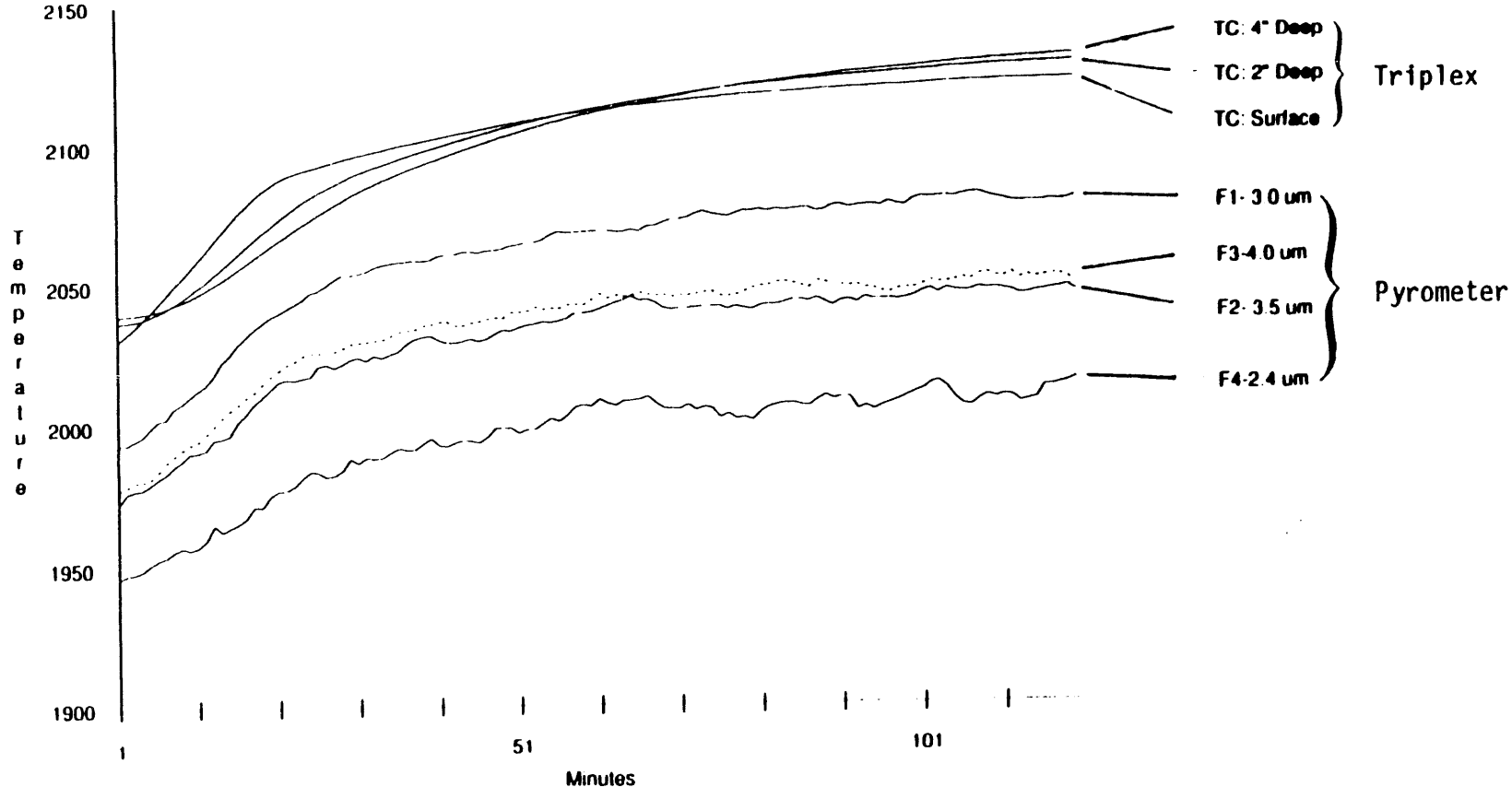

Figure E-4. Transient gradient data.

isothermal temperature that yields the same emission, and (3) assigning this calculated temperature to a given, fixed depth. As stated above, the Viskanta equation can be used to estimate the error associated with this procedure through analyzing a wide range of profiles that might be encountered. The results of this analysis indicate that the depth where the temperatures coincide do not vary significantly. Thus, little error is introduced by simply assigning an invariant depth to the calculated isothermal temperatures.

Figure E-5 shows how this was applied to the present data. Each of the four wavelengths generates one data point at a specific depth for specified time. The close relation between the temperatures, and the gradients suggests the power of the approach. It is worth noting that this is a very mild gradient, only corresponding to 7°F/inch.

Another alternative was used to analyze the data. Here, a temperature profile is hypothesized, and the Viskanta equation is used to calculate the expected radiant emissivities at each wavelength. These are then compared to the measured values. The error is used to adjust the trial temperature profile and the procedure is repeated until the error between the calculated and measured radiance values is minimized. This procedure is appropriate for any arbitrary temperature profile. For instance, the temperature can be specified at four depths, and a spline routine can be used to derive a physically realistic functionality between the points that can be integrated with the Viskanta equation. An alternative is illustrated here in which a specific functionality is assumed for the temperature, and the parameters within the functionality are adjusted to minimize the error.

The functionality is based on the steady gradient observed during the experiments. Heat is extracted from the bottom of the crucible, which establishes a piece wise, linear temperature gradient through most of the glass. At the surface, heat can enter the glass through convection and radiation. Radiation dominates, and the heat is absorbed not at the surface, but throughout the optical depth. Examples of this kind of temperature profile are shown in Figure E-6, in which the gradient is zero at the surface, and builds towards its final

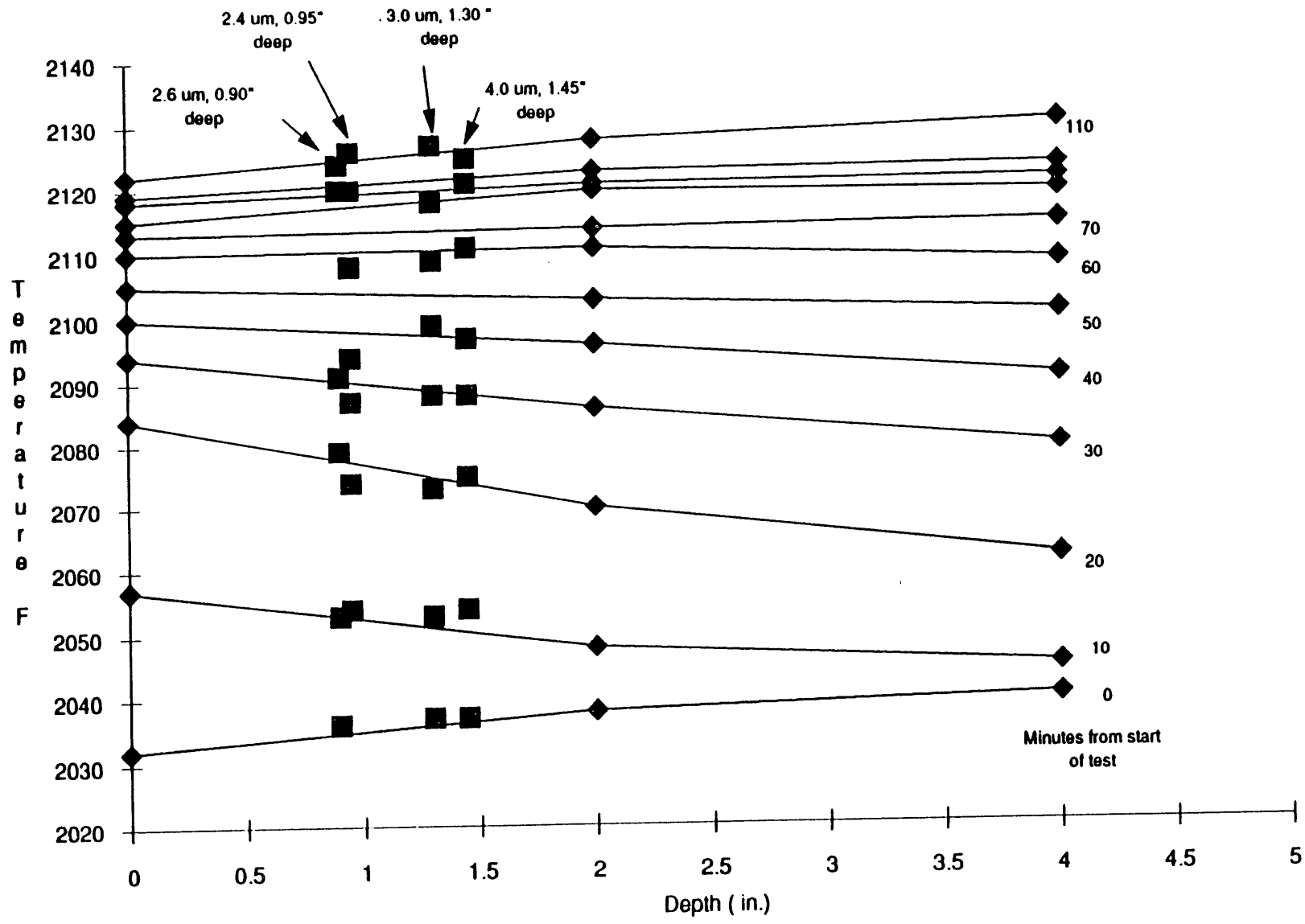

Figure E-5. Referee TC profile and depth measurements.

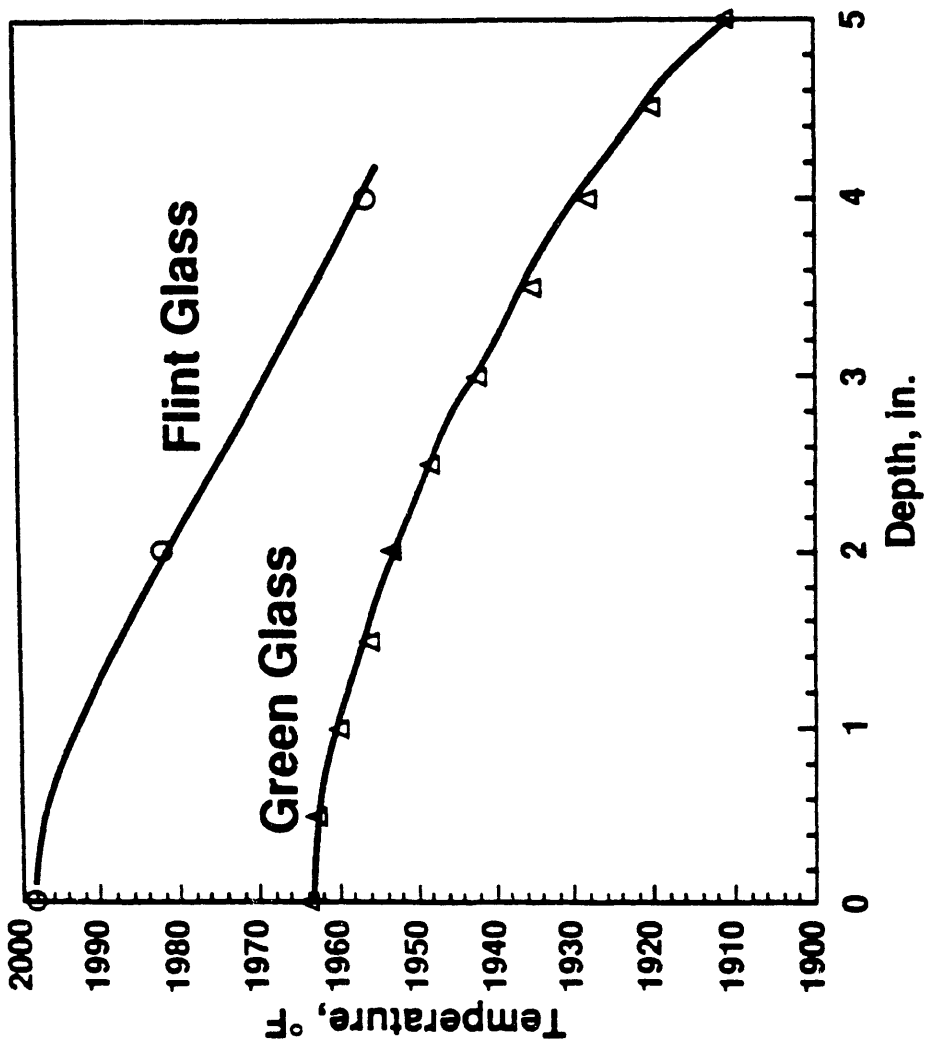

Figure E-6. Glass thermal profiles.

value as radiation is increasingly absorbed with depth. A functionality which reproduces this behavior (*i.e.*, zero gradient at the surface, linear gradient at depth) is:

$$T(y) = T_s - a_1 y - a_1 a_2 \exp[-y/a_2]$$

where T_s, a_1, and a_2 are adjustable parameters (a_1 represents the linear temperature gradient, T_s represents the *projected* surface temperature based on this gradient, and a_2 is the characteristic depth over which the temperature approaches the linear gradient. Note that a_2 is closely related to the optical depth of the glass, over which the incident radiant energy is absorbed.

In the example, the values of the parameters for flint are T_s=1311•K, a_1=3.1, and a_2=1.2. In application we would not know these values, but instead we would have measured the radiance at the four wavelengths. One numerical approach is to fix two of the values and vary the third. For each value, the Viskanta equation is integrated to yield the calculated radiances at each of the four wavelengths. The error between the measured and calculated values is expressed as:

$$\varepsilon = \sum_{\lambda_1}^{\lambda_4} | E_{calc}(\lambda_i) - E_{meas}(\lambda_i) |$$

Figure E-7 shows how this composite error is minimized for the correct value of a_2. This procedure would be repeated iteratively for each of the variables in turn, until the error of all the variables are minimized in concert. In practice, any of the common methods of multivariable error minimization (*e.g.*, method of steepest descents) could be used to arrive at the correct temperature profile. It is important to remember that this iterative approach does not require significant time to calculate. Also, the general approach is applicable to any temperature model, not just the one illustrated here.

It is felt that the simplified procedure is appropriate for well-behaved temperature profiles, *i.e.*, monotonic profiles that do not vary too much from

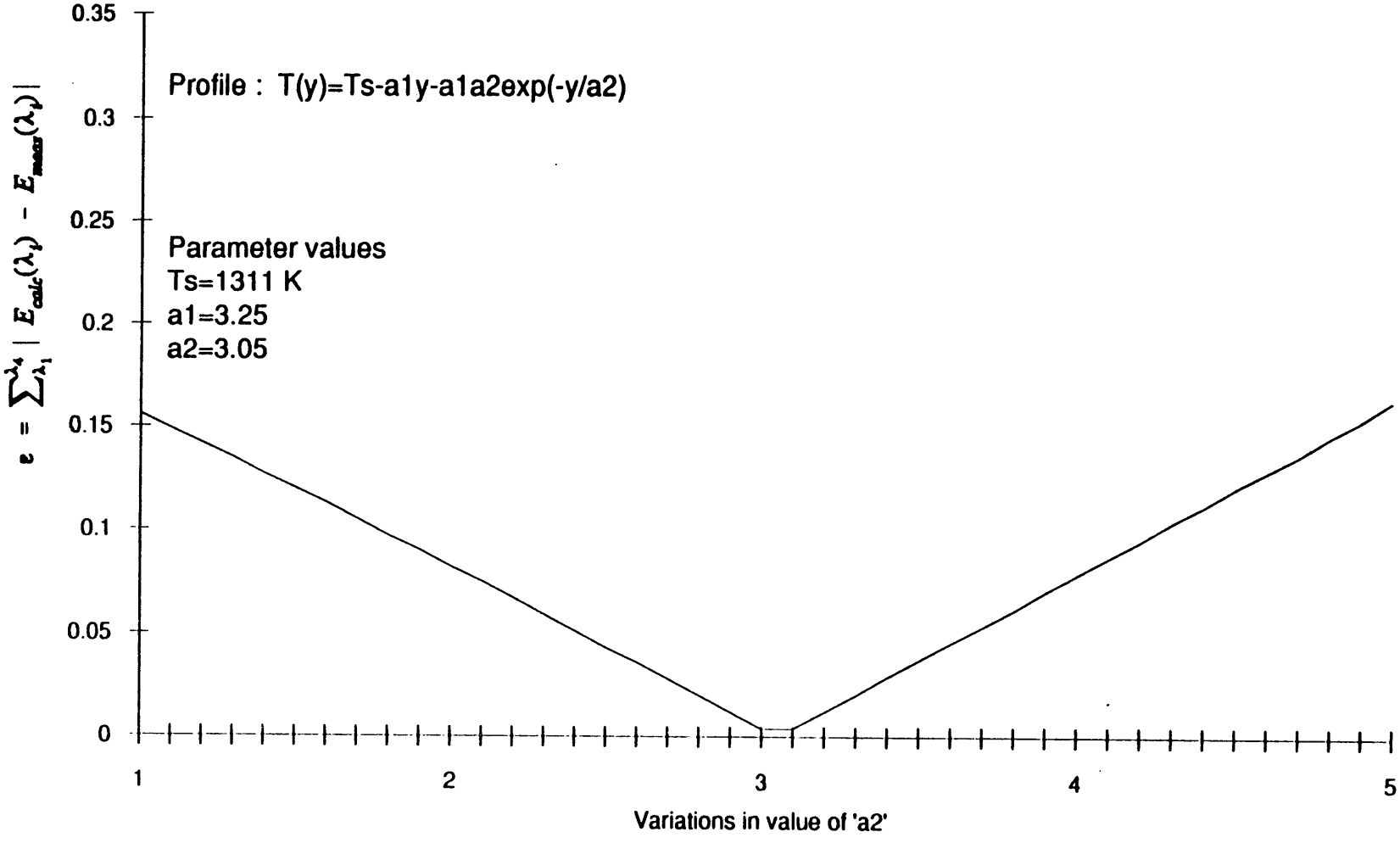

Figure E-7. Composite error in profile as a function of a2.

linear. The iterative approach may be used under more severe conditions.

Experimental Conclusions

A significant advancement of the state of the art was made toward satisfying the program objectives. Full functionality of the instrument system was demonstrated including:

- multiple sensors communicating over an optical fiber network to a common, remote, multiplexing spectrometer
- in situ, sensor specific black body calibration
- temperature profile resolution with two highly diverse container glasses
- operational compatibility with the process environment (temperature, reradiation, and combustion gases)

The most significant design shortfalls were:

- depth measurement of 2" demonstrated, target of 6"
- a demonstrated accuracy of ±4°F, target of ±1°F

The former shortfall resulted from what turned about to be a non-optimum choice of visible, near infrared measurement wavelengths. This is easily corrected, requiring only the replacement of band pass filters in what is the high resolution operating regime of the instrument.

The breadboard tests identified two general areas where design improvements to the system are needed to enhance accuracy performance. The first is noise. In general the signal to noise ratio for the recorded data was between 160 and 650. Noise in this range was determined not to be influencing data quality. However,

it is suspected that the noise arises due to some slackness in the chain drive that rotates the multiplexer wheel. One modification that should reduce the noise is to replace the chain with a notched rubber drive belt, or with a direct gear drive. This is planned for the next design iteration.

The second area of concern is drift. For many data sets, the average signal outputs stayed constant over runs of several hours. There were instances, however, where the signal of all four wavelengths would inexplicably begin drifting in the middle of an otherwise invariant run. This behavior was even noted during long term runs with the calibration source, which eliminated changes in the glass properties as an explanation. Although the reasons for the drift have not been fully defined, it is suspected to come from the detector. Specifically, the detector is mounted on a solid-state thermoelectric cooler that is designed to maintain the detector temperature at a constant value. This is critical because detector response varies strongly with temperature. It is thought that the current design does not provide sufficient contact between the detector and the cooler, so that under some conditions the detector temperature can drift, yielding the unexpected signal change. This issue will be explored and corrected during the next series of tests.

1.0 INTRODUCTION AND OBJECTIVES

This report describes the results of a Phase I Development Program to develop a non-contact, advanced optically based thermal analysis system for applications in the glass industry. Energy and Environmental Research Corporation (EER) is conducting the program under joint funding from the Department of Energy, Office of Industrial Technology, the Center for Materials Production (CMP), and EER in response to DOE Solicitation Number DE-PS07-89ID12781, entitled "Development of a Process Control Sensor for the Glass Industry." The overall goal is to improve product quality control and to minimize energy requirements on the glass forming line. The key optical elements of the thermal analysis system (TAS) were previously developed by EER and the Southern California Gas Company. This program builds on this background work by focusing on additional hardware and software development for a glass furnace-specific application (Phase I), and prototype analyzer testing on a forehearth in commercial operation (Phase II).

As applied to the glass industry, the TAS consists of an advanced narrow band, multicolor infrared radiometer. The system uses a fiber optics communication network, which allows the detectors and electronics to be located away from harsh environments. A novel optical multiplexer allows optical signals from a large number of fiber sensors to be processed through a common signal processing system. This represents a considerable cost savings in the hardware investment needed for multipoint measurements. A number of optical temperature sensing approaches were evaluated to remove reflected radiation from the measurement and obtain a true thermal emission signal.

1.1 Glass Manufacturing Needs

Thermal control in the glass manufacturing industry has two main goals. Firstly, the quality and packing efficiency (low rejection/loss) of the product is tightly coupled to the temperatures encountered at various points in the process. Thus, thermal control is synonymous with quality control. Secondly, process economics are heavily influenced by energy use.

Presently, the manufacturing line is controlled by a combination of operator empirical experience, batch monitoring of product quality and limited direct or inferential (indirect) thermal measurements. The monitoring of glass internal temperatures is particularly difficult. In most operations, the operators adjust firing rate, excess air, and throughput based on experience and inferential measurement of structural temperatures (crown and bridgewall). Limited use of ceramically sheathed thermocouples is also made, but these are expensive and have poor response, high drift, and short operating life. There is generally no satisfactory way to account for relative temperature variations between different locations or at various depths. Knowledge of the internal temperature distribution of the melt and molds would allow optimum thermal profiling. This should increase productivity, reduce furnace rejects, and improve energy efficiency.

Discussions with glass manufacturers and review of the literature have identified three critical points in the process where improved temperature measurement is needed. These are:

- Forehearth. The temperature of the glass as it is moved from the melting furnace to the forming step is critical if the melt is to have the correct viscosity and surface adhesion properties for forming the product. The thickness of the glass flow at this point suggests that a surface temperature is of minor utility, while a full thermal profile is difficult to obtain. Conventional optical pyrometry measurements are difficult because high background radiation levels that interfere with the measurement. Also, broad-band optical pyrometry tends to yield a mixed signal consisting of surface contributions at longer wavelengths and interior contributions at the shorter, more transparent wavelengths.

- Gob. This is the semimolten glass piece that is separated from the forehearth flow for insertion into the mold. Again, control of viscosity and surface properties are critical for optimum molding behavior. This operation takes place in a low background radiation

environment. Although conventional optical pyrometry is more easily performed, the gob is cooling at a rapid rate. Thus, the appropriate measurement technique must respond quickly, and would ideally look beyond just the surface.

- Molds. The surface temperature is critical to obtaining appropriate surface finishes, and to obtaining good release of the product. This measurement also takes place in the absence of significant background radiation.

Thus, the critical requirements of any optically based thermal sensor should include: (1) the ability to operate accurately in regions of high background radiation, (2) the capability to "look" into the glass melt a various depths and resolve internal temperature, and (3) the achievement of an essentially real-time signal.

1.2 Optical Approaches

Several measurement approaches, each using the basic TAS system, were identified for study under the proposed program. These approaches use four-color pyrometry (as opposed to two color temperature which ratios the emission intensity at two wavelengths) to deconvolute temperature profiles from radiosity measurements. Two approaches are used to eliminate background radiation interference. These are the Brewster's angle approach and the normal angle approach.

Brewster's Angle Approach. The first approach is based upon using Brewster's angle of reflection to eliminate background radiation from the collected signal. A principle discussed in many introductory physics textbooks is that light reflected from a smooth dielectric surface (glass, for example) is preferentially polarized in a plane perpendicular to the plane of incidence. This is the phenomenon that results in the "glare" that Polaroid sunglasses remove effectively. At a specific angle of reflection, known as Brewster's angle, 100 percent of the reflected light is polarized. Thus, by observing the

surface of a glass melt at Brewster's angle it is possible by the use of polarized filters to completely eliminate the background radiation.

Brewster's angle reflection measurements can be coupled with another property of glass melts to obtain depth temperature profiles. The transparency of glass melts is a function of the wavelength of light. Thus by varying the wavelength of collected light it is possible to "see" the change in temperature with distance into the glass melt.

Normal Angle Pyrometry. The second approach involves normal angle emission signal collection. One property of glass melts is that at wavelengths away from specific absorption bands only about four percent of the normal incident light is reflected. Aligning optics at the normal angle is much simpler than alignment at Brewster's angle and the associated alignment of a polarized filter. Thus, for a low background environment, detection alignment normal to the melt surface offers a means for enhancing the signal-to-background ratio. Normal angle signal collection can be combined with variable wavelength measurements to obtain depth temperature profiles. This approach should be very successful in obtaining time-temperature-depth profiles in the gob where no significant background radiation is present.

1.3 Technical Approach

EER has implemented a two-phase project. In Phase I, a breadboard TAS was designed, assembled and used to measure glass temperatures in a laboratory pilot scale furnace. The "proof of concept" test has provided key data for the design of a prototype instrument. The focus of Phase I was evaluation of the two concepts, normal and Brewster's angle, multicolor pyrometry. In Phase II, the prototype instrument will be constructed, installed, and tested on a glass forming line. Gallo Glass Company, a large bottle manufacturer, has submitted a Letter of Intent to participate as a host demonstration site.

This project has received considerable support from industry. The Glass Packaging Institute, Glass Firing Task Group has provided project review and

guidance to ensure that the TAS will be optimized to meet industry needs. The CMP, cofunded by Pacific Gas and Electric, has also supported the Phase I Project.

The Phase I Development and Laboratory Evaluation objectives were to:

1. Develop the sensors and appropriate signal processing instrumentation which enables remote measurement of surface and subsurface radiosity in the mid infrared and visible wavelengths.

2. Develop radiation models which will determine glass temperature based on sensor indications.

3. Conduct pilot-scale furnace studies to verify that the EER Thermal Analysis System will determine glass and refractory temperatures.

4. Select a glass manufacturing application and assess its cost effectiveness.

5. Develop a plan and design a full-scale system for field evaluation in a suitable glass furnace or process.

These objectives were fulfilled in a six task development program, Figure 1-1:

- Task 1--Assessment and Applications Characterization
- Task 2--Sensor System Development
- Task 3--Laboratory Scale Furnace System Development
- Task 4--Laboratory Study and Verification
- Task 5--Engineering Design and System Economics
- Task 6--Phase I Report

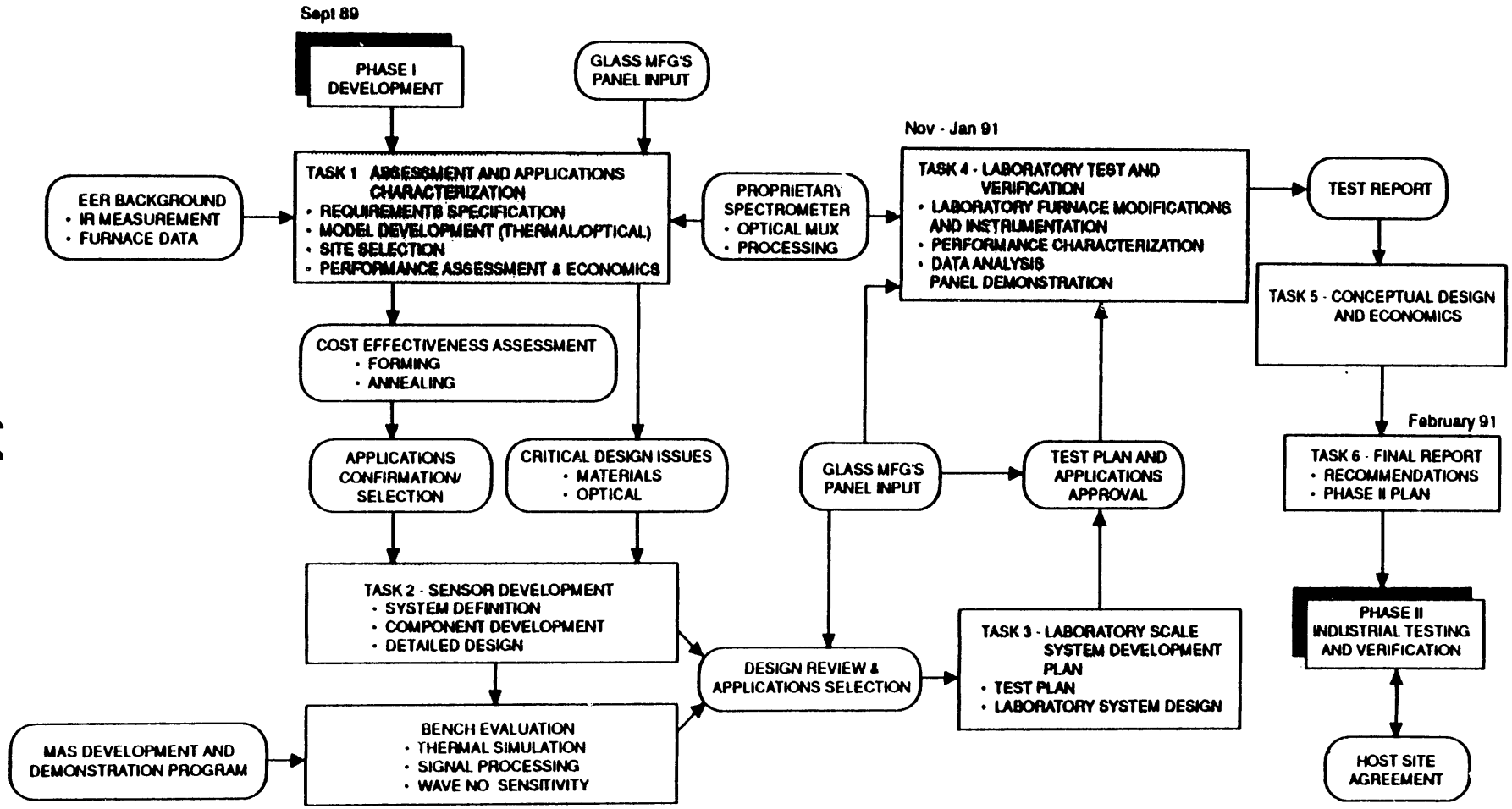

Figure 1-1. Phase I development plan.

2.0 ASSESSMENT AND APPLICATIONS

An assessment of potential TAS applications within those industries requiring significant thermal processing was performed. Although primary emphasis in support of Task 1 was focused on the glass industry; metals processing was also briefly addressed.

This section describes the rationale for selecting container glass manufacturing as the target process, and the forehearth and forming operations of the glass production line as the most cost effective application for the subject technology. This conclusion is based upon discussions with plate and container glass manufacturers, the manufacturers for forming equipment, and various consultants, associations and agencies connected with the industry. New technology developments such as light weighting of containers for production cost reduction is also considered. It is noteworthy that glass container and press and blown manufacturing, both of which use forehearths, consume about 64% of the energy used in glass manufacturing [1, 2]. Further, post melting operations, the activity most impacted by good forehearth control, uses 25 percent of the total glass industrial total. Preliminary order of magnitude economics using reasonable assumptions suggested energy and production savings should result in a payback on total capital costs of less than a year and perhaps as low as half a year.

An aggregate market for steel, glass, and cement applications is estimated at 2865 units and is comprised of systems configured with 8 to 32 sensors. Glass applications dominate this market, comprising about 1800 units.

2.1 Approach

The technical assessment, Task 1, was conducted in the following steps, Figure 2-1:

- Discussions with industrial experts (end users and furnace manufacturers) with regard to instrument needs and performance.

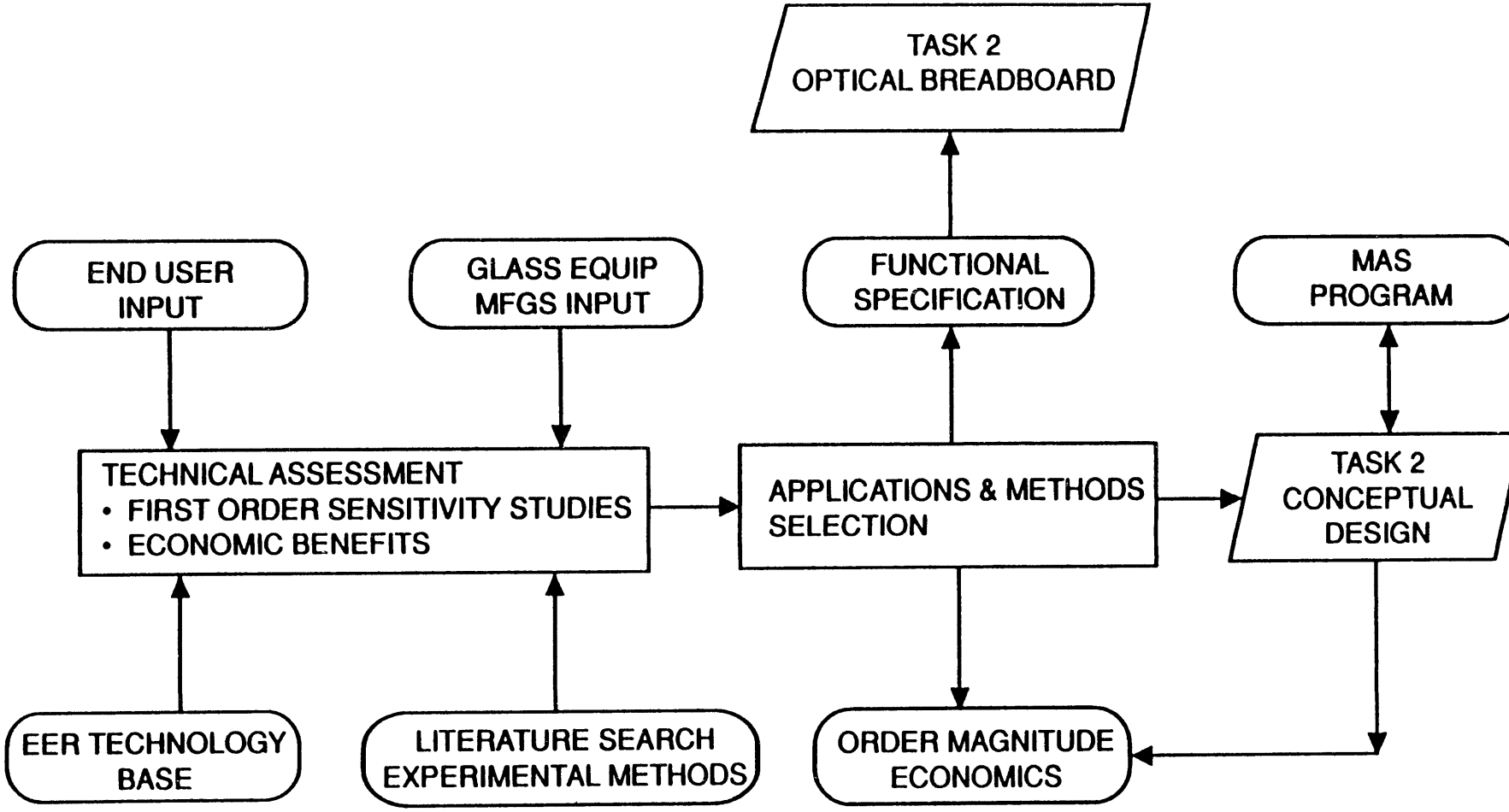

Figure 2-1. Task 1, technical assessment work plan.

- Identification and quantification of the energy intensive glass manufacturing processes.

- An evaluation of the various optical methodologies and their potential incorporation into the TAS multiplexed instrumentation.

- Conceptual design and cost effective assessment (although discussion is deferred until Section 5.0).

The data base thus established was then used to select an application and to develop a functional specification for the instrument.

The development of the functional analyzer specification was initiated by defining furnace operating and glass temperature along the glass path. Conditions are generally characterized by:

- Melt bulk and profile temperatures which are substantially influenced by boundary conditions surrounding the melt

- The atmosphere over the melt, typically IR radiating gases containing H_2O and CO_2 at higher temperatures and cooling air at lower temperatures

- Progressively lower temperatures and gradients as the glass flows from the melting tank (2800°F) to the annealed product (1100°F)

The advanced sensor should have performance at least as good as the current state of the art, Pt-Rd triplex, submerged thermocouples:

- 50°F drift over life

- ability to look between 4" to 6" into the glass

- installation through a 1" diameter hole in refractory walls

- compatibility with a wide range of glass optical properties (color and absorptivity)

- precision and accuracy close to the ± 1 to 2°F usually claimed for competing measurements

The resulting functional specification, Table 2-1, was discussed with forehearth manufacturers and the Glass Firing Task Group of the Glass Packaging Institute, and revised in light of their recommendation. The result of this activity and the development efforts of a parallel sister program, the development of a moisture analyzer (MAS), were then integrated. MAS component design modifications (optical and software) were identified which were needed to implement the functional specification and the contemplated measurement methods. The resulting conceptual design was then used to develop a provisional capital cost, and estimate the economics of the selected application.

2.2 Industrial Assessment

The industrial assessment was performed by integrating user and equipment manufacture input, a literature search, and considerations as to the inherent capability of the proposed instrument. The first activity was to identify those segments of the glass industry having large energy consumptions on both a unit production as well as average plant basis. Major manufacturing sectors identified by SIC code are:

- Container glass

- Pressed and blown glass

- Fiber glass and

- Plate glass

TABLE 2-1. GLASS SENSOR APPLICATIONS AND FUNCTIONAL SPECIFICATION FOR GLASS PACKAGING INSTITUTE PANEL REVIEW

1. Process Description

1.1 Location	Melt Depth Inch	Temp °F		No Temp. Sensors	
		Surface	Melt	Surface	Subsurface
a) Glass Tank		2800-2900	2300-2600	12-24	na
b) Refiner	36-60	2700	2100-2300	3-6	3-6
c) Forehearth	4-8	2200-2400	2100-2300	12-18	12-18
d) GOB/Spout	1-3	-	1900-2100	1-4	1-4
e) Mold, ON/OFF	1/16-1/4	100-500	1900-1200	1-3/section	na

1.2 Interferences

a) Wall Radiation, differential °F	100-500
b) Atms	12% H_2O, submicron particulate

1.3 Glass Properties

a) Index of Refraction	1.30 to 1.48
b) Transparency, %	0 to 80, 3.3 to 1.5 μm

2. Instrument Performance

2.1 Repeatability, °F	±1
2.2 Precision, °F	±1
2.3 Calibration/Stability, °F/mo.	±2

3. Instrument Interfaces

3.1 Installation Considerations

a) Component Interconnection	
- Sensor to Shop Floor,m	Ground Level, 20-40
- Cabinet to Control Room,m	100-200
b) Sensor Environmental	
- Temperature, °F	140°F
- Vibration	60-200 Hz
- Contamination	Oil Mist

TABLE 2-1. GLASS SENSOR APPLICATIONS AND FUNCTIONAL SPECIFICATION FOR GLASS PACKAGING INSTITUTE PANEL REVIEW (Concluded)

c) Mounting	
• Permanent Furnace Locations	Thru Refractory
• External Tripod Mount	Portable or Bracket
• Structural Interfaces	1" Penetration thru Ceramics
d) Utility Support - Power	110V, 60Hz
- Purge Air	10 scfh/Sensor
3.2 Operator Interaction	
a) Control Strategy	Feed Forward, Cascade Back
b) Maintenance Access -	Sensor Head Quick Disconnect
-	Electronics Floor Level
c) Displays	LCD/CRT
4. Design Characteristics	
4.1 Hardware	
a) Sensor Hardening	Passive, SS
b) Electronic Chassis/Enclosure	NEMA 4
c) Computer Architecture	Std Bus
4.2 Communications	
a) LAN Configuration	Star, Multi-Drop Daisey
b) Software/Firmware	DOS/Std Bus
c) Diagnostics	Self
d) I/O Devices/Ports	RS232, 16 I/O Count
4.3 Control	
a) Internal Instrument	Digital, "C" Language
b) External Loop	PID Direct and Cascaded
4.4 Maintenance	
a) System Level	PC Card Replacement
b) Spare Parts	10% of Cost
4.5 Cost	
a) Investment[1]	2200 to 8000 $/pt
b) O&M[2]	200 to 800 $/pt/yr
c) Payback, yrs	1 to 2

[1]Based on current cost of tri-level, submerged thermocouples.

[2]10% of investment, current submerged TC's need replacement every 9 to 36 months at over $500/unit.

2.2.1 Industrial Energy Use Profiles

Profiles for these SIC codes, Table 2-2 [2], shows glass containers dominating total industrial energy use. They use well over 40 percent of the energy and are substantially higher than any of the other SIC codes with respect to value of goods shipped. Therefore, container and pressed and blown glass are the areas to be focused upon. As it turns out, this industrial segment has also shown the most interest in the technology. The proposed sensor technology is probably most cost effective where internally consistent, 3-dimensional temperature profiles can materially assist in improving the production and energy efficiencies. A noncontact optical system measuring multiple points within the glass melt, both surface and in depth, with common signal processing hardware could satisfy this requirement. The physics of glass (absorption coefficients) constrain measurement depths to about 4 to 6 inches, depending upon the type and transmissivity; therefore, the melter and probably the refining area of the process would be inappropriate or constrained applications of the technology. Also, the environment and access to the melt surface are substantially more difficult in these areas and for a first industrial application probably would be unadvisable.

In order to quantify energy consumption actually impacted by an advanced glass sensor, energy use was allocated to the post melter process steps, Figure 2-2. These results confirm that container and pressed and blown glass have the most energy intensive post melting steps, Table 2-3 [3], and should therefore be good candidates for the first application, i.e. 25 percent of the total industrial. Of the two top contenders, container glass is preferred since the plants individually have higher production rates, typically in excess of 300 ton/day pulls whereas pressed and blown plants have a high diversity factor, representing anything from very small specialty productions to major high-production facilities approaching several hundred ton per day.

TABLE 2-2. GLASS INDUSTRY ENERGY USE PROFILES

Process	SIC	% of Industry Use	Annual Tons (10^6)	Value $\$(10^9)$	Post-Melting %
Container	3221	42	13.5	4.9	11
Press and Blow	3224	22	2.2	2.7	14
Fiber	3211	18	2.0	2.3	10
Flat		18	3.1	1.7	3

Ref: Battelle Rept PNC 5640, June 86.

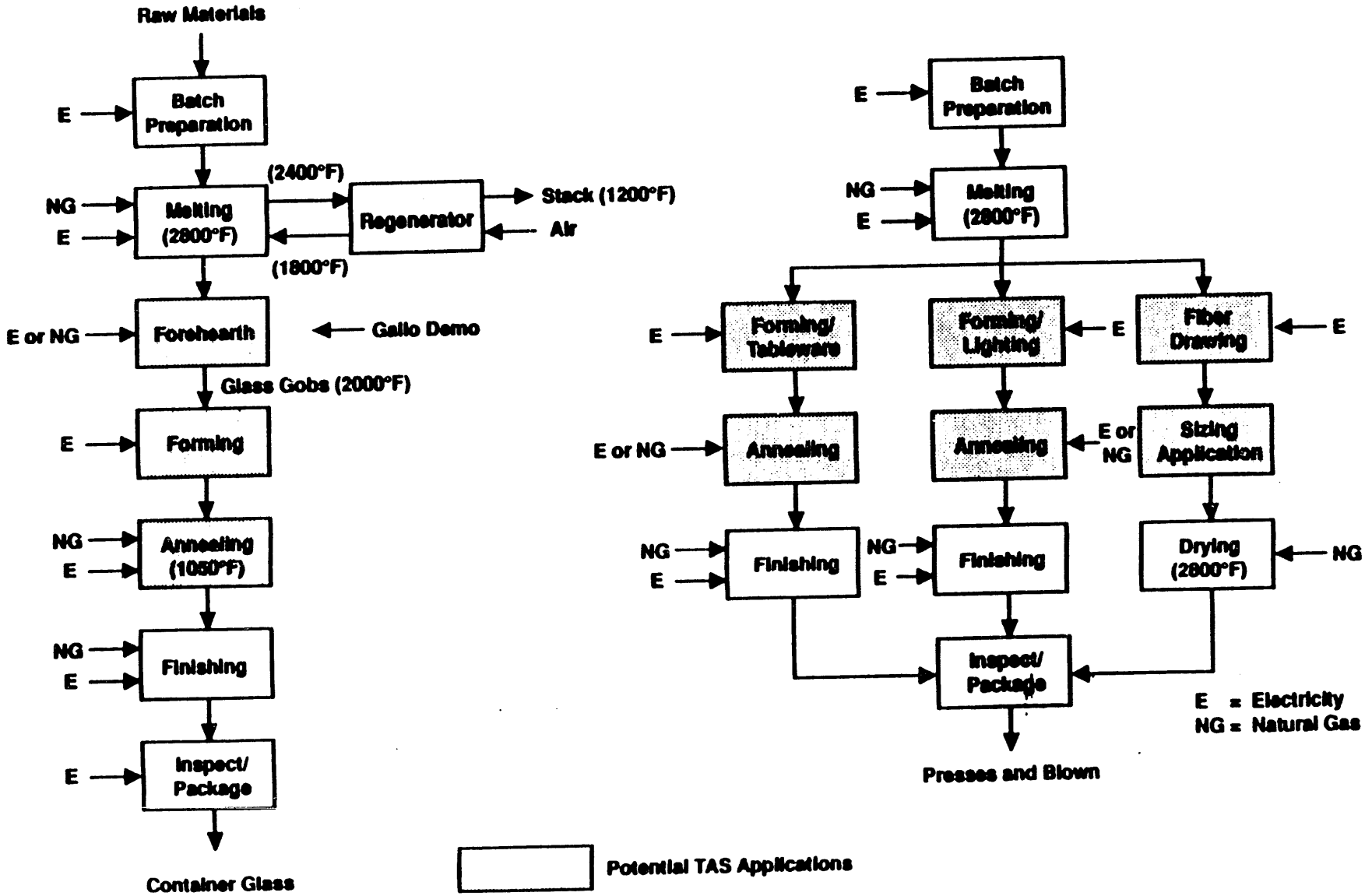

Figure 2-2. Processing steps in the production of high energy consuming glasses.

Reference: Battelle Rept. PNL-5640/UC-95f, Potential for Energy Conservation in the Glass Industry, June '86.

TABLE 2-3. (a) TYPICAL ENERGY USE IN THE FOREHEARTH

Plant	Pull ton/da	No. Hearths	Fuel Use M^2Btu/da	Efficiency M^2 Btu/ton
A	245	2	55	0.22
A	147	2	75	0.51
A	142	3	74	0.52
B	200	2	34.8	0.17
B	200	2	77.0	0.38
B	200	2	22.0	0.11
(b) TYPICAL ENERGY USE IN ANNEALING LEHRS				
A	245	2	17	0.069
A	147	2	53	0.36
A	142	2	24	0.1

2.2.2 Forehearth and Forming Applications

The most critical manufacturing step is glass conditioning (temperature and degassing) in the post melting operations. Glass conditioning effects production throughput, packing efficiency (shipped to melted weight ratio), and energy use. Temperatures typically are in the range of 2250 to 2400°F at the rear of the forehearth, and are progressively cooled and homogenized as the melt progresses to bowl, typically at 2100 to 2200°F, Figure 2-3. On a modern forehearth temperatures are measured with triplex Pt-Rd thermocouples, Figure 2-4, at three cross sections (centerline and edges) for a total of nine positions.

In order to effect a control algorithm (usually feedback, sometimes feed foreward) the TC measured gradients are normalized to a single weighted temperature commonly referred to as the "temperature gradient efficiency." The control strategy drives this efficiency toward a target (set point) value, close to 100% (no gradient).

The control logic determines where and how cooling, heating, or some combination are to be applied, Figure 2-4. Forehearths are typically 3 to 4 ft wide and 24 to 30 ft long. Glass surfaces are smooth because of low linear velocities and viscosity. Temperatures in the bowl around the plunger are the most critical and difficult to measure. Gob delivery (weight repeatability and formability) is highly dependent on viscosity at this point. Optical paths through the head space above the melt are typically 2 to 6 inches.

Forehearths are elevated from the plant floor some 8 to 10 ft and are surrounded by hot ambient, misty (oil release) environments. Thus, a TAS capable of relatively passive sensing and having a remote, floor mounted signal processing subsystem would significantly improve reliability and maintainability. Optical systems must be able to look around any optically interfering combustion products (H_2O or CO_2) above the melt to avoid interferences which could confound the radiosity measurement.

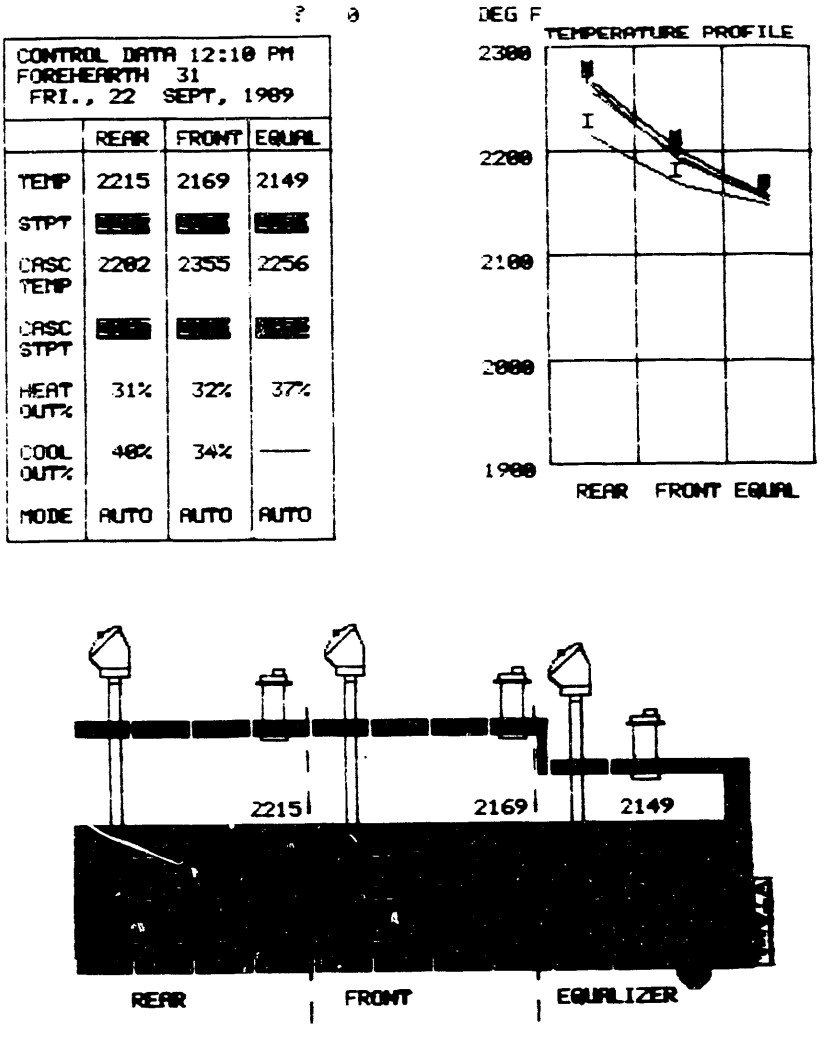

Figure 2-3. Typical container glass forehearth temperature profiles.

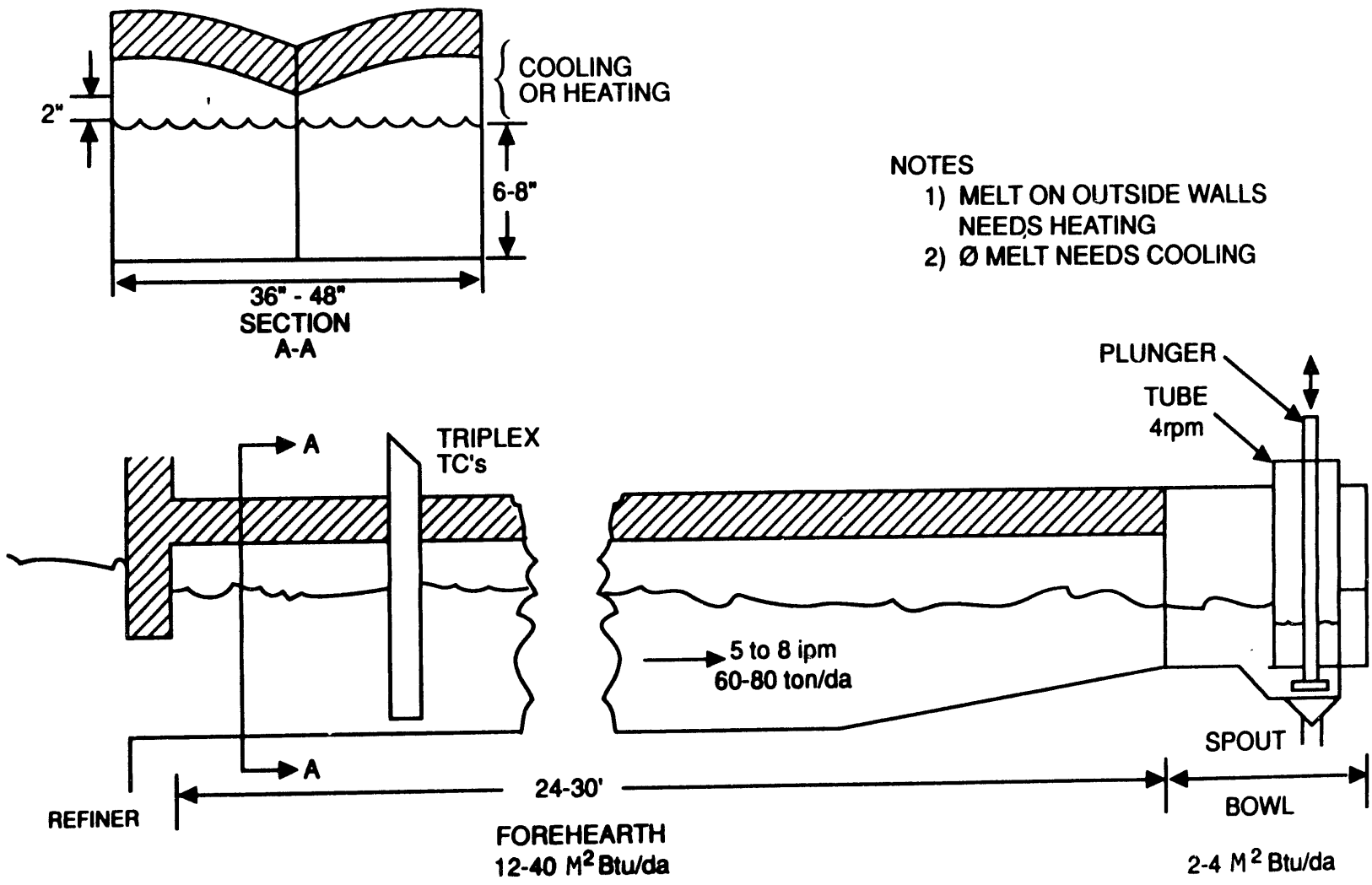

Figure 2-4. Forehearth, spout & GOB geometry and process data.

2.2.3 Annealing and Tempering Lehrs

Lehrs are large convective conveyor ovens which anneal or temper formed glass usually as part of a continuous production line. Annealing lehrs are not major energy consumers since the containers enter at high temperature from the mold machines and are typically held at about 1000°F over 10 to 20 minutes. Tempering furnaces usually start with a cold product and are therefore about twice as energy intensive.

Annealing lehrs process about the same tonnage as forehearths, but with a heat input of about half, Table 2-3. Temperature distribution (and variances) across the oven (ware and convective gases) and in the machine direction are critical. Any method of improving this control has two major benefits.

- Improved productivity, particularly when the melting and forming production are similarly improved.

- Better quality control since the conveyor line production rate is matched to the cross conveyor ware position having the shortest temperature-time profile.

Line production increases would be most significant for tempering operations since their speed is independent of melter pull rates and they are about twice as energy intensive. Annual energy consumption for tempering is not well documented and generally limited to laminated plate glass and kitchen ware, certainly well under 25 percent of the annual glass production and, again, with less overall impact than the forehearth application. Thus, convective ovens are significantly less energy intensive and do not have the economic leverage of the conditioning and forming operations.

2.3 Measurement Methods

Measurement methods have tentatively been selected from a review of the literature [4 through 15] and incorporate both current practice, Table 2-4, as

TABLE 2-4. CURRENT GLASS PRACTICES IN INSTRUMENTATION AND CONTROL

Primary Steps	Glass Temp. ^{o}F	Efficiency M^2 Btu/Ton Range	Efficiency M^2 Btu/Ton Avg	Current Practice
		0.015-.04	.021	
Melt	2600-2800	3-8	5	Bridgewall Temp/Models
Refine	2200-2400	0.05-0.2		Submerged Probe/ Pyrometers
Condition	1900-2100	0.1-0.5	0.3	Submerged Probe/ Pyrometers
Form	1900-2000	0.015-.04	.02[1]	Pyrometer at Setup
Temper	1000-12000	2.5-6	4[1]	Recirc. Air Temp
Anneal	900-1200	0.05-.5	.20	Recirc. Air Temp

[1]Primarily electrical, converted to fuel equivalent assuming a utility heat rate of 11,800 Btu/kW-hr.

well as experimental procedures developed by glass researchers. Current state-of-the-art optical pyrometers, Table 2-5, primarily use single narrow band or broad band radiation in two distinct regions of the glass transmissivity curve, Figure 2-5. These are nominally in the .7 to 1 micrometer, which is visible to very near infrared, and the 4-1/2 to 5-1/2 micrometer which is mid-infrared. Glass optical characteristics at each of these two wavelengths have unique properties which enhance functionality; for example, at near infrared (almost visible), glass has a very high transmissivity. Instruments sighted at these wavelengths typically measure radiation coming from both the surface and the bulk glass, perhaps representing an average some 2 to 3 inches into the glass. The measurement is susceptible, however, to reflected radiation since glass is also fairly reflective in this wavelength range; i.e., its apparent emissivity is relatively low. Conversely, when moving to the mid-infrared range the glass emissivity is very high (glass is almost opaque) and therefore its reflective characteristics are relatively low. This, then, provides a fairly accurate surface temperature but gives no indication of the temperature gradient below that surface. Other important analyzer features are the compatibility of optical sensors with optical fiber signal transmission and multiplexing to a timeshared signal processing system. Those sensors compatible with optical multiplexing (up to 24) and multi-color radiosity measurements (4 preferred) should have superior cost and measurement features relative to post melting applications.

The ability to transmit narrow or broad band radiation signals over optical fibers provides significant operational enhancements:

- The signal is immune from electromagnetic radiation frequency interferences caused by electrical machinery.

- Sensitive signal processing (electro-optic and electronic) can be remote from process.

The mid IR range prohibits the use of the more common high purity silica materials. However, heavy metal fluoride optical fibers have good transmissivity over the operating range. These fibers, although approximately an order of

TABLE 2-5. COMPARISON OF ADVANCED NON-CONTACT TEMPERATURE SENSORS

Item	Mfg.	Product	Optical Fibers[1]			Pyrometry[2] Color, μm			Target	Signal Processing	
			Sensor	Tran.	S/P	1	2	4	Ref.	MUX[3]	μP
1	EER	Thermal Analysis System	X	X 20m	X			1/4	Diode Laser	Optical 8-Chan.	X
2	Ircon	Mirage OR Series		X 3m			0.7/ 1.08				
		OZ Series				0.7/ 1.08					
		T Series				2/4					
3	Raytek	Thermalert II				X					X
4	Bloom	Energy Eye					X		X		X
5	Williamson	Tru Temp 9100	X	X			0.71/ 0.81			Optical 5-Chan.	X
		Fiber View 6200EP	X	X		2.0/ 2.4					
6	Pyrometer Instruments					X 0.865			IR Laser		X
7	Vanzetti	TM-2 & Vanguard 2		X Couples Sensor to Detector		X 4.5/5.2	X Bifurcated Fiber			Electronic	X
8	Land	WTA 135/System 3		X 3m		0.7/1.0	0.7/1.1	Second Sensor on Wall			X
9	Accufiber	Model 100	X	X	X					Electronic 8 Chan.	X

Notes:
[1](Trans) signal transmission between sensor and detector, (S/P) spectrometer components.
[2]1 (one color broad board with no corrections), 2 (two color ratio, gray body assumption), 3 three color grey body correction), Ref (with special target for reflected radiation or emittance).
[3]Optical (optical with common detector) or electronic (MUX after detectors).

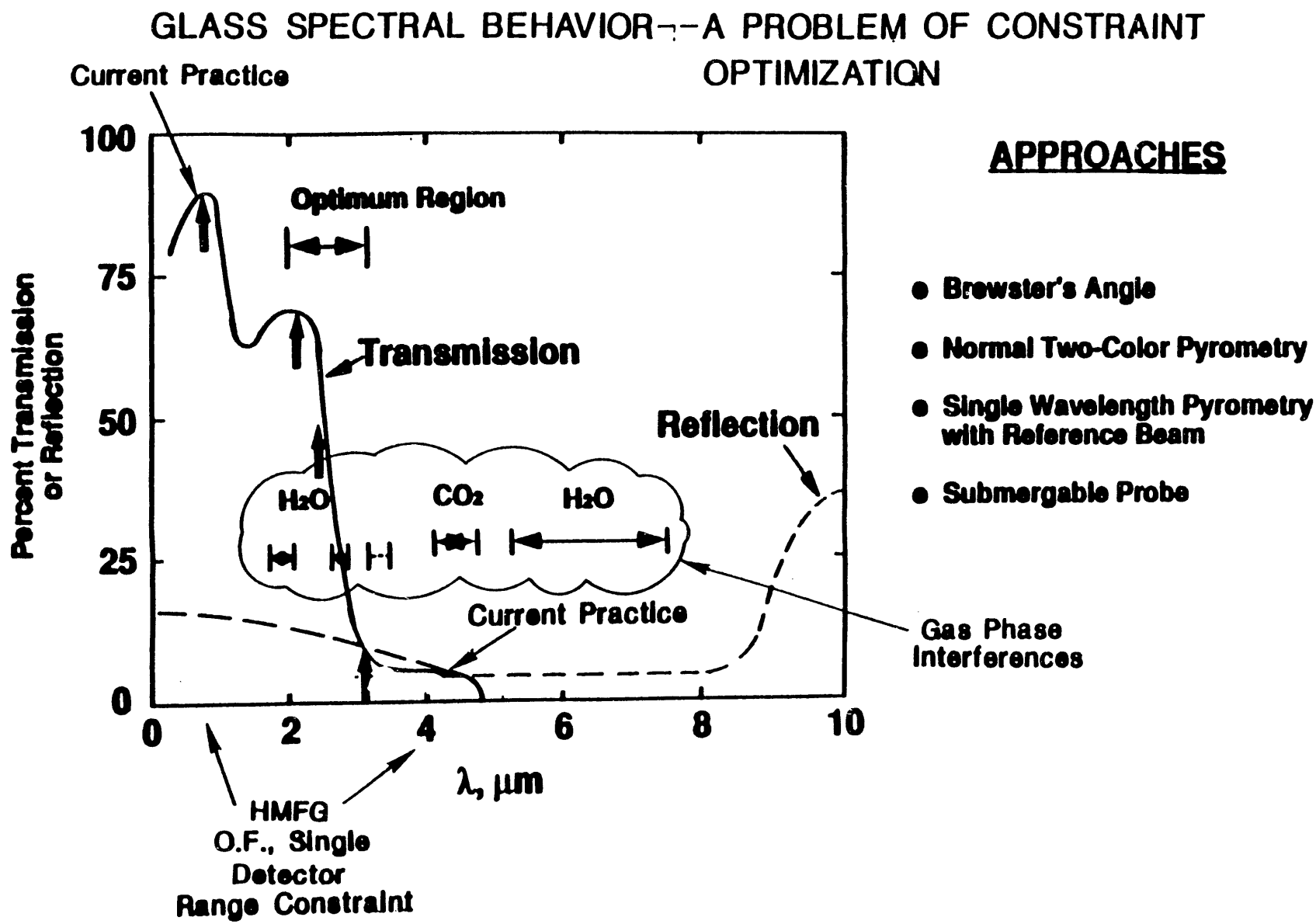

Figure 2-5. Optical approaches using various glass properties.

magnitude more expensive, are priced consistent with the general economic and cost requirements of the project. This allows good transmission of broad-band optical signals between one and four micrometers, well within the range of the various measurement methods proposed, except for those using a black body pyrometer at about 5 μm. Wavelengths beyond this provides very little information content and would require moving to even more exotic optical fiber materials such as chalcogenides which are, in the quantities currently available, extremely expensive and subject to deterioration. This suggests that the Brewster's angle affect could also be used to make a measurement of subsurface temperature, but in a wavelength region which is more compatible with the optical technology. This angle is a function of the index of refraction and is somewhat wavelength dependent. Sighting a sensor at or below this angle and using a polarization filter allows one to make an unconfounded temperature measurement; i.e., one that isn't affected by surface reflection from hot or emitting refractory surfaces surrounding the glass melt.

Glass temperature gradients with depth have been experimentally measured using multiple, narrow band multi-wavelength radiometers. Discussions with Professor Viskanta of Purdue University [12, 14] and other literature [15], suggest, that depending upon the physical properties of the glass being measured, between three and five IR wavelengths are optimum. Additional wavelengths to more precisely resolve the temperature vs. wavelength curve, unfortunately also require a higher level of mathematical inversion with its own errors. There is actually an optimum number in the range of 3 to 5 wavelengths. Therefore, it would appear that the optical design criteria for the proposed instrument should include:

- A minimum of four widely separate measurement wavelengths incorporating the range approximately between .7 and 4.5 micrometers.

- The ability to look deep into the glass without being concerned about boundary conditions at the glass, ceramic back wall interface.

- The ability to transmit this collected light over a fiber optic communication system with low attenuation.

- The ability to sight off normal by about 45°.

The literature generally indicates that IR radiation internal to the glass much below 6 inches will not provide sufficient signal to deconvolute temperature. Therefore, the technology is constrained to those parts of the glass manufacturing process where the glass melt or product is relatively thin; i.e., forehearths, gobs, forming mold machine and post-forming tempering and annealing.

2.4 Market Assessment

The potential TAS market (application and size) is estimated in this section for high temperature thermo processing industries like steel, ceramics, and nonferrous.

2.4.1 Applications

The proposed glass sensor incorporating the EER Temperature Analyzer System is suitable for a large number of high temperature thermal processing applications. Those that are energy intensive and require a knowledge of temperature profiles (temporal and spatial) for good results (quality control and/or productivity) are primary candidates. Table 2-6 lists processes corresponding to these criteria, and includes ferrous and non-ferrous metals, ceramic and cement production.

Currently, workpiece temperature is typically controlled using an inferential temperature measurement and furnace operating variables are set based on operator experience. Large, high production equipment may employ more sophisticated sensing and control like optical pyrometers and computerized process models. The practice varies somewhat depending on type of furnace (batch or continuous) and type of thermal process (ferrous or non-ferrous metals, and ceramics).

TABLE 2-6. OTHER INDUSTRIAL APPLICATIONS AND THEIR ENERGY USE PROFILES

	Description		Energy Use Unit Level		Annual Total
	Work Temp, ^{o}F	Type Furnace [1,2]	Input M^2Btu/hr	Efficiency M^2Btu/ton	10^{12}Btu/yr
1. Fabrication					
1.1 Steel Reheat	1800-2400	C(3-4)	30-100	1-1/2 - 2-1/2	100
1.2 Steel Forge	1600-2300	B(3-9)	3-15	2-5	60
1.3 Al Forge & Reheat	1000-1400	B(2-6)	1-20	3/4 - 1	20
1.4 Clay - Ceramic Firing	1800-2200	B(10-16)	5-20	2 - 3-1/2	100
1.5 Glass Annealing	800-1200	C(1-2)	5-20	1 - 1-1/2	50
2. Metallurgical					
2.1 Steel Heat Treat	1000-1700	B(2-10)	>1-5	4-8	20
2.2 Al Heat Treat	600-1000	B(2-8)	1-20	1-1/2 - 2-1/2	20
3. Cement	2200-3500	C(2)	>100	4-5	297

NOTES: 1, C (no zones) continuous 2, B (cycle hours) batch

Batch furnace (mostly metallurgical and shuttle kiln) work temperature is most easily measured and controlled because:

- Work volumes are relatively small and reach isothermal conditions well before thermal processing is completed; therefore, the temperature of the furnace environment in a better measure of work temperature.

- Stationary product can be monitored with surrogate temperature instrumented or temperature sensitive (i.e., ceramic cones) workpieces and with thermocouples embedded in the work stack (pallets, fixtures, etc.).

Therefore, these low production processes will usually not materially benefit from improved temperature sensing unless extremely critical temperature tolerances must be held, e.g., silicon metals and ceramics in the electronic industry. On the other hand, energy intensive continuous processes like:

- Steel reheating for rolling and forging

- Aluminum and steel stripmills

- Container, pressed and blown, and fiber glass conditioning and forming

- Portland cement kilning

are good candidates and are briefly explored as markets.

Steel Reheating and Processing.

Steel reheat furnaces commonly found in primary and secondary steel forming may be particularly attractive TAS applications because:

- They have a high per unit heat input and are one of the largest energy users at the four digit standard industrial code level.

- They are a continuous process with a high production throughout.

- There is potential for a high degree of process variability because different product lines require different levels of furnace heat input and because of frequent holds and idle conditions due to delays in the rolling mill or forge lines.

- There is a need for the steel industry to modernize with cost effective technology to remain competitive internationally.

- There is recent industrial history in accepting high technology to solve its problems.

The primary control problem in reheat furnace operation is that the critical process variable, the steel temperature, is not usually directly measured. Recent developments with dual-head in-furnace pyrometers have provided methods to minimize the effect of reflected radiation from the furnace interior. These effects can confound the steel temperature measurement and result in inaccurate readings. However, these are difficult to protect, calibrate and maintain in the operating environment. For large furnace volumes a large number of cost effective sensors is desired to resolve spatial and temporal temperature profiles of the work in process. Commonly used pyrometers will yield only the surface temperature of the steel and will not generally correct for deviations from grey body conditions or reflected radiation.

The traditional control strategy involves selecting furnace zone temperature set points on the basis of operator experience. Under steady production conditions, this methodology can be successful. However, the control problem is exacerbated by variations in heated product size (thickness, width, length), grade of steel, charge temperature, production rate and production delay time. Any supervisory control system must dynamically adjust for variations in

these parameters, each of which have an optimum heating curve within each furnace zone. Compounding the problem are rapid changes in production throughout because of product changes and bottlenecks elsewhere in the production line. Product temperatures in these furnaces are almost always controlled through an inferential measurement of zone combustion gas or wall temperatures which are infrequently calibrated by pyrometry or temperature-instrumented surrogate workpieces. More recently, an attempt has been made to couple the power of computers with real-time furnace heat transfer models.

In 1982, Battelle estimated a potential for 10 percent energy savings from increased throughput in the steel processing industry if internal work temperatures could be measured accurately. Subsequent advances in heat-transfer modeling have increased the potential savings. Much of this work has been conducted in Germany and Japan. In Germany continuous casting speed has been optimized to improve efficiency in aluminum production. In Japan an integrated system has been developed whereby a conduction heat-transfer model is used to optimize billet reheating by controlling furnace temperature as well as firing conditions. However, there is frequently poor correspondence between the model predictions and the billet temperature during the initial transient state. Thus, some combination of modeling and measured boundary (surface) temperature measured by a multisensor system should significantly improve the control of large metal reheating furnaces.

The domestic market for TAS systems for these applications can roughly be scoped in terms of the number of reheat furnaces operating in integrated and mini mills. The Directory of Iron Steel Plants published by the Association of Iron and Steel Engineers has been used as the primary data source:

	Plants	Furnaces
Integrated Plants	181	400
Mini-Medi Mills	95	95
Total	276	495

It is estimated that each integrated facility on average has 2.2 reheat furnaces and each mini-medi facility one reheat furnace. A typical large reheat furnace in a rolling mill could require 16 to 24 sensors configured TAS.

Specialty steel producers typically manufacture forged or cast products and have a large number of smaller reheat and heat treating furnaces. These would require no more than an 8 sensor configured TAS. Numbers of furnaces are difficult to estimate, but probably exceeds the number of reheat furnaces in several hundred facilities. The Western Steel Industry Data Book (1985) lists 73 continuous annealing systems on various coating and heat treating lines which are also potential candidates for TAS systems. Telephone discussions were conducted with the Center for Metal Processing (Gary Walzer), Tamco Steel (Gary Howel), and the Iron and Steel Institute (Bill Dennis and Dave Sampson), all of whom felt a TAS would be beneficial to their operations or industries. Thus, a reasonable market and industrial interest is forecast for continuous steel processing applications.

Glass Conditioning and Forming

Discussions have been held with a number of glass industry end users, equipment manufacturers, and industrial associations, Table 2-7. There was a substantial consensus that a TAS performing to the specification of Table 2-1 would be of significant benefit in the container, pressed and blown segments of the industry. Float glass applications are a potential, but the TAS primary application would probably be in flat glass and in specialty manufacturing requiring the tempering of special shapes.

The glass conditioning, forming, and heat treating processes were described in Section 2.2. The domestic market for TAS systems can be roughly scoped knowing the number of forehearths. About 550 container glass and 100 pressed glass forehearths are estimated. The 650 total excludes fiber glass applications. Each forehearth requires between 18 and 24 sensors, depending on size and temperature sensitivity.

TABLE 2-7. GLASS INDUSTRY CONTACTS

Contact	Organization	Tel	Comments
Mike Mees	Gallo Glass	(209)579-3411	Mfgs. container glass, flint and green forehearth demonstration site
Phil Ross, Div. V.P.	Kerr Glass	(714)557-3770	Mfgs. container glass, heads Industrial Panel for project
Walt Van Saun	Latchford Glass	(213)587-7221	Mfgs. container glass
Frank Bubon	Emhart Glass	(203)688-8551	Mfgs. forehearths and controls, and mold machines
Robert Douglas	Maul Technology	(317)584-2101	Mfgs. mold machines
Richard Wissinger Group Mgr.	Sweldow	(714)893-7531	Mfgs. specialty windows for the aircraft industry
Vern Jensen	Pittsburge Plate	(209)264-4136	Mfgs. plate glass from float process
GB Samuel	BHF Inc.	(419)891-4009	Mfgs. forehearths and controls

Other potential applications include glass tempering and annealing furnaces and mold machines. Of the two, the rotary and forming machines are the more attractive, and could require up to two sensors for each mold and each gob, a total of about 20 to 26 for 8 and 10 section machines. The number of glass annealing furnaces should approximate forehearths, about 650. Since the economic leverage is not high for this application, they probably would not support more than the minimum sized, 8 sensor configured TAS.

Cement Kilns

No attempt was made to quantify the size or receptability of this market. However, it is believed to comprise several hundred installations. Temperature time profiles are critical to clinker formation, but it is unclear as to whether multiple temperature measurements are of benefit.

2.4.2 Projected Market

A market potential for various configurations of TAS was estimated for those industries and processes where a high penetration can be projected, Table 2-8. There are other specialty high value added applications not addressed such as continuous manufacturing lines found in high production consumer goods (automobile and appliance paint lines [16] and the electronics industry, ceramic solid state devices) where temperature/time critical control is also required. The provisional market breaks down by TAS configuration as follows:

- Large Scale Systems, 16-32 sensors, 1795 units
- Small Scale Systems, 8 sensors, 1070 units

TABLE 2-8. PROVISIONAL MARKET ASSESSMENT

Application[1]		Equipment		TAS Config.		
Industry	Process	Temperature Range, °F	Units	# Sensors	#λ	Note
Steel	Reheat-Mill	70-2200	495	16-24	3-4	2
Steel	Reheat-Forge	70-2400	500	8	3	2
Steel	Annealing	70-1400	70	8	3	2
Glass	Forehearth	2000-2400	650	16-24	4	3
Glass	IS Mold	1000-2000	650	16-32	3-4	3
Glass	Anneal/Temper	800-1200	500	8	3-4	3
Cement	Kiln	2200-3500	-	8	2-3	2

Notes:

1, Continuous, high production, large equipment volumes or lengths.
2, Instrument corrects for reflection and/or departures from grey body.
3, Instrument measures glass radiance at different depths.

3.0 PRELIMINARY DESIGN AND DEVELOPMENT

Within the context of the Task 1 Assessment conclusion a review of the existing moisture analyzer system (MAS) technology base, a two-color near IR fiber optics based reflective spectrometer, was performed. The objective was to identify modifications required in the critical optical and electro-optic components and firmware to achieve the performance objectives of the TAS functional specification, Table 2-1. This design was also used to:

- develop capital cost estimates to support a system economic evaluation, Task 5
- initiate the detailed design of a preprototype, optical and electronic components within a breadboarded instrument system to perform proof of principle bench tests, Task 4.

3.1 Approach

A number of design activities and their interfaces with the then leading MAS instrument development program, were implemented to support various program work elements, Figure 3-1. The TAS instrument design is sufficiently flexible to implement the following:

- Brewster's angle (wavelength polarized) for reflectance free subsurface and surface temperature measurements
- Normal angle, multiwavelength for melt temperature profiling
- Multiplexing of 8 sensor positions per optical bench, up to 3 optical benches per chassis
- In-situ black body calibration
- Data acquisition and storage (DAS) for off line data analysis

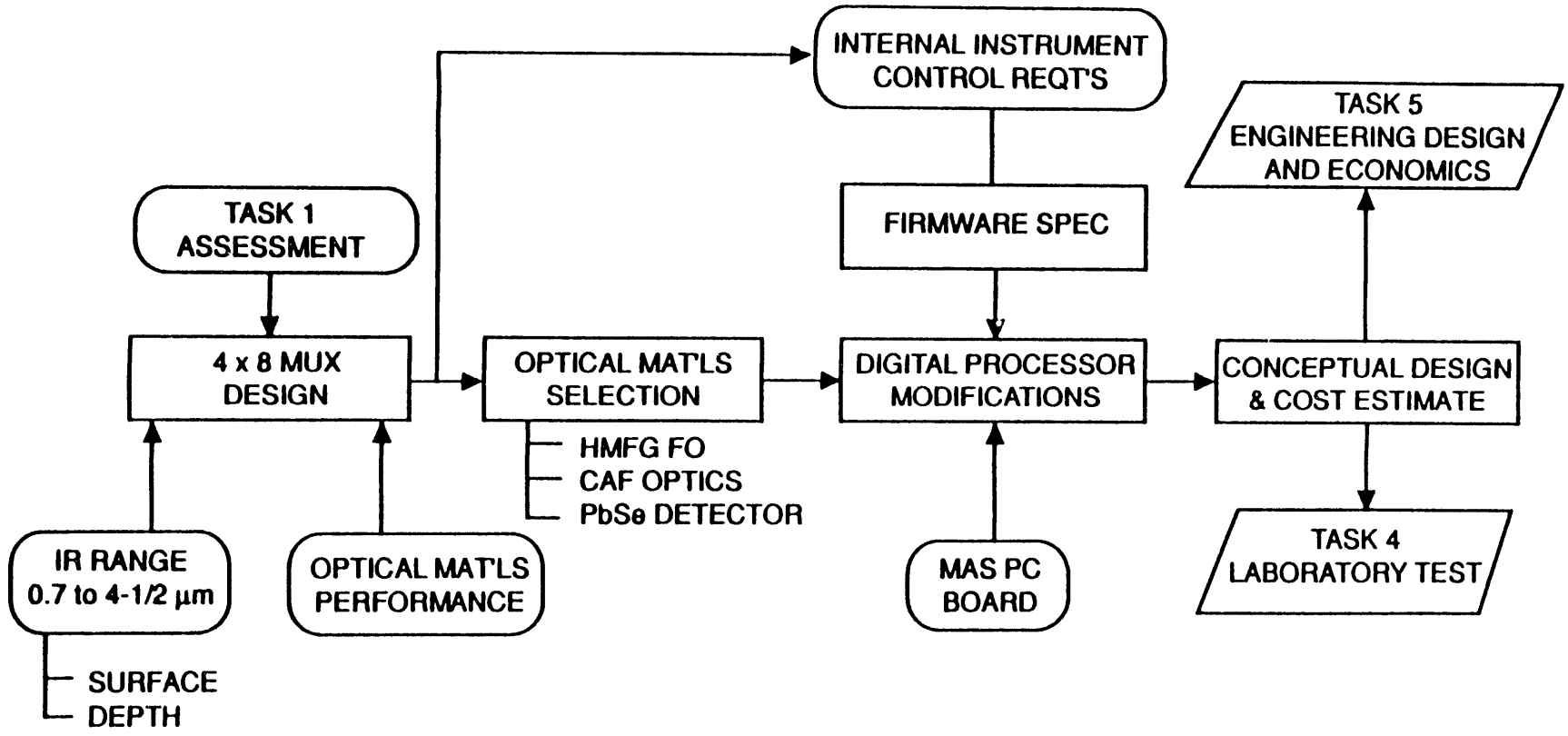

Figure 3-1. Task 2, sensor development and preliminary design plan.

Matching these functions to the MAS capabilities identified a number of areas of significant commonality including the compatibility with the basic optically multiplexing concept and generic compatibility with internal instrument control functions such as:

- standard bus digital architecture
- internal power supplies for electronic components
- detector thermal control with Peltier (thermo-electric) cooling
- data synchronization, A/D conversion, and memory mapping

However, the then existing MAS required the following functional modifications:

- Change from a two to four wavelength (band pass filter) instrument
- Broaden the IR processing range from 0.7 to 2.1 to 0.7 to 4-1/2 μm
- Decrease primary sensor (optical telescope) diameter from 4" to 1" diameter
- Increase the capacity and execution speed of the microprocessor

3.2 Preliminary Design

The following major MAS component design changes were implemented to accommodate the TAS measurement methods:

- The optical MUX was increased in size to accommodate two additional filters on the mask, Figure 3-2, and the detector spectral response improved (lead selenide) to obtain a broad IR range.

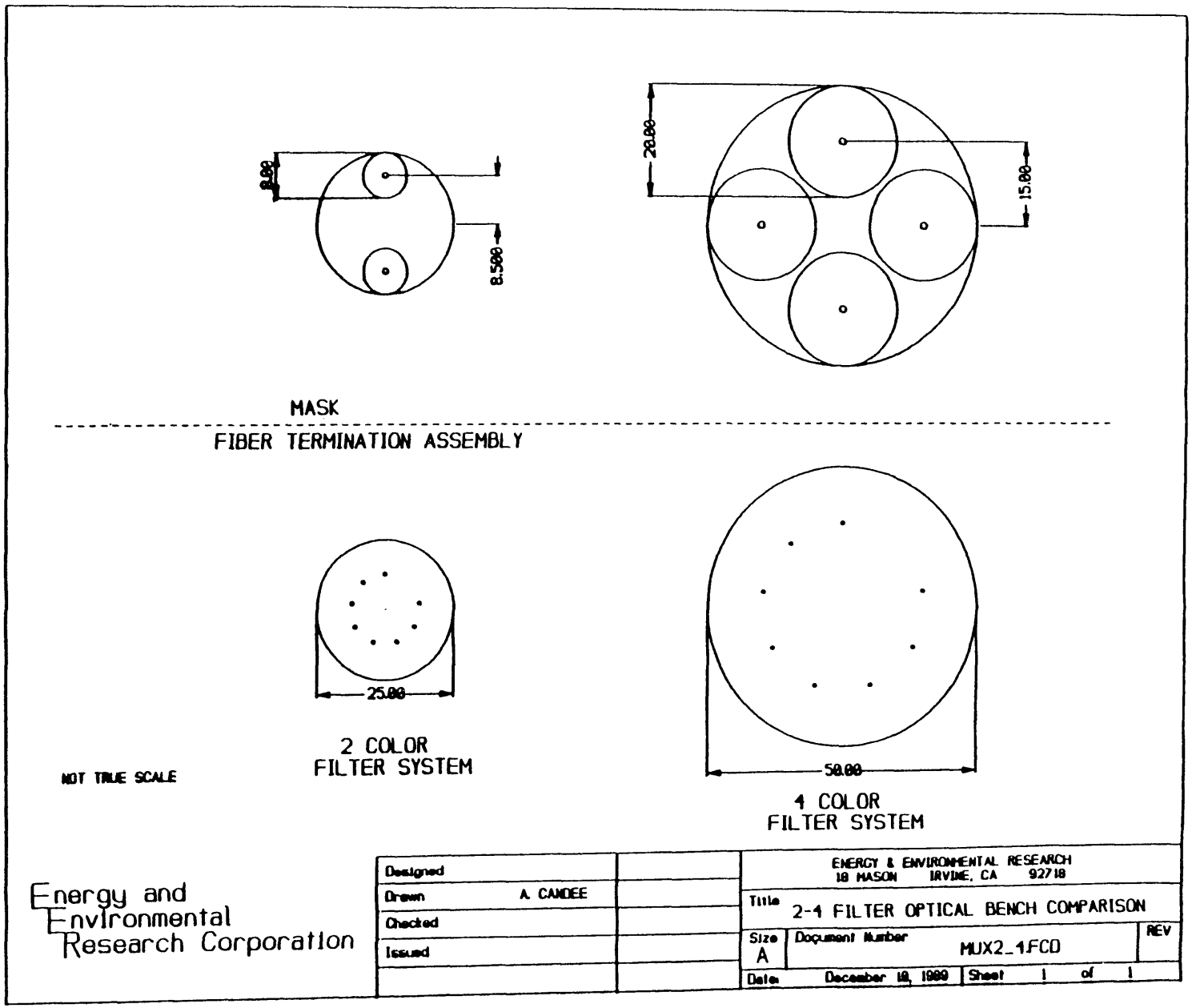
20.00
15.00
8.500
MASK
FIBER TERMINATION ASSEMBLY
25.00
2 COLOR
FILTER SYSTEM
50.00
4 COLOR
FILTER SYSTEM
NOT TRUE SCALE
Energy and
Environmental
Research Corporation
Designed
Drawn A. CANDEE
Checked
Issued
ENERGY & ENVIRONMENTAL RESEARCH
18 MASON IRVINE, CA 92718
Title 2-4 FILTER OPTICAL BENCH COMPARISON
Size A
Document Number MUX2_4.FCD
REV
Date December 18, 1989
Sheet 1 of 1

Figure 3-2.

- The MUX optical materials were changed from crown glass to calcium fluoride and an additional lens was added to reduce chromatic aberrations over the increased IR wavelength range, Figure 3-3.

- The transmitting fibers were changed from high purity silica to heavy metal fluoride, Figure 3-4.

- Firmware modifications were implemented to synchronize and store 8 digitized sensor measurements.

- An off axis parabolic mirror was selected to focus collected light into the optical fiber, Figure 3-5.

design, Figures 3-6 and 3-7, is comprised of five major subsystems:

- the sensing head, which gathers emitted and reflected optical radiation, and if appropriate transmits reference signals to or from the process environment. This communicates broad band spectral data over optical fibers to a remote, multiplexed photo spectrometer

- an optical bench for spectral and temporal processing of the sensor broad band spectra to wavelength, time and channel resolved electrical pulses, Figure 3-8.

- an electronic printed circuit board which digitizes and decodes electrical pulses, and outputs to a standard bus.

- an electronic printed circuit board for distributing power to the optical MUX (brushless motor) and standard bus chassis.

- a purchased standard bus compatible central processing unit (CPU), EER firmware programmed, which provides control functions to the instrument components, acquires and analyzes data, and interfaces with various output devices (RS232, CRT, etc.)

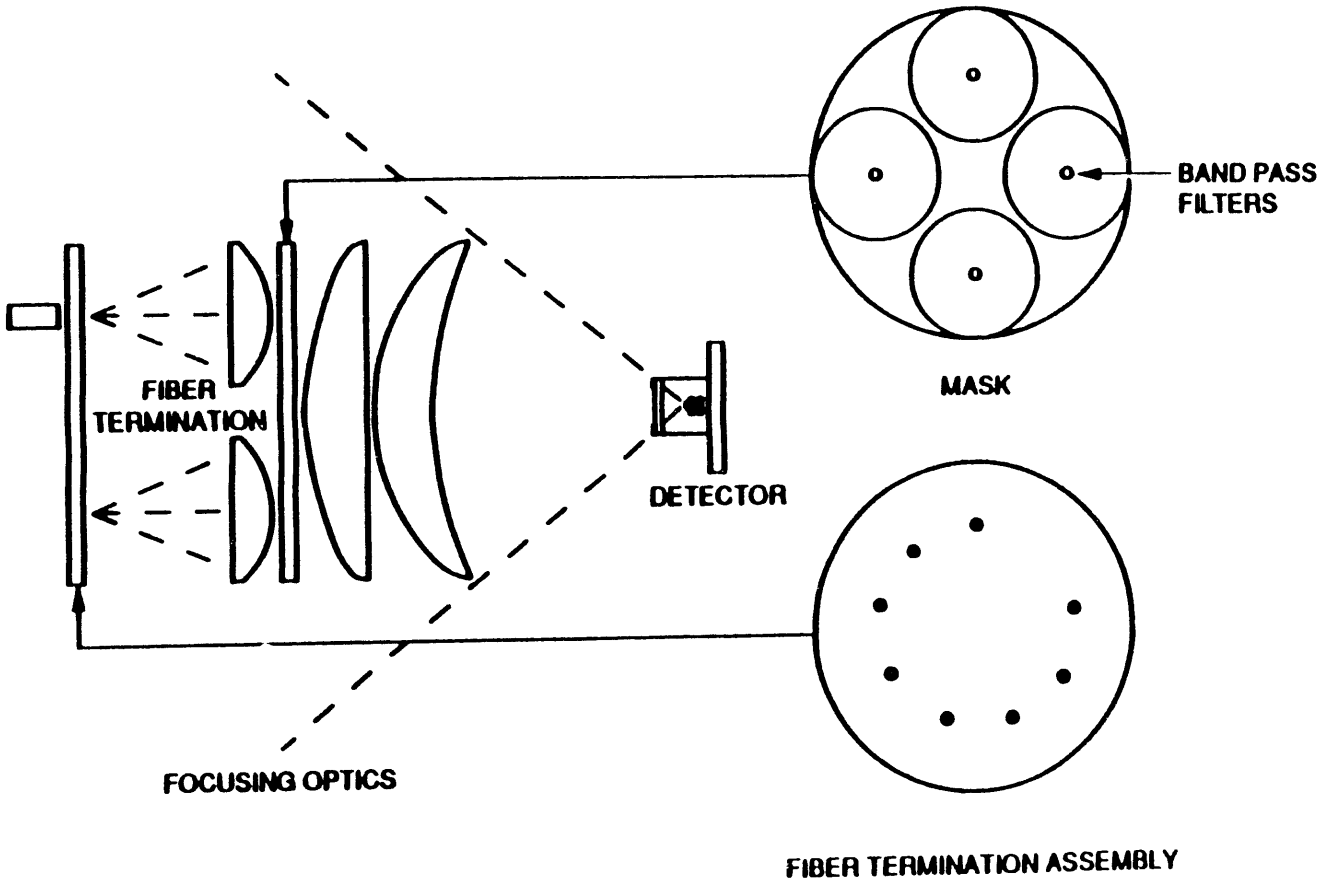
BAND PASS
FILTERS
MASK
FIBER
TERMINATION
DETECTOR
FOCUSING OPTICS
FIBER TERMINATION ASSEMBLY
NOT TRUE SCALE

Figure 3-3.

INFRARED
FIBER
SYSTEMS, INC.
2301-A Broadbirch Drive • Silver Spring, MD 20904 • (301) 622-9546
FAX (301) 622-7135

FIBER TECHNICAL SPECIFICATIONS

- Fiber diameters available range from 50 to 650 microns clad o.d., with the core diameter typically 80% of this.
- Fiber N.A. from .1 to .2 (glass clad) and .6 (plastic clad).
- Bend radius: ~8 mm for a 200 micron diameter fiber.
- Coating: u.v. acrylate

Fiber loss shown below (glass clad) is reproducible over long lengths (greater than 100 meters). Upon request, lower loss is possible using purer raw materials; please call for our latest results.

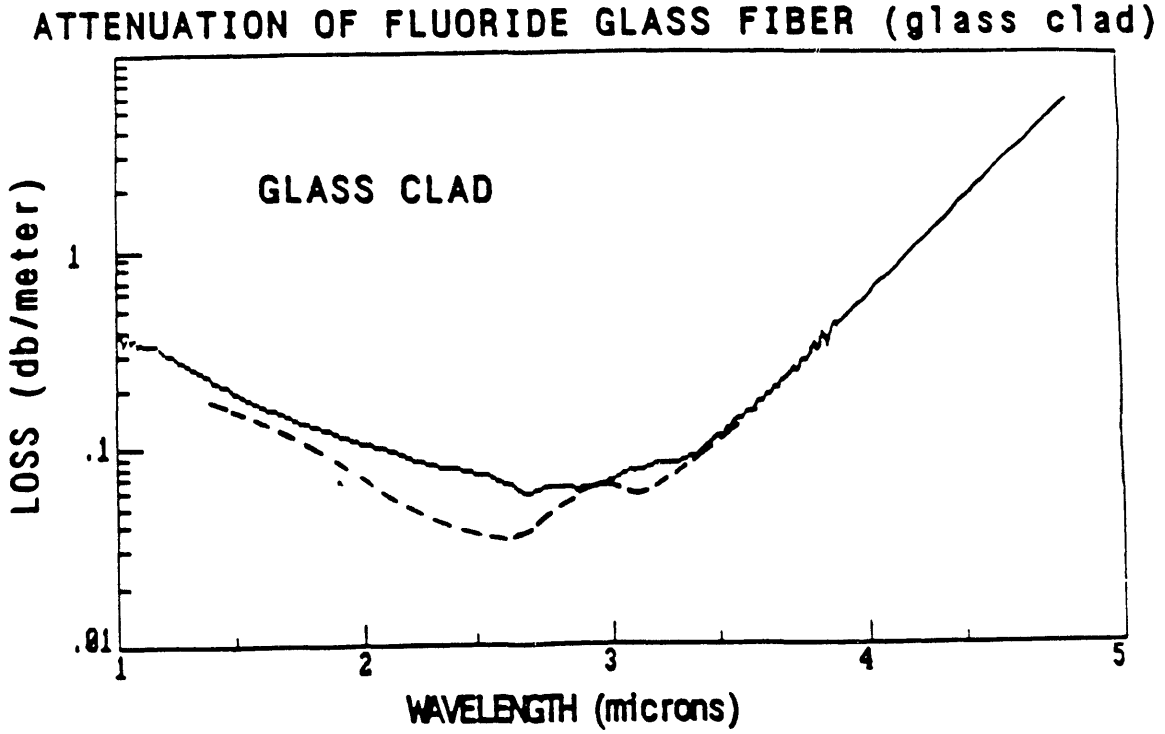

Solid line indicates attenuation obtained with reagent-grade materials. Lower attentuation can be obtained using purer raw materials (broken line).

5/17/88

Figure 3-4. Fluoride fiber specification.

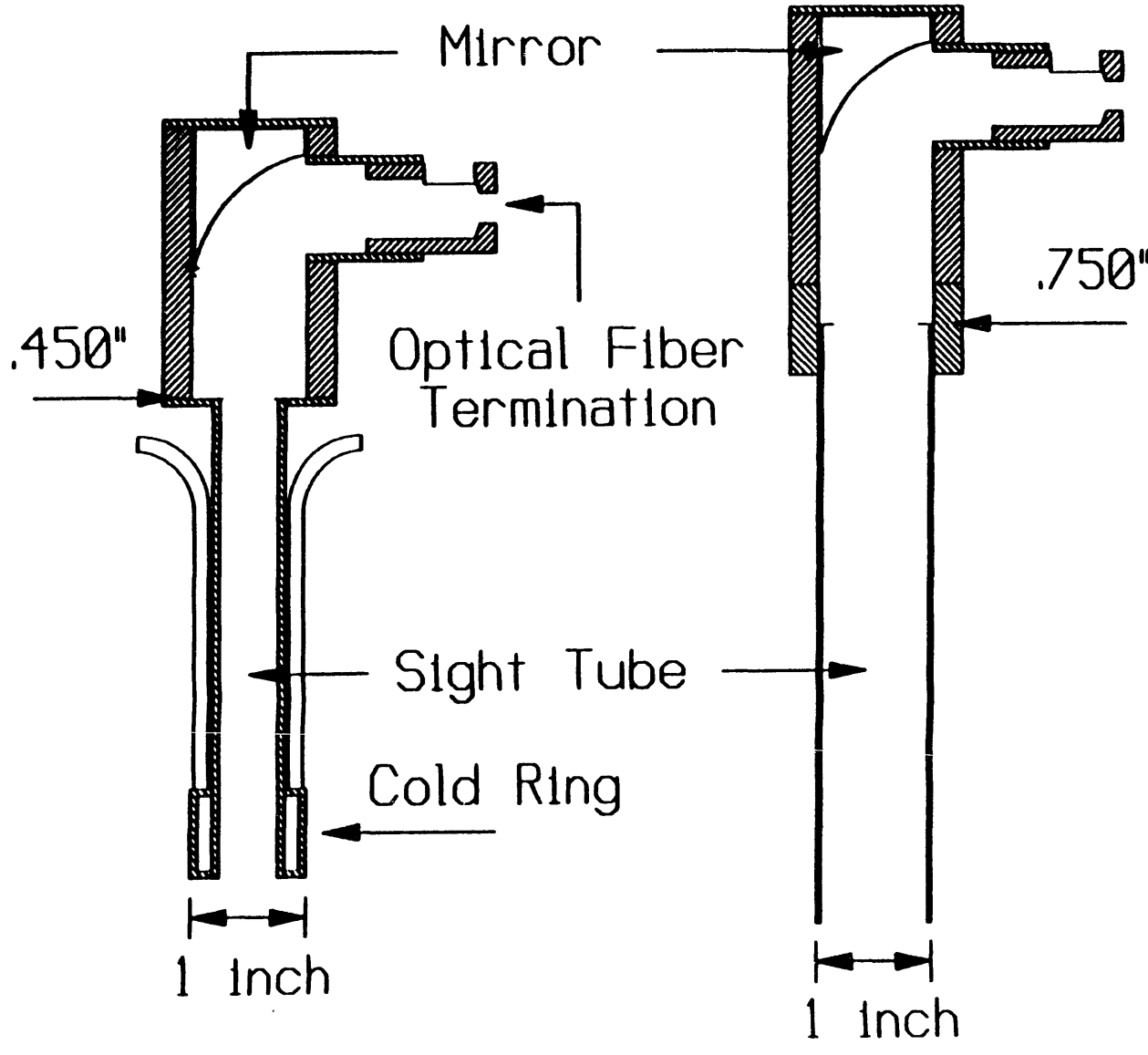

Figure 3-5. Temperature analyzer sensors.

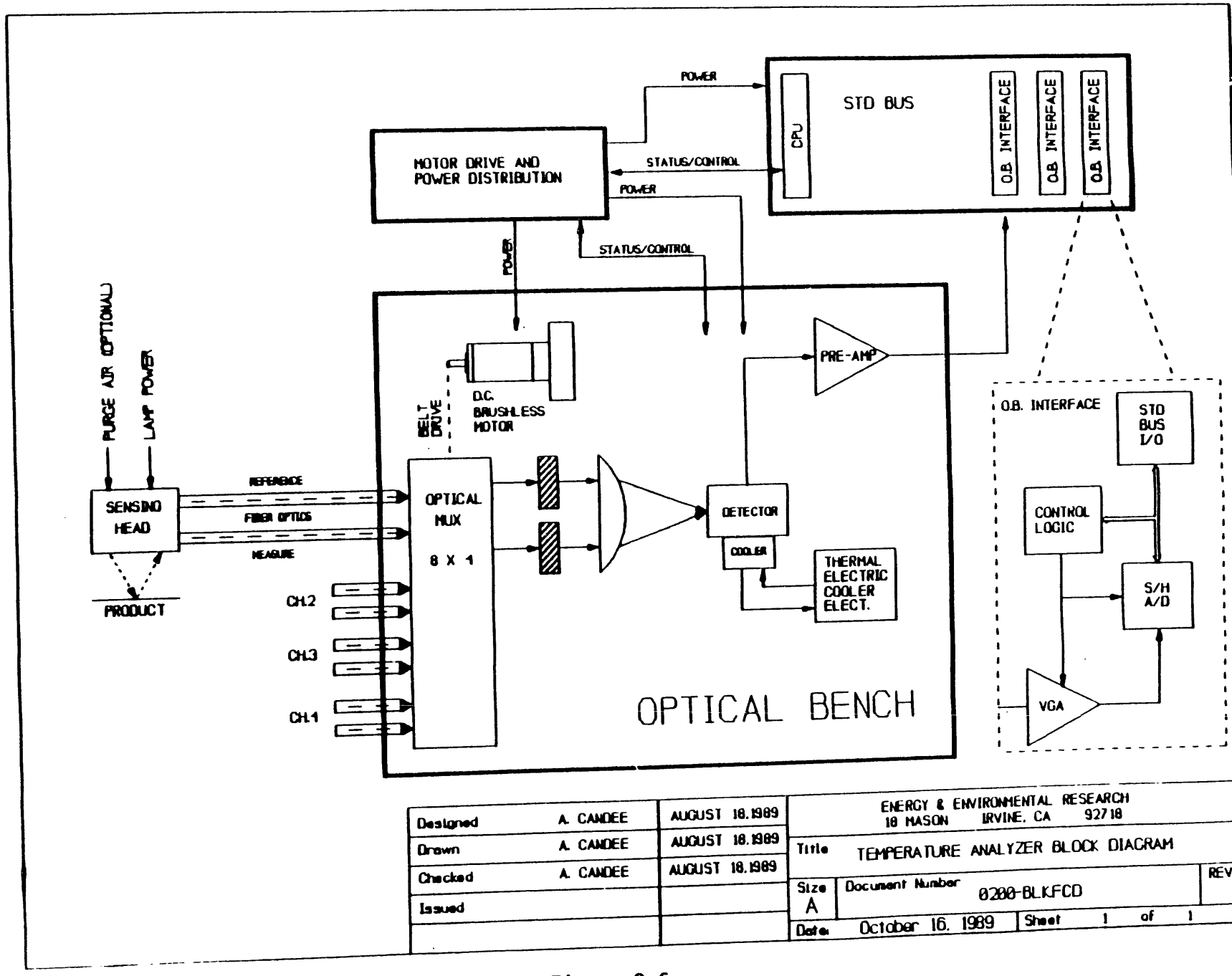
POWER
STD BUS
CPU
O.B. INTERFACE
O.B. INTERFACE
O.B. INTERFACE
MOTOR DRIVE AND
POWER DISTRIBUTION
STATUS/CONTROL
POWER
POWER
STATUS/CONTROL
PURGE AIR (OPTIONAL)
LAMP POWER
BELT DRIVE
D.C. BRUSHLESS MOTOR
PRE-AMP
O.B. INTERFACE
STD BUS I/O
CONTROL LOGIC
S/H A/D
VGA
REFERENCE
FIBER OPTICS
MEASURE
SENSING HEAD
PRODUCT
OPTICAL MUX
8 X 1
CH.2
CH.3
CH.1
DETECTOR
COOLER
THERMAL ELECTRIC COOLER ELECT.
OPTICAL BENCH
Designed A. CANDEE AUGUST 18.1989
Drawn A. CANDEE AUGUST 18.1989
Checked A. CANDEE AUGUST 18.1989
Issued
ENERGY & ENVIRONMENTAL RESEARCH
18 MASON IRVINE, CA 92718
Title TEMPERATURE ANALYZER BLOCK DIAGRAM
Size A
Document Number 0200-BLKFCD
REV
Date October 16. 1989
Sheet 1 of 1

Figure 3-6.

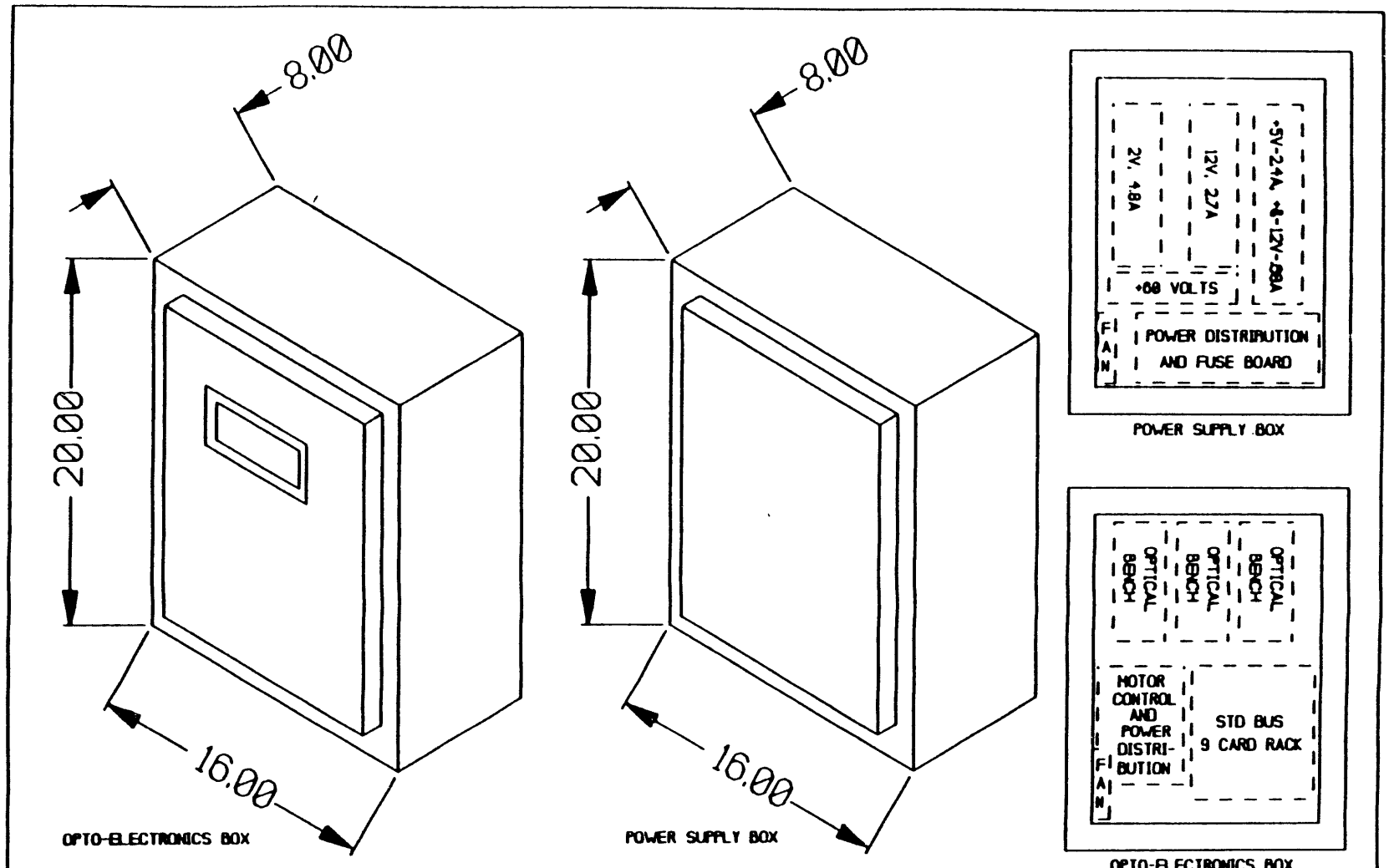
8.00
20.00
16.00
OPTO-ELECTRONICS BOX
8.00
20.00
16.00
POWER SUPPLY BOX
2V, 4.8A
12V, 2.7A
+5V-24A, +&-12V-08A
+08 VOLTS
FAN
POWER DISTRIBUTION AND FUSE BOARD
POWER SUPPLY BOX
OPTICAL BENCH
OPTICAL BENCH
OPTICAL BENCH
MOTOR CONTROL AND POWER DISTRI-BUTION
FAN
STD BUS 9 CARD RACK
OPTO-ELECTRONICS BOX
Energy and Environmental Research Corporation
Designed A. CANDEE JUNE 27, 1989
Drawn A. CANDEE JUNE 27, 1989
Checked A. CANDEE
Issued
ENERGY & ENVIRONMENTAL RESEARCH
16 MASON IRVINE, CA 92718
Title TEMPERATURE ANALYZER - GLASS SENSOR
NEMA 4 PACKAGE
Size A
Document Number GSPACK1FCD
REV
Date October 16, 1989
Sheet 1 of 1

Figure 3-7.

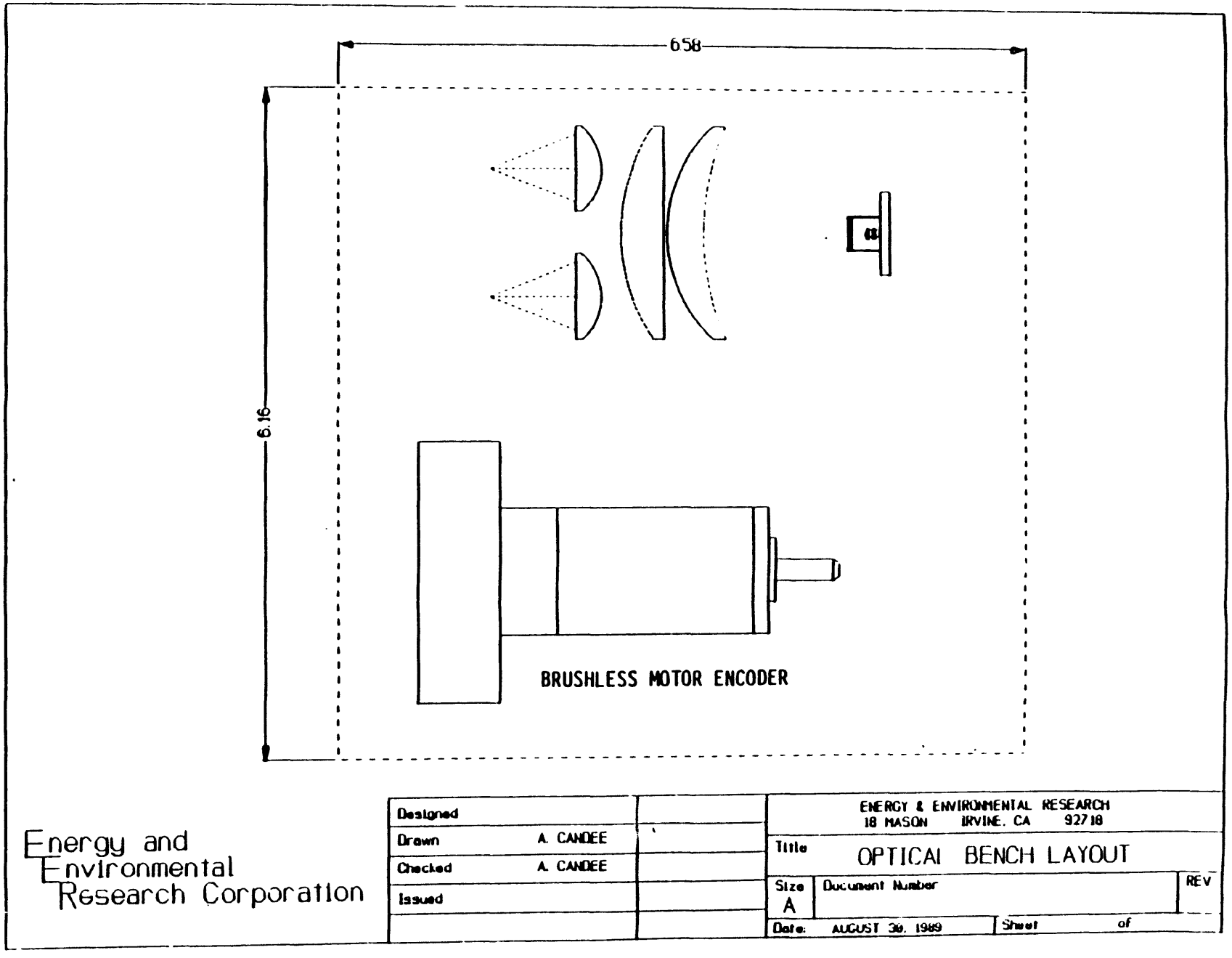
6.58
6.16
BRUSHLESS MOTOR ENCODER
Energy and
Environmental
Research Corporation
Designed
Drawn A. CANDEE
Checked A. CANDEE
Issued
ENERGY & ENVIRONMENTAL RESEARCH
18 MASON IRVINE. CA 92718
Title OPTICAL BENCH LAYOUT
Size A
Document Number
REV
Date: AUGUST 30. 1989
Sheet of

Figure 3-8.

On the basis of these changes critical breadboard development hardware was first constructed for subsystem testing (fit and function). Fabricated hardware addressed those components which are not sensitive to the measurement method, e.g. optical and electro-optical components, and digital signal processing electronics.

3.3 Component Description

Most of the hardware as previously described are modifications or derivatives of an earlier Moisture Analyzer System development and demonstration program.

Optical Multiplexer

A detailed design of an optical multiplexer capable of wavelength (4) and 8 channel (sensor) processing through a common, remote signal processing system has been completed. The design consists of focusing optics, Figure 3-3, mounted on a rotating hub which positions each of four optical band pass (wavelength) filters in front of a stationary fiber optic cable (8) termination assembly. The optical lens configurations (compound) and materials (CaF) have been selected to provide low light loss and good chromatic focusing (low aberration) over the operating wavelength (0.7 to 4-1/2 μm). The four chopped optical signals are serially focused on a common photodetector (PbSe) for each optical fiber (sensor) channel. The hub (up to three) is driven by a common brushless DC motor with a chain belt, Figure 3-8, connecting drive sprockets. Butyl "O" rings in compression hold the assembly together and a guide key and selective parts tolerances assure proper alignment. The optical MUX is mounted to an optical bench (frame) which also contains provisions for mounting the detector/preamp printed circuit card. The printed circuit board also contains a temperature control circuit for maintaining detector temperature to close tolerances (±.1°F) using a two stage thermo-electric cooler (reverse thermocouple) to improve sensitivity.

Electronics

The optical bench interface card (a standard EER proprietary component) amplifies and digitizes the pulsed detector (electro-optical transducer) electrical analog output signal. The input card is a four layer board and also contains back plane connections for communicating with the "standard" data bus and the position encoder on the motor. The position encoder information is used to identify the pulsed signals generated by the optical bench. The EER proprietary motor control card provides power and speed control for the motor. It also distributes other status and control signals not handled by the STD bus. It is a two-layer board. A standard bus computer architecture is used to digitally communicate, store and process data, Figure 3-9.

Optical Sensor and Cabling

The bulk emitted radiation from the melt is collected in focusing optics and transmitted via fiber optic cable to the remote multiplexer. The use of an off axis, parabolic mirror insures high light collection efficiency over a very broad spectral range with a very small acceptance angle, Figure 3-5. The mirror can be axially positioned within the sight tube for fine alignment. The optical fiber is the least efficient of all the optical components. A heavy metal fluoride fiber, glass clad, 500 μm id, in armored cable, Figure 3-4, was selected after an exhaustive search. Two 10 m lengths were purchased. Maximum attenuation is 1 db/m over the intended operating range.

3.4 Breadboard Tests

The engineering design of several components and subassemblies required verification testing with breadboard mock-ups prior to being implemented in a final design. The breadboard tests were designed to prove functionality or determine operational parameters of one or a series of integrated components. Two basic subsystems were breadboarded and tested. The optical (path) system transmits light from the emitting source to the detector, and the black body calibration source.

CPU-188
80188 Single Board Computer

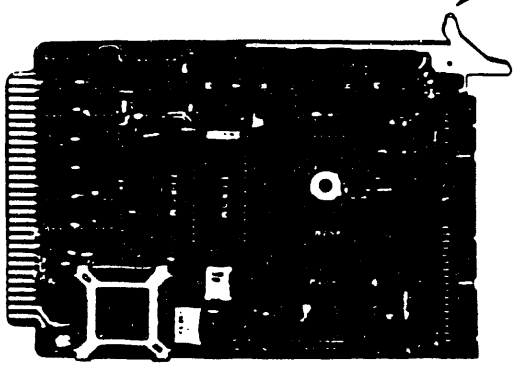

Description

The CPU-188 single board computer features a 16-bit processor, serial communications, and software configurable PIO and event counters. It is designed to combine and maximize the strengths of the STD Bus and MS-DOS software. The STD Bus offers a wide range of low cost industrial I/O hardware. MS-DOS compatibility provides state-of-the-art software development tools.

The CPU-188 provides all the functions needed for most industrial applications: a 16-bit 80188 processor, up to 1M of DRAM, up to 128k of EPROM, two RS-232 serial communications channels, 28 parallel I/O lines, six 16-bit event counters, an SBX connector, and a watch-dog timer. The 80188 processor provides object code compatibility with MS-DOS-based application software, while maintaining compatibility with the standard 8-bit STD Bus memory and I/O peripherals. One of the two serial channels may be configured for RS-232 serial communications or RS-485 multi-drop communications. The 50-pin PIO connector is directly compatible with a 24-channel solid state relay rack. Up to six of the PIO lines may be software configured to be event- counter inputs.

With all these on-board functions, fewer boards are needed for the system, thus lowering system costs. In fact, for many applications, the CPU-188 can be used as a single board computer outside the STD Bus environment. Expansion can be handled by using the SBX connector or by going to the STD Bus.

Features

- 16-bit internal 8-bit external architecture
- 8088 code capability
- 8 or 10 MHz operation
- 64k, 256k or 1M of DRAM
- Up to 128k EPROM
- Two serial communication ports, one configurable for RS-485 multi-drop
- 28 parallel I/O lines
- Six 16-bit event counters or timers
- One DMA channel
- STD Bus interface with Z80 peripheral compatibility
- Industry standard SBX interface
- Watch-dog timer
- Optional battery-backed real-time clock/calendar
- Optional math co-processor

Software Development

Computer Dynamics' software tools provide an ideal environment for developing ROM-based systems. Your application software may be written and compiled, using a variety of languages, under MS-DOS or PC-DOS. Your development system is a standard PC compatible with a serial connection to the actual target system. Source level debugging in the actual target hardware is done with Remote DSD. Computer Dynamics' ROM Tools package helps you to easily move your final application program from diskette to EPROM. See page 4 for a complete description of software development tools for embedded applications.

As the heart of Computer Dynamics' DOS-188 system, the CPU-188 provides an MS-DOS-compatible, disk-based environment as an alternative for software development. See page 23 for a description of the DOS-188 system.

STD Bus Memory and I/O Addressing

The CPU-188 supports up to 128k of STD Bus memory using MEMEX. The full memory addressing capabilities of the 80188 processor (1M) are utilized on board, but under program control, the 128k of STD Bus memory can be mapped in. This allows battery-backed RAM or EPROM to be resident on the STD Bus and fully accessible by the CPU-188.

The CPU-188 STD Bus I/O interface emulates the Z80 and will access any of the 512 port locations on the STD Bus using the lower 8 address lines and IOEXP. Up to three wait states can be programmed for STD Bus accesses.

A Z80-compatible interrupt structure is provided. The STD Bus timing is compatible with Z80 peripherals and can support mode 2 interrupts directly.

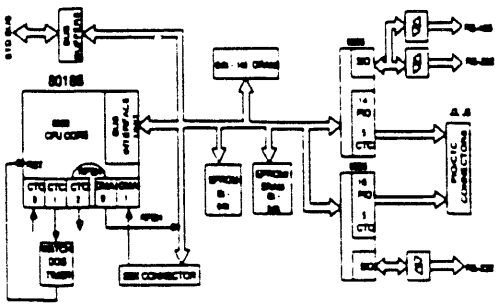

Computer DYNAMICS 107 South Main Street, Greer, SC 29650
Phone: (803) 877-8700 FAX: (803) 879-2090

Figure 3-9. Standard bus central processing unit and auxiliaries.

CPU-188

80188 Single Board Computer

Specifications

CPU	
• Type	8088 compatible (80188)
• Oscillator	16 or 20 MHz crystal
• CPU speed	8 or 10 MHz
• External wait state	STD Bus or SBX generated
• Programmed wait states for any memory or I/O access	375 ns max at 8 MHz
Memory, On-board	
• DRAM	Dynamic 1 bit x 1 page mode
-- Capacity	64k/256k/1M
-- Minimum access time	120 ns
• SRAM/EPROM/EEPROM	CMOS or NMOS, JF standard
-- Capacity	8k minimum (two devices) 128k maximum (two 64k devices)
-- Speed	250 ns
Memory, Off-board	
• RAM type	Static
• Capacity	128k (using MEMEX)
• Minimum access time	Z80 type timing 8 MHz no wait states - 125 ns 3 wait states - 500 ns
Watch-Dog Timer	
• Software selectable enable and refresh rate	1s max @ 8 MHz
Serial I/O	
• Serial communications channels	Two
• Communications device	8256 MUART
• Interface	Two at RS-232 async -or- One at RS-232 async One at RS-485 async
• Baud rates	50 to 19.2k
Parallel I/O - CTC	
• Interface bit count	28 lines (cable compatible for 24-channel solid state relay rack)
• CTC	Six 16-bit event counters or timers
SBX	
• Small Bus eXpansion	Intel Multibus iSBX IEEE P959
• Compatibility	Single width (meets STD Bus size)
• Size	Double width (outside cage)
• Clock	10.24 MHz
STD Bus Interface	
• Address lines	16
• Data lines	Eight
• Memory addressing	128k (using A17 as MEMEX), up to 3 programmable wait states
• I/O addressing	512 ports (using A9 as IOEXP), up to 3 programmable wait states
• Timing and interrupt type	Z80 emulation
• DMA	1 channel
Typical Power Requirements	+5 Vdc @ 1.37A +12Vdc @ 30 mA -12Vdc @ 30 mA

RS-485 Multi-drop Communications

Communications with remote STD Bus systems are made possible by the RS-485 multi-drop capability of the CPU-188. Serial channel A is supplied with an RS-485 interface in addition to the RS-232 interface.

RS-485 is a twisted wire pair, 32-node multi-drop EIA standard communication interface that allows data transmissions up to 4000 feet. With this interface, asynchronous bit rates of up to 19.2k bps are possible. Up to 32 CPU-188s in different locations may be interconnected on a single twisted wire pair. One CPU-188 may be connected to the low speed RS-485 network, while the user accesses higher speed networks such as BITBUS, CHEAPERNET or STARLAN through the SBX interface. Please consult the factory for SBX interfaces and software services.

Ordering Information

- CPU-188-8-64 – 8 MHz, 64k DRAM fixed
- CPU-188-8-256 – 8 MHz, 256k DRAM fixed
- CPU-188-8-1M – 8 MHz, 1M DRAM fixed
- CPU-188-x-x-CMOS – Low power option
- CPU-188-MATHCO – 8087 math co-processor
- 10 MHz versions available in all above memory configurations
- CPU-188-DSD – Remote dynamic symbolic debugger for CPU-188 target system and IBM PC host; includes debugger/monitor PROM and PC cable
- ROM Tools – MS-DOS-based ROM conversion utilities
- CPU-188-DSDS – CPU-188 monitor, debugger/monitor PROM (included with CPU-188 DSD)

Computer DYNAMICS 107 South Main Street, Greer, SC 29650
Phone: (803) 877-8700 FAX: (803) 879-2030

Figure 3-9. Standard bus central processing unit and auxiliaries. (Continued)

Optical System Tests

The primary objective of this test was to determine the appropriate diameter for the fluoride fiber to be used in the testing outlined in Task 4. The tests also served to shakedown all the optical components and confirm the theoretical predictions of power transmission levels for the optical sensor system.

A miniature tube furnace with a cavity temperature similar to that of the box test furnace was set-up as a radiation source for the measurements. An optical system was assembled to collect radiation into a 450 micron fluoride fiber and transmit it to the optical bench optics and PbSe detector. Both broad band and narrow band measurements were made. The broad band measurements were made with a Scientech radiometer for reference purposes and the narrow band measurements were made using a PbSe detector. The narrowband measurements were designed to indicate whether or not a smaller fiber diameter could be used to lower fabrication costs.

The theoretical prediction of the power received at the detector was made by first predicting the power incident on the fiber end. This was done by calculating the irradiance of the source and then estimating the solid angle, or collection efficiency, of the sensor optics. The test was conducted using a narrow band pass filter with a 33 nanometer band width centered at 3.5 microns. Using a 1800°F source, the power received at the fiber was predicted to be 7.8 microvolts. The optical system, including the 1 meter fiber, was calculated to have a total transmittance of 40% which reduced the power at the detector to 3.1 microvolts. The chopped signal output of the detector was measured in peak to peak volts and displayed on an oscilloscope screen. Given the literature value of the detector responsivity and the amplifier gain the theoretical prediction of detector output was 4.1 volts.

The breadboard tests of the optical system showed a mean repeatable detector output of 1.4 volts with a signal to noise ratio of about 30. Though the comparison of experiment to theory shows a 65% shortfall, the test was highly

successful considering uncertainties in the detector responsivity and the inability to compensate for unknown optical misalignment problems. The results of the optical system breadboard test indicated the filter band widths should be increased to 100 to 200 nm in order to improve the signal level, and the fiber core diameters should be kept at 450 microns to insure good signal throughput.

Calibration Source Tests

Several on-line concepts for calibration sources were designed, assembled and tested for functionality. The most difficult aspect was to find a design that would heat up rapidly and have a very uniform and high surface temperature. The above conditions are somewhat mutually exclusive, a rapidly heatable surface with sufficient surface area to extend beyond the sensor field of view also losses heat rapidly. The surface temperature of the source should be at least 600°C in order to maintain sufficient calibration accuracy.

The first cal-source element considered was a small 1-1/2" square with a grooved surface. Literature showed this design is frequently used as a secondary standard for black bodies and it appeared to have potential for implementation as an on-line calibrator. The element was fabricated out of nichrome wire and a castable refractory and molded with a cross hatched surface. Applying current to the element showed it was capable of reaching the desired temperature, but it was visually obvious that the surface was far from isothermal. This design was immediately dropped from consideration.

The second design simulated a commercial black body source. This source had a conical cavity 1" in diameter and 5" deep. It was wrapped with heating element wire and heavily insulated. Testing with this element showed it performed better than the first, but was still unacceptably nonisothermal.

Failure of the first two designs indicated that further testing of potential on-line designs would delay the test program and an easy alternative should be expedited. A black body element was molded using silicon carbide castable refractory. The shape used was a conical cavity which according to

theory had an emissivity of about .99, which is sufficient for the accuracy requirements of the test program. This black body was placed in the furnace and suitably temperature instrumented. Its use is described in more detail in Section 3.5.3.

3.5 Model Development

Several mathematical and conceptual (physical) models were developed to predict and describe the physical phenomena associated with making noncontact temperature measurements of a glass melt. In this section the most important and extensive models developed for this program are described. They have been used to perform parametric, sensitivity studies to define theoretical measurement resolution and to deconvolute multicolor radiance measurements to yield melt temperature profiles.

3.5.1 Glass Radiative Transfer Model

The literature recognizes that optical pyrometry measurements can be used to extract an approximate average temperature to a given depth in a glass melt by appropriate selection of wavelength. In the present approach, a simultaneous evaluation of a number of wavelengths is used to develop a more rigorous means of constructing a temperature vs. depth profile.

Viskanta [12, 14] developed the general radiative transfer equation for a glass melt of finite thickness whose upper face is exposed to an atmosphere and whose lower face is bounded by an opaque solid. Viskanta developed a number of simplified versions of the equation which are appropriate for special cases, but not for this proposed application.

Differences include:

- The glass layer is sufficiently thick (top to bottom surface) such that multiple internal reflection are not important. (Note that IR wavelengths can always be selected to satisfy this assumption.)

- In spite of the fact the glass is optically thick relative to the back wall, a thermal gradient exists within the glass.

The implications of these assumptions on Viskanta's general equation are that the terms for the external radiance, the underlying media, and the reflections and interreflections of the bottom (2nd) interface can be ignored. Hence the general equation reduces to the following:

$$N_\upsilon^+(0,\mu) = [1-\rho_{1\upsilon}(\mu)]\,[\frac{n_{0\upsilon}}{n_\upsilon}]^2 \int_0^L n_\upsilon^2 N_{b\upsilon}(y)\, e^{-\tau_\upsilon(y)/\mu} K_\upsilon \frac{dy}{\mu}$$

The following terms appear in the equation:

$N_\upsilon^+(0,\mu)$ = emissions at wavelength leaving surface of the glass into the atmosphere at directional cosine μ

$\rho_{1\upsilon}(\mu)$ = directional reflectivity of interface 1

μ = direction cosine within glass

n_υ = refractive index of glass

$n_{0\upsilon}$ = refractive index of media over glass (air)

$N_{b\upsilon}(T)$ = spectral radiance of a black body at temp T. given by Planck's law

K_υ = spectral absorbtion coefficient

τ_υ = optical thickness

$[1-\rho_{1\upsilon}(\mu)]$ = directional transmissivity of interface 1

Viskanta indicated that the temperature dependent nature of this equation can be more readily shown by integrating by parts and noting that

$$d[n_\nu^2 N_{b\nu}(y)] = \{\frac{d[n_\nu^2 N_{b\nu}(T)}{dT}\}(\frac{dT}{dy})\,dy$$

After evaluating the integral we find that the general solution for the temperature and depth dependent Radiative Transfer Equation becomes

$$N_\nu^+(o,\mu) = [1-\rho_{1\nu}(\mu)](\frac{n_{o\nu}}{n_\nu})^2\{n_\nu^2 N_{b\nu}(T)\,[1-e^{-\tau_{L\nu}/\mu}] + \int_0^L \frac{d[n_\nu^2 N_{b\nu}(T)}{dT}(\frac{dT}{dy})\,e^{-\tau_\nu}$$

By varying wavelength, this equation can form the basis for the development of a depth vs. temperature characteristic. Closed form solutions are available for the isothermal case, in which the equation reduces to Planck's equation modified by an emissivity, and for the case of a linear temperature profile. The latter is reproduced here:

$$N_\nu^+(0,\mu) = [1-\rho_{1\nu}(\nu)](\frac{n_{o\nu}}{n_\nu})^2[1-e^{-\tau_{L\nu}/\mu}]\{n_\nu^2 N_{b\nu}(T)\,[1+\frac{(dT/dy)\,c_2 e^{c_2/\lambda T}}{\kappa_\nu \lambda T^2(e^{c_2/\lambda T}-1)}]\}$$

where $C_1 = 1.175 \times 10^{-11}$ W cm^2

$C_2 = 1.4388$ cm °K

Glass transmissivity ($\tau_{L\nu}$) varies substantially with wavelength in the infrared. Thus, at long wavelengths the glass will behave as an opaque medium. At other wavelengths, considerable radiation from within the glass will be detected at the surface. By judicious selection of several wavelengths, optical

pyrometry can be used to develop a temperature vs. depth characteristic for a glass melt.

3.5.2 Theoretical Sensitivity Studies

The technique of measuring the temperature distribution was described in Section 3.2. The characteristics of Window glass will be used as an example to quantitatively illustrate the detection technique and its gradient resolution using wavelengths from 2.4 to 4.0μm.

The example case assumes a forehearth application with a glass melt eight inches deep at 2250°F surface temperature and no background radiation. This exercise was primarily designed to determine the degree of accuracy required to differentiate the temperature gradient in a glass melt. Figures 3-10 and 3-11 show radiation curves for four different linear window glass temperature gradients at four different wavelengths. The optical thickness (t) at each of the wavelengths is indicated on the plots and is defined as the thickness within which 99% of the emitted light originates. These same temperature distributions are considered in each of the plots including an isothermal case where dT/dy = 0. A normal viewing angle was used in the radiation predictions.

Figure 3-10 shows that the temperature gradient has only a small effect on the total radiation. For a wide range of gradients the radiation level only changes 0.6%, which corresponds closely to the accuracy of the instrument. This degree of accuracy will indicate the temperature to within 1°F. Therefore despite the fact that light is being detected from half a centimeter glass depth, total radiation is reasonably predicting surface temperature.

Figure 3-10 shows the radiation emitted over a broader optical depth from the same slab of glass at a narrow radiation window centered at 3.0μm. With an accurate measure of the surface temperature using an essentially opaque measurement at 4.4μm a prediction could be made for the radiation level at 3.0μm assuming an isothermal slab. A degree of departure from the predicted isothermal and the actual detected radiation would indicate a strong or weak temperature

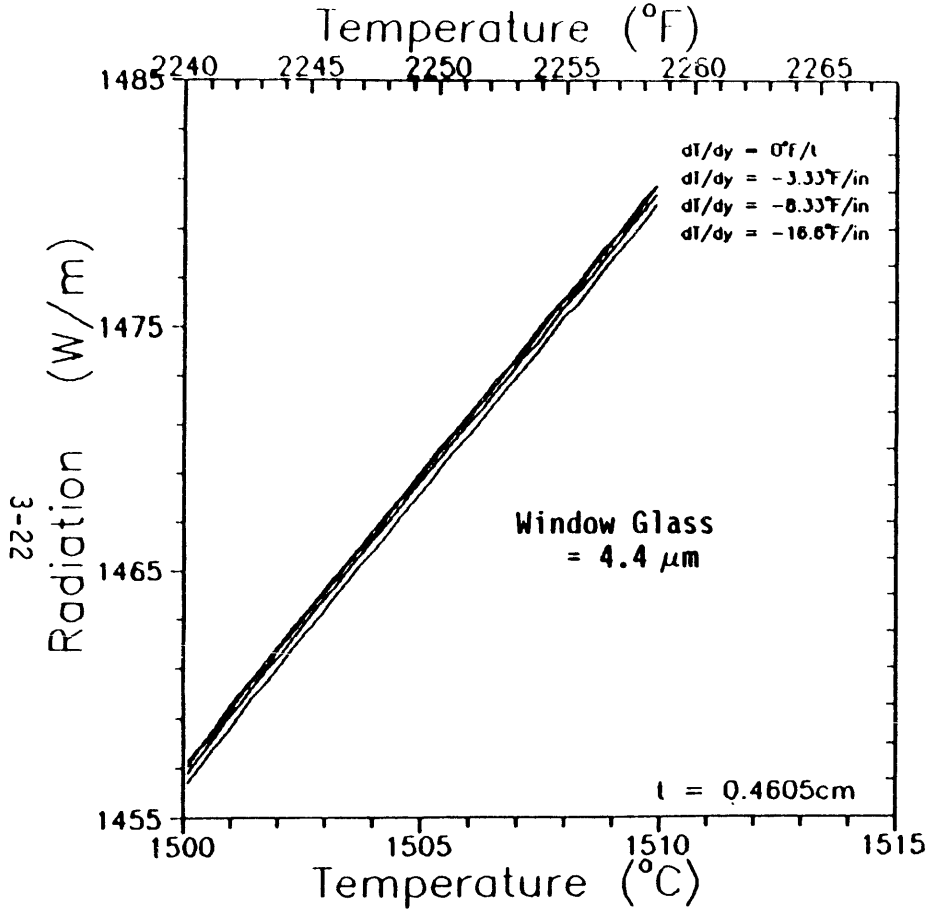

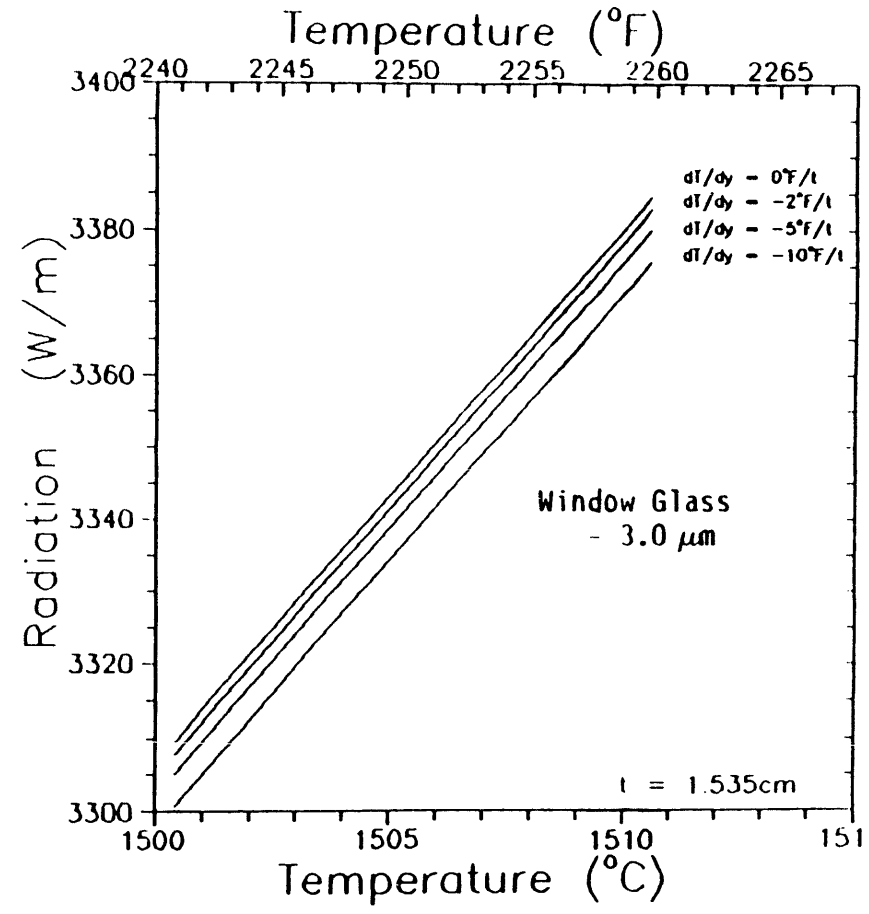

Figures 3-10 (a) and 3-10 (b). Variation in radiation with wavelength: 4.4 and 3.0 microns.

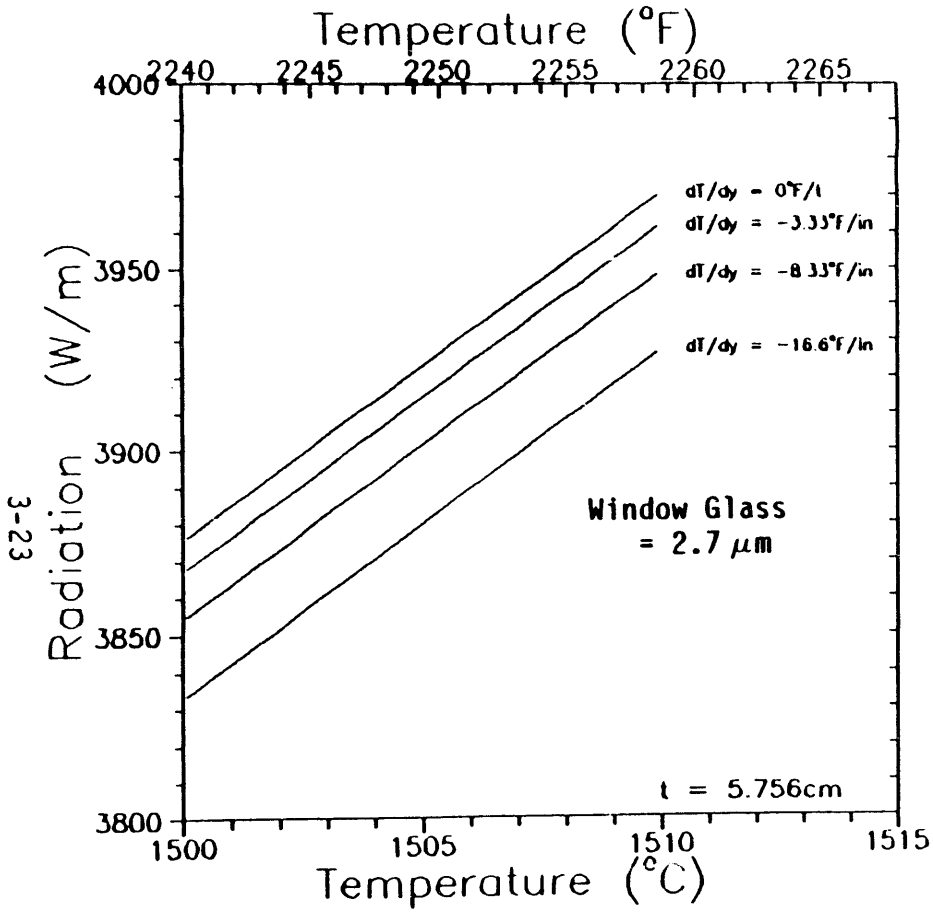

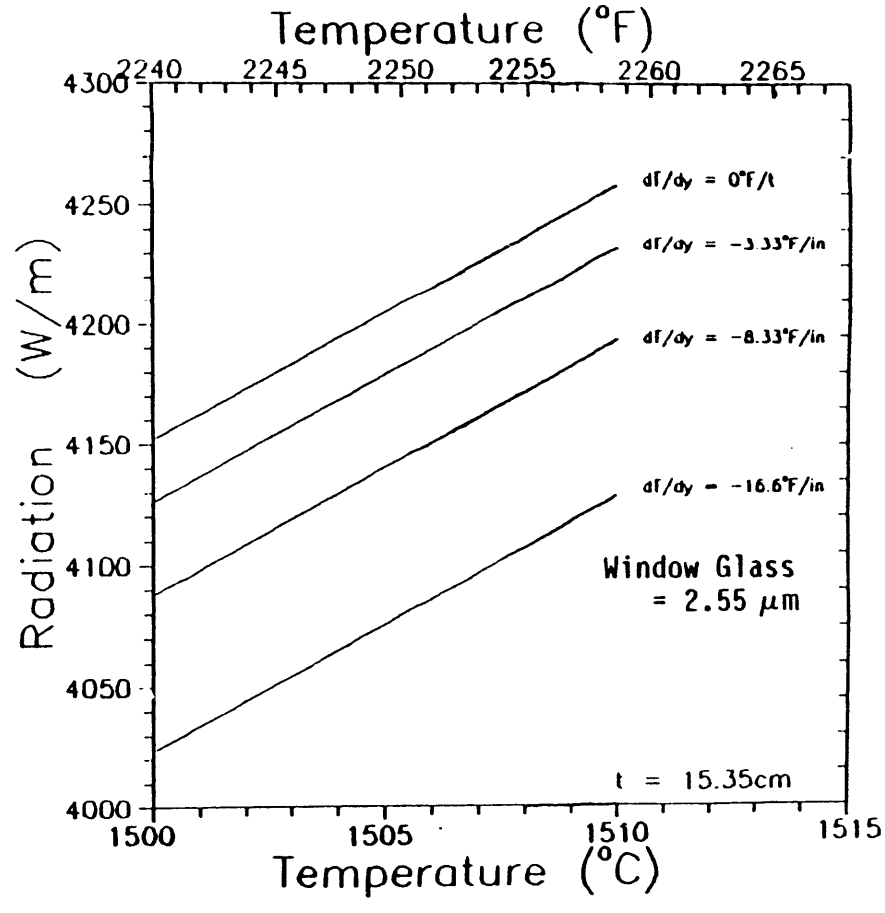

Figures 3-11 (a) and 3-11 (b). Variation in radiation with wavelength and temperature gradient:2.7 and 2.55 microns.

gradient in the first 1.5 cm of the slab. The bottom curve shows a case where the temperature changes 10°F over the optical thickness. This curve is .27% below the isothermal curve (referenced to surface temperature) and should be easily detected.

Figure 3-11 shows the effect of these temperature gradients on the radiation at 2.7μm. At this wavelength a measurement would readily indicate a temperature gradient relative to an isothermal radiance prediction referenced to the 4.4μm surface temperature measurement. The fourth plot at 2.55μm (Figure 3-11) shows an even greater resolution of the temperature gradients, and hence demonstrates that radiative measurements at four wavelengths can be deconvoluted to indicate the temperature history of the glass.

3.5.3 Calibration Methodology

The methodology for calibrating the system was modeled to determine the necessary technique and hardware for producing accurate temperature measurements. Optical non-contact temperature signals can be broken into five basic variables. These quantities are defined as follows: the radiance L ($Wm^{-2}sr^{-1}$) of the surface to be measured; the responsivity $\Re$ (V/W) of the detector and optics combined; the area A (m^2) of the sensor aperture; the solid viewing angle Ω (sr) of the sensor; and the output voltage V_{out} of the detector. The detector output is defined as

$$V_{out} = \Re_\lambda L_{\lambda T} \Omega A .$$

The radiance is the only quantity not defined by the sensor system and is a well characterized function defined by Planck's equation of black body radiation. Thus, by aiming the sensor at a black surface of known temperature, and hence known radiance, a calibration constant can be calculated which represents both the responsivity and sensor constants. This is defined as

$$c_\lambda = \Re_\lambda \Omega A.$$

Calibrating the system in this manner works very well providing there are no changes in the system in time. In reality this may not be the case. The responsivity will inevitably show gradual changes in time, due to ageing of the fiber and detector. Short term changes in system output will result from contamination of the optics and will require an active calibration system. Since contamination of the optics will only affect Ω and A terms, all wavelengths may be affected equally.

Calibration of the system consists of aiming the sensors at an isothermal black body surface of known temperature and whose area extends beyond the field of view of the sensor.

3.5.4 True Radiance Model

The calibration theory described in 3.5.3 was implemented in a spreadsheet to automate the calibration procedure. The spreadsheet was designed to calculate the filter calibration constants which convert the output voltage from each channel to a value indicating the level of radiation detected. The spreadsheet requires entering pertinent optical data for each filter used in the multiplexer. The spreadsheet also requires the calibration source temperature and the mean output voltage for each filter. During the course of the calibration test the sensors are aimed at the black body source.

The model uses the filter halfwidth points and the source temperature to calculate a theoretical value of the radiance emitted from the source. The radiance is a temperature and wavelength dependent function which is defined by integration of Planck's equation of black body radiation over the interval ($\Delta\lambda$) between λ_1 and λ_2:

$$L_{\Delta\lambda} = \int_{\lambda_1}^{\lambda_2} \frac{c_1 \lambda^{-5}}{\pi \left(e^{c_2/\lambda T_s} - 1 \right)} d\lambda$$

where $c_1 = 3.7418 \times 10^{-12}$ W cm^2, $c_2 = 1.438786$ cm K and T_0 is the calibration source temperature. The integration results in a moderately simple equation which is described as follows:

$$L_{\Delta\lambda} = \frac{c_1}{\pi}\left(\frac{T_\circ}{c_2}\right)^4 \sum_1$$

where the summation is defined as,

$$\sum_1 = \sum_{m=1}^{\infty} \exp\left(\frac{-mc_2}{\lambda_2 T_\circ}\right) m^{-4}\beta_2 \; - \sum_{m=1}^{\infty} \exp\left(\frac{-mc_2}{\lambda_1 T_\circ}\right) m^{-4}\beta_1$$

and,

$$\beta_1 = x_1^3 + 3x_1^2 + 6x_1 + 6$$

$$\beta_2 = x_2^3 + 3x_2^2 + 6x_2 + 6$$

$$x_1 = \frac{c_2}{\lambda_1 T_\circ}$$

$$x_2 = \frac{c_2}{\lambda_2 T_\circ}.$$

The summations are shown above as an infinite sum, however for the wavelengths of interest an accurate value can be obtained with a few (5-10) iterations. This equation was used in the spreadsheet to calculate the theoretical value for the radiance detected through each filter and was used for exact predictions of radiance in units of (W/cm^2 sr). The radiance values were used to generate a calibration constant for each output channel of the multiplexer by dividing the output voltage by the theoretical radiance. The calibration constants in the measurement mode convert the detector output to a meaningful measurement of radiance or color temperature.

3.5.5 Data Analysis

The radiance equation just described is a very exacting model for predicting radiant energy emitted from a body of known emissivity at temperature T. However due to its iterative nature it is not easily applied in a spreadsheet to a large quantity of data. Further, it is difficult to implement because its summations preclude transforming the equation to solve for temperature as a function of radiance. Since all the data are logged as a measure of radiance, it is convenient to have a single equation to estimate temperature.

Fortunately this can be approximated from Planck's integral. As we recall this equation describes the radiances for a particular wavelength integral as

$$L_{\Delta\lambda}(T_i) = \varepsilon_\lambda \int_{\lambda_1}^{\lambda_2} \frac{C_1}{\pi\lambda^5 (e^{C_2/\lambda T} - 1)} dy$$

Since the kernel of this equation is well behaved, the integral is closely approximated by multiplying the kernel by the band width $\Delta\lambda$ and evaluating at the center wavelength λ_{cw}. This gives a much simplified new equation which can be solved for T_i ($L_{\Delta\lambda}$).

$$L_{\Delta\lambda}(T_i) = \frac{\varepsilon_{\lambda_{cw}} C_1 \Delta\lambda}{\pi\lambda_{cw}^5 (e^{C_2/\lambda_{cw} T_i} - 1)}$$

The accuracy of this equation was checked against the integral/summation model and was found to give a maximum temperature error of 0.3°F. This was deemed acceptable for the analysis of the breadboard data.

3.5.6 Thermal Deconvolution

Multiple radiant energy readings (measurements) associated with spectral radiation bands are required to describe or model the actual thermal profile.

Information regarding the glass melt optical properties (spectral absorbtion) and glass radiative emission properties is also necessary. The fundamental difficulty is that the highly non-linear integral equations describing radiant exchange are not explicit in the unknown variable, temperature. The determination of the temperature profile, T (y), from the energy measurements E (λ) therefore requires a deconvolution or inversion technique, ultimately in real time.

One approach (but by no means the only one) is to make an initial assumption as to the form of the thermal profile. With the general form of the profile assumed, adjustments in the algebraic equation modeling the profile are, in principle, made to match the energy measurement, given the physical properties of the glass.

From this premise several approaches are discussed below, each differing in complexity and relative accuracy. The best approach depends on the application, the needed precision, the number of data points for each measurement, and the shape of the thermal profile.

Simple Approach

One simple approach is appropriate if the temperature profile is monotonic and well-behaved. In this approach the radiance is measured at a particular wavelength. The Planck equation is used to evaluate the fictitious isothermal temperature that is equivalent to the radiance coming from the nonisothermal melt. In practice this fictitious temperature will agree with the melt temperature at some depth. It turns out that this depth is fairly constant for a wide range of temperature profiles. Thus, the procedure is to measure the equivalent isothermal temperature associated with each wavelength, and assign these temperatures to specific depths. The Viskanta equation can be integrated for a few profiles to establish these depths.

Analytical Approach

A potentially more accurate approach is the deconvolution of the generalized equation defining temperature profile using measured radiance at length. The temperature gradient can be defined from linear segments which are progressively deeper in the glass, or as a continuous function. Deconvolution is easiest if temperature is known at one of the interface surfaces. The usual requirement is that one of the measurements be made at a wavelength where the glass is considered to be opaque such as the surface temperature (T_s) at $\lambda > 4.5$ μm. Again, as in the previously described approach, the energy measurements can be assigned a unique depth.

With the exception of the surface temperature measurement, each energy measurement is a linear temperature gradient representation of its respective depth segment. In this way the thermal profile is approximated by a series of linear temperature profiles representing progressively deeper segments. This method was provisionally selected at the beginning of the pilot furnace test and verification task.

The greatest drawback of this method is that it relies heavily upon making an accurate surface temperature measurement. Any errors in the surface temperature measurement will propagate through the algorithm creating gross errors in the deepest measurement. Slight variations in the physical properties of the glass could also propagate errors with depth.

Precise Approach

An alternative more precise approach is based upon an established iterative technique. This approach is initialized by assuming a functional form of the temperature profile, T(y). The assumed profile then predicts theoretical energy $\dot{E}(\lambda_i)$. This is compared to the actual measurements to yield an error of the prediction. The next step is to systematically adjust the temperature profile T(y) with a recursive procedure such that the sum of the errors are reduced. The calculation is completed when the errors are minimized or fall within an

acceptable limit, yielding the measured temperature profile. This approach can be very accurate, although a certain amount of mathematical art is required to adjust T(y) in a way to rapidly and economically converge to minimum error.

It is concluded that the deconvolution method can be made as simple and complex as needed and will inevitably be determined by experimentation and the needed accuracy, precision, and system response required by the end user.

4.0 LABORATORY DESIGN, SENSOR TEST AND VERIFICATION

A two step test plan was proposed to evaluate the functional performance of the TAS within both controlled laboratory and simulated field environments. In Task 1 - Assessment and Selection of Potential Application, the rationale for selecting Gallo Glass's forehearth processing line was described. The plan to characterize the TAS at pilot scale and then use it to implement an energy and production saving strategy was described. The development test work (Phase 1) consisted of:

- laboratory tests at the component and subsystem level to characterize analyzer sensitivities to measurement (IR) wavelengths;

- pilot scale laboratory furnace tests over a range of environmental, thermodynamic, geometry, and process variables to characterize the TAS performance sensitivities to process and design variables;

In a proposed follow-on Phase II, the developed sensor will be installed on a glass forehearth and used to:

- confirm analyzer functional performance and durability;

- systematically adjust the forehearth operating parameters based on 3-dimensional temperature measurements to optimize process performance (energy and production).

The Phase I work was accomplished using glass melts which are generically representative of the container industry and Gallo's major production. A range of glass products were selected having physical and chemical characteristics which may affect analyzer performance. Specifically, two products were characterized in detail which present variations in the following characteristics:

- emissivity

- absorbtion coefficient (IR transparency)
- glass chemistry

Process variables which were selectively investigated include:

- gas phase atmospheric interferences (CO_2 and H_2O)
- temperature dependent glass properties
- nonisothermal boundary conditions
- temperature gradients (positive and negative)

Design variables investigated are:

- IR wavelength combinations
- optical cabling distances
- sensor design alternatives
- viewing angles (normal and Brewster's)
- calibration procedures

4.1 Approach and Test Plan

The preliminary bench scale testing of components and subsystems was outlined in Section 3.4. The following section describes the objectives of the laboratory tests, the test plan designed to achieve those objectives and the test equipment used to conduct the experiments.

The basic premise of the pilot furnace tests was to construct a prototype of the TAS and characterize its sensitivities and operational parameters in a laboratory environment similar to that encountered in the actual process application. The prototype TAS used unhardened, but fully configured components suitable for lab testing. A commercially available box furnace was purchased and modified to melt glass samples at temperatures up to 2200°F. A data acquisition system was assembled with the appropriate hardware and software to record raw data from the TAS optical multiplexer and referee thermocouples. The system was designed so the data could be digitally filtered to reduce noise prior to being recorded directly on the computer hard disk. Data sets from individual test runs were analyzed off-line after the test was completed.

The test program objectives were to evaluate the glass characteristics, process variables, and design variables listed in 4.0 with respect the TAS sensitivity and performance.

The tests were conducted according to the test matrix shown in Table 4-1. This matrix gives a listing of the system variables manipulated to systematically evaluate each of the test objectives. Each test objective was evaluated by only varying those parameters influencing the objective with all other independent variables kept constant. Different types of sensors were designed to reduce stray background radiation detection by the sensor at a normal viewing angle. Sensors sighted at the Brewsters angle accomplished the same objective by taking advantage of reflected light polarization effects. Combustion gas interference tests sought to reveal any effects of molecular absorption at the selected filter wavelengths at furnace temperature. The configuration sensitivity tests addressed the issue of whether there is any unforseen effect of sensor height that could introduce measurement error.

The last test objective evaluated system ability to measure internal glass temperatures and gradients. In addition to the measurement variables indicated in Table 4-1, variations in the use of the deconvolution algorithm were implemented to optimize its accuracy. (See Section 3.5.6).

TABLE 4-1. TEST MATRIX

Test Objective	Product	Filter Wheel Combination	Temperature, °F	Temp. Gradient, °F/in.	Atmosphere	Sensor Type	Viewing Angle	Fiber Length, m	Sensor Standoff, in.
Normal Angle Background Control	Gallo Green	# 1	2000	0	Air	Cold Aperature Hot Aperature Open Aperature	Normal	10	1/2
Brewsters Angle Background Control	Gallo Green	# 3	2000 2100 2200	0	Air	Open Aperature	45 degrees 53 degrees 65 degrees	10	1/2
Atmospheric Interferences	Gallo Green	# 2	2000	0	Air Nitrogen Combustion	Best of Above	Normal	10	1/2
Configuration Sensitivity	Gallo Green	# 1	2000	0	Air	Cold Aperature	Normal	10	1/2 4
Measurement Sensitivity	Gallo Green Gallo Flint Kerr Flint	# 1 # 2 # 3	1900 2000 2100	0 10 20 40	Combustion	Best of Above	Best of Above	10 20	1/2
Test Variables									
	Gallo Green Gallo Flint	# 1 # 2	1900 2000	0 10	Air Nitrogen	Cold Aperature Hot Aperature	Normal 45 degrees	10 20	1/2 4

4.2 Pilot Furnace Design

EER designed and constructed a pilot test furnace at their Irvine facility specifically for conducting the laboratory test program. The test stand was designed around a commercially available box furnace and equipped with sufficient work space and all required utilities, such as shop air, water, and 115/230 electric power. In addition to the basic necessities, electronic instrumentation interface cards were incorporated into an automated, PC based data acquisition system. Figure 4-1 diagrams the test setup used to conduct the laboratory test.

4.2.1 Data Acquisition System

The main components of the data acquisition system were a PC with custom software, the TAS, and multiplexing thermocouple electronics. The PC was used to control the operations of the TAS and to log data to disk for off-line analysis. Custom software was created which accomplished these tasks. The software allowed the operator to choose to record any combination of Tri-plex thermocouple or TAS data. In addition to logging data and controlling the TAS, real-time table and graphic displays were available to assist the operator with pretest setup.

4.2.2 Furnace and Operating Instrumentation

The furnace purchased for the test program was a Cress model C-122012-TCZ-HLC box furnace. The furnace chamber volume (12" W x 20" L x 12" H) allowed two crucibles to be heated at once. The furnace was modified by adding a timer override switch to enable continuous 24 hour operations. A number of furnace penetrations were made to allow cooling water and purge gases to be introduced. Roof penetrations for sensor viewing (1" dia) and triplex thermocouples are shown in Figure 4-2.

The maximum furnace operating temperature is 2250°F for intermittent operation. Continuous operation was specified at 2000°F. This limited the practical test matrix to the range of 1800°F to 2150°F. The maximum design

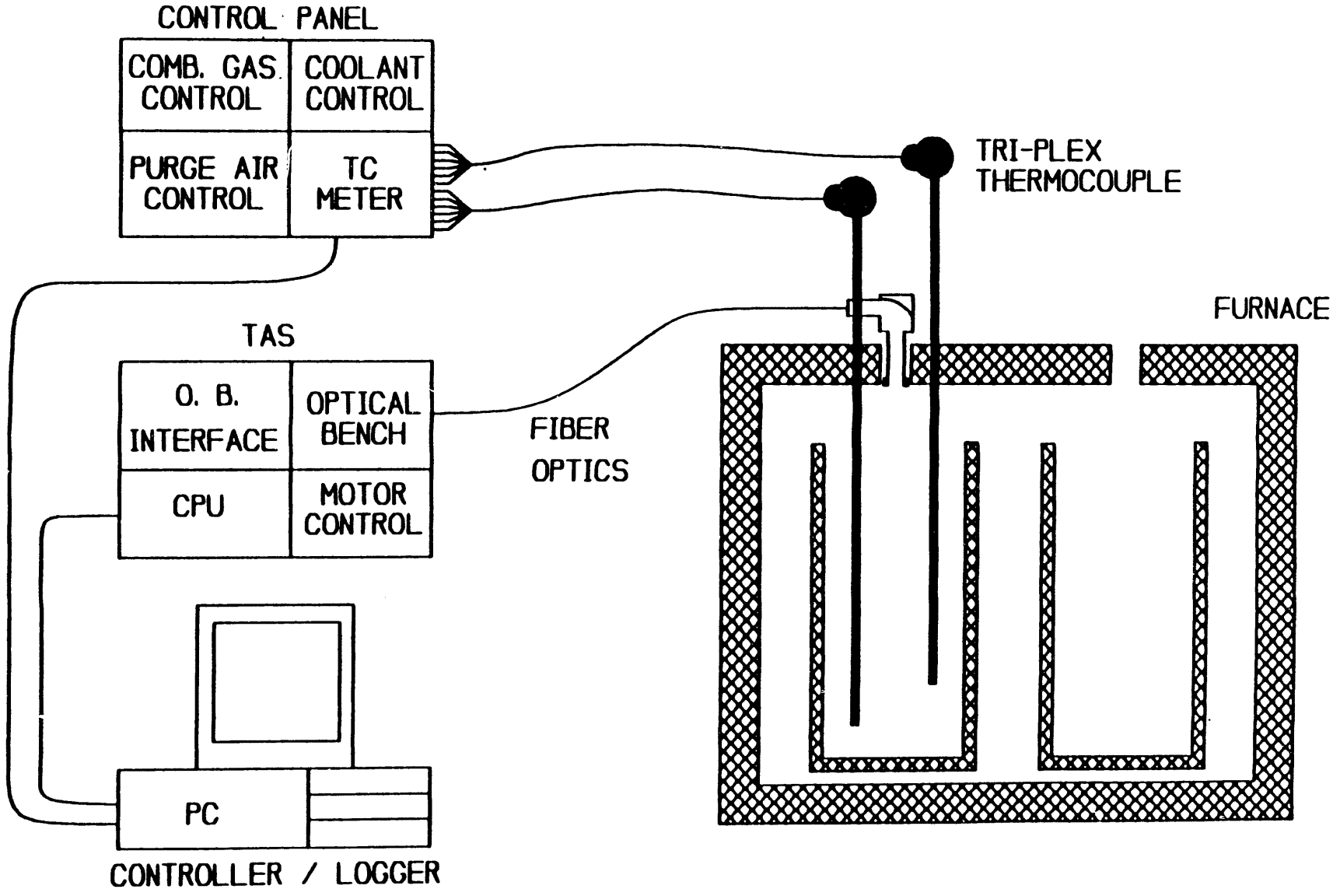

Figure 4-1. Temperature analyzer test setup.

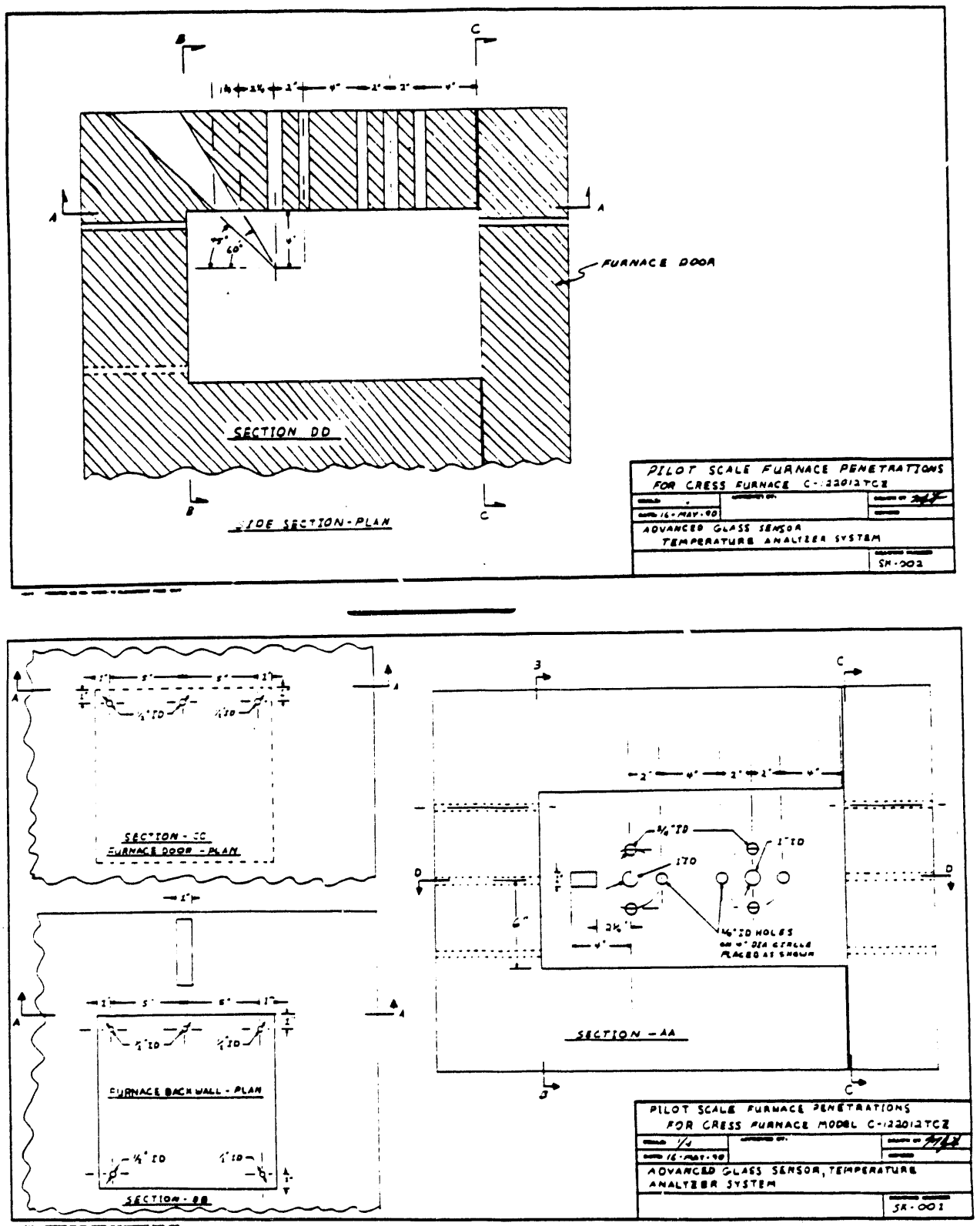

Figure 4-2. Pilot scale furnace modifications.

operating temperature was not used to avoid thermal overloading and potential heat element failure.

Two types of crucibles were used to contain the glass melt samples during testing. Crucibles were size #50 having an 11" height and 6-3/4" diameter. Since this height was too high to allow for angular viewing of the glass, the crucibles were cut to reduce the height to 9". Other shorter size crucibles were available but no standard sizes could accommodate the thermocouple probes on each side of the viewing area. The crucibles were obtained in two materials, Zirconia and a silica based refractory. Both materials are inert to molten glass and can withstand the high furnace temperatures. The Zirconia crucibles worked the best of the two types, though, due to the strong contraction of the glass during cool down, it was subject to fractures after 1 to 2 firings. Despite these fractures the Zirconia crucibles held up well after four firings. The silicate crucibles were purchased because they were inexpensive and had a very short lead time. Their performance in the furnace was satisfactory although due to a greater contraction on cool down, they failed completely after one firing.

To test for possible gaseous atmosphere interferences caused by molecular absorbtion of IR radiation combustion products were introduced into the furnace chamber. Several methods of combustion flue gas simulation were considered. The final configuration used a small catalytic combustor placed directly on the furnace. The catalytic combustor consisted of a quartz tube with a small wad of platinum wire lodged inside. The platinum wire acts as a catalyst to sustain combustion of a premixed fuel mixture of air and methane. Once ignited the tube was inserted into a port on the furnace to purge the chamber with IR absorbing combustion products (mostly CO_2 and H_2O). This design had the advantage of a small flow rate (11 SCFH) and no heat loss of the gases prior to entering the furnace. The air and methane flows were controlled on the flow control panel.

The test plan requires producing a stable glass sample temperature gradient in order to test the deconvolution method. A negative gradient was created with a water cooled coil or "cold plate" under the crucible to lower the bottom

temperature. The cold plate coil was made of 1/4" O.D. stainless steel tubing and the water flow was controlled at the flow panel.

The largest gradient achieved was about 10°F/in. Tests using the cold plate were performed first because uncooled tubing could not withstand the high furnace temperatures. After gradient tests were completed, a sequence of isothermal tests were performed with the cold plate off. At the end of the test the furnace was cooled. If the crucible was intact it was reused and the now destroyed cold plate discarded and replaced.

The furnace and flow panel were installed on a specially designed steel table. A steel unistrut supported cable tray was constructed over the furnace to support communication wiring for the sensors and referee triplex thermocouples. The structure allowed the sensors to be properly aligned in a manner that was unaffected by the thermal distortion of the outer furnace shell.

Referee measurements were made by precision triplex thermocouples purchased from Engelhard. These thermocouples (Figure 4-4) were a Platinum B type thermocouple (±1°F accuracy) which is a standard of the glass industry. Two thermocouples were purchased, each with the three sensing points separated by two inches. In typical testing the triplex TC's were placed on each side of the viewing area (out of view of the sensor) with the highest TC point at the glass surface. These thermocouples gave the best possible reference for the pyrometric measurements.

4.2.3 Sensor Calibration

Sensor calibration was one of the most critical test procedures. Preliminary evaluations of two calibration source designs were outlined in Section 3.4 and showed that the most expedient method was to place a temperature instrumented silicon carbide element inside the furnace. The sensor calibration was made prior to each test sequence. After the test, calibration constants were calculated so the output signals could be translated into a meaningful measure of irradiance in W/cm^2. The sensor calibration configuration is shown in Figure

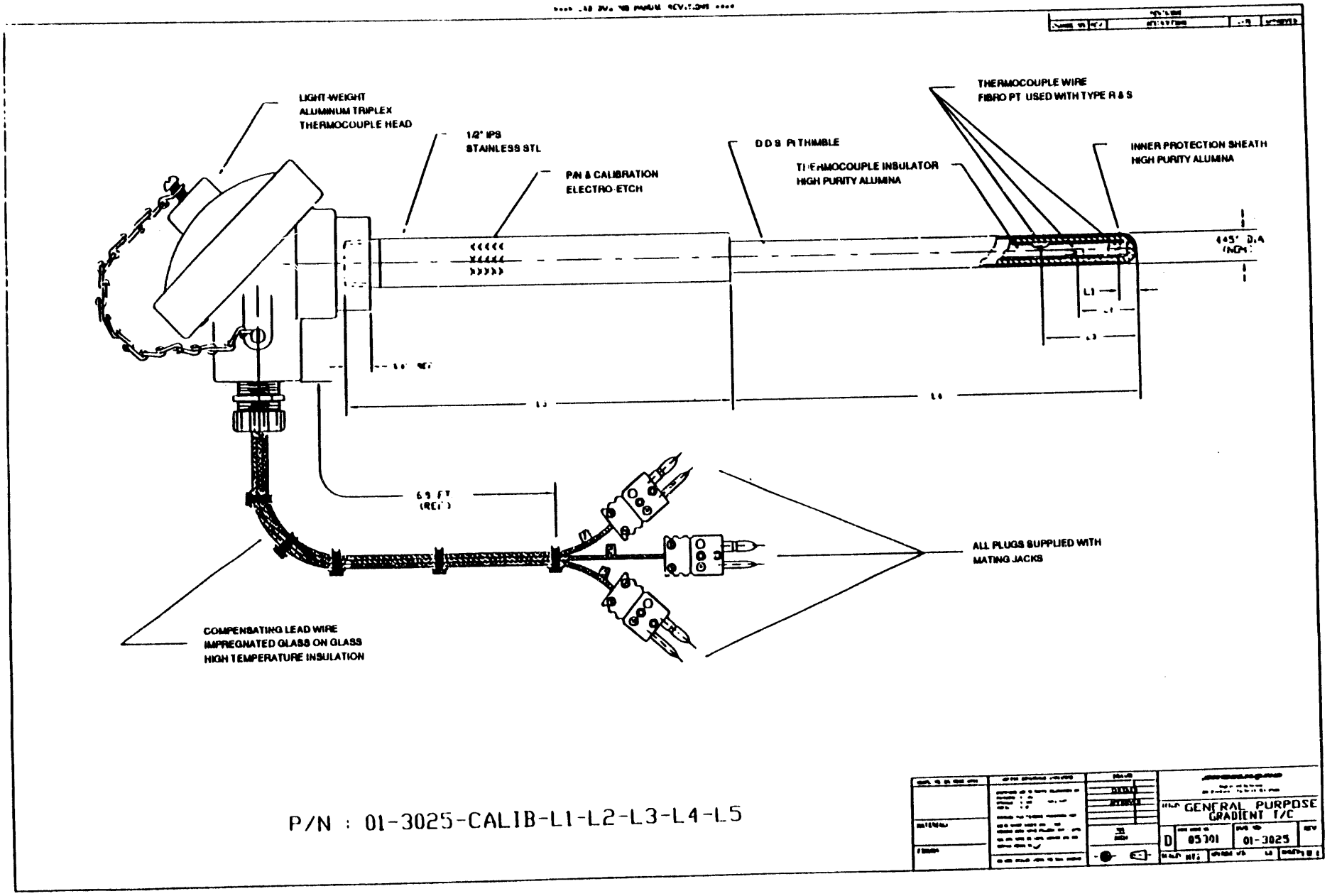

Figure 4-4. Reference thermocouple.

4-5 and uses one of the viewing ports. The glass filled crucible is under the other. The element consisted of a cylindrical block of silicon carbide cast with a conical depression. Silicon carbide was chosen for its very high emissivity (.98+) and the conical cavity is a classical design to enhance the emissivity (.99+). This design is very close to being a true isothermal black-body. A referee temperature measurement was made by placing a thermocouple on the rim of the cone. Not shown are cylindrical radiation shields enclosing the element which served to thermally damp transients from the heating elements and insure the thermal uniformity.

The calibration procedure was to install the sensor over the black-body element and record the digitized output signals overnight. This assured that a very isothermal condition was achieved over a large number of data points. The data was entered into the calibration spreadsheet to calculate the ratio of signal output for each filter wavelength to the predicted radiance for the recorded black-body temperature. The calibration constant is calculated as the mean output divided by the predicted black-body radiance.

Calibrations made at two different temperatures should follow Plancks' temperature dependency if the optical system has a linear response. Calibration data from two temperatures were compared to determine how linearly the detector responds to radiation. Measured radiance levels at 1520°F were compared to radiance predictions for 1520°F based upon calibration constants measured at 1980°F (Figure 4-6). This test showed a maximum of 10°F error in one of the channels. This translates to a calibration error of 2°F per 100 degree change. This was determined to be acceptable for the test program. Calibration factors can be developed and implemented in the data analysis software to correct the error if required. This error is a likely result of a nonlinearity in the relative detector response at significantly different input levels.

4.3 Parametric Studies

The parametric studies were designed to evaluate the physical principles governing and affecting the noncontact temperature measurement of glass melts.

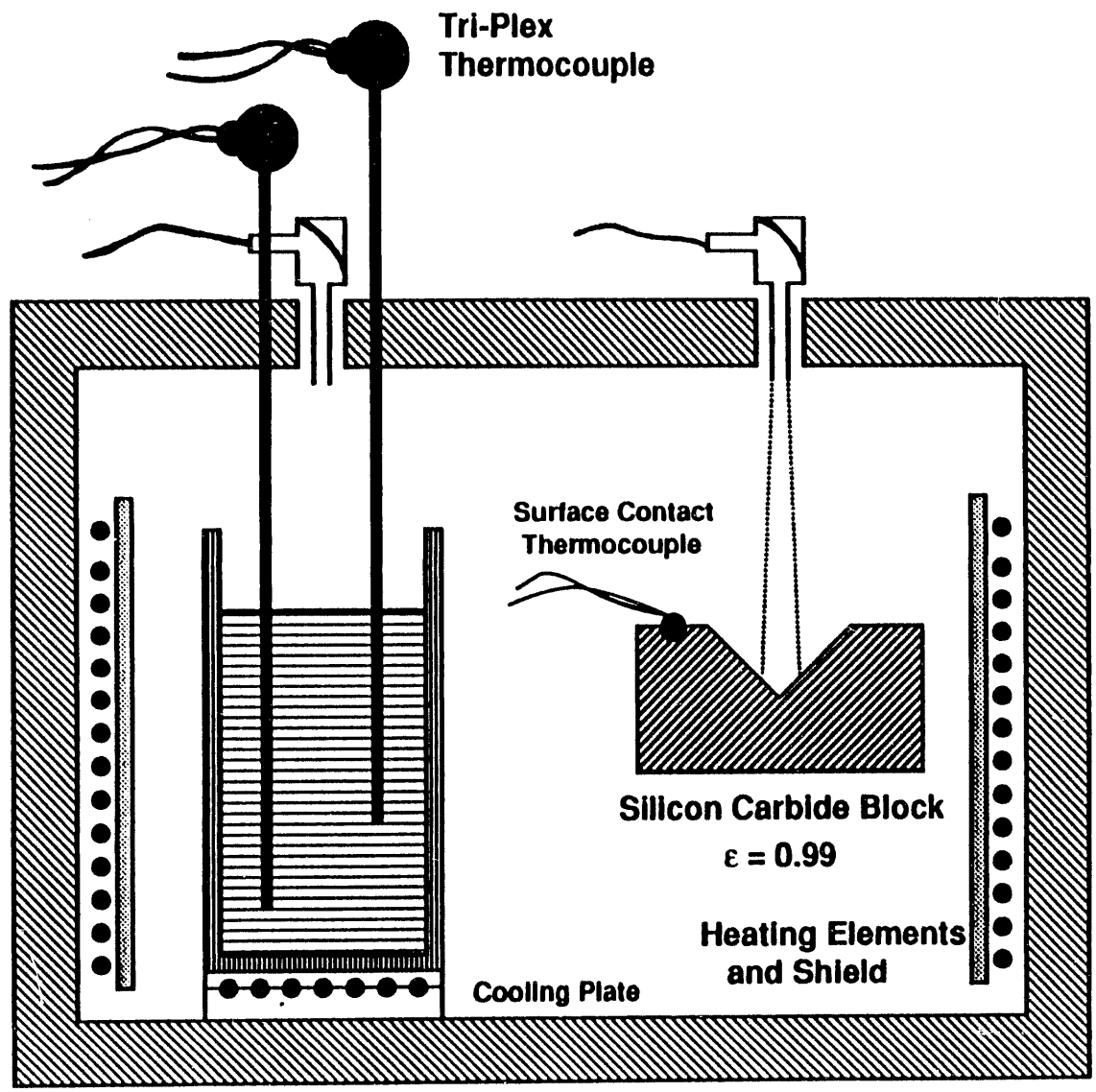

Figure 4-5. Furnace calibration configuration.

Factors Included in Calibration

- In-furnace, air atmosphere
- Mirror reflectivity
- Fiber properties, including launch losses and transmission
- Multiplexer transmission, including filter properties
- Detector sensitivity
- Electronic amplification

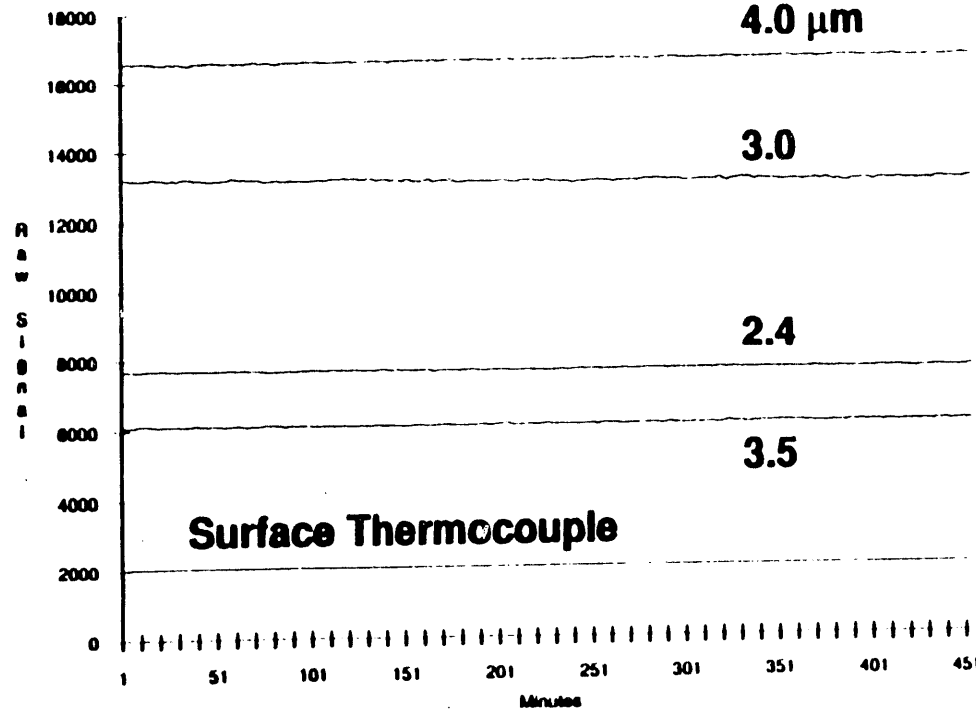

- Single point calibration: Maximum expected error in operating range is 10°F

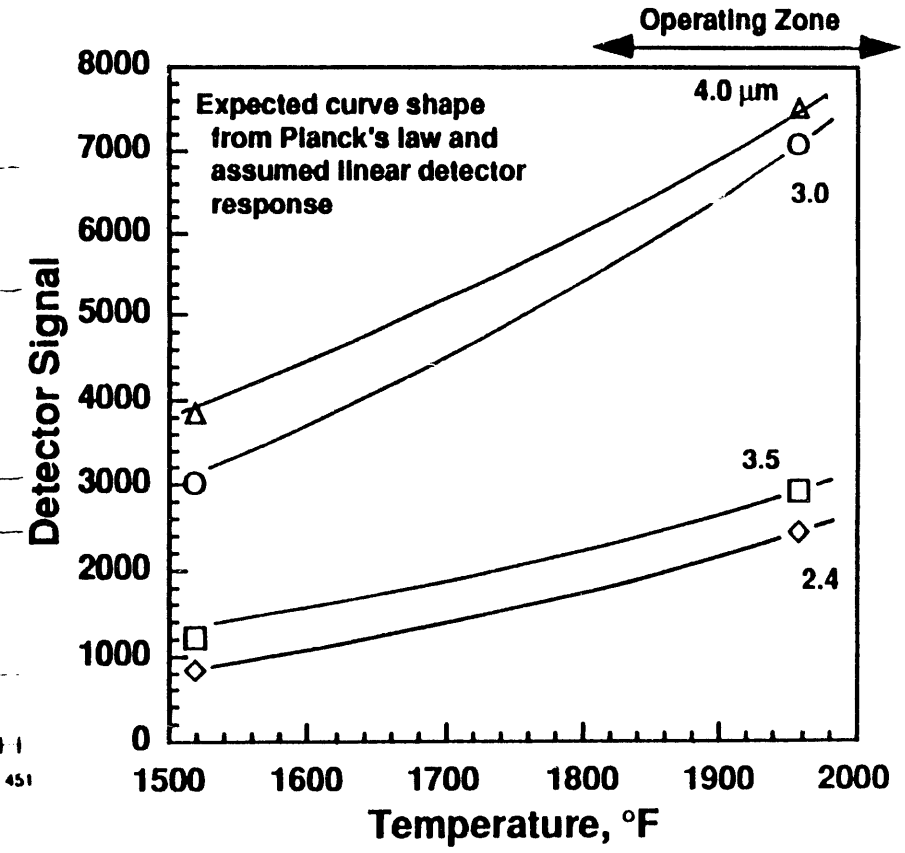

Figure 4-6.

The test plan (Table 4-1) outlines the test objectives and the respective parameters to be studied. The following section describes the tests conducted and the results of the analysis. The following parameters were evaluated; Gas phase interferants, surface reflection mitigation, and glass type.

4.3.1 Interference Sensitivities

All optical detection methods are influenced by interferences imposed by the intervening medium between the element to be measured and the sensor. Since no particulates are expected in the forehearth atmosphere, the remaining potential interferants influencing the measurement are combustion products occupying the space between the glass and the probe. Molecular IR absorbtion from gaseous combustion species is primarily a result of water and CO_2.

The primary method of mitigating interferences due to molecular absorbtion was to study the absorbtion spectra of the species expected to be present and select measurement wavelengths that are not coincident with any strong absorbtion bands. Figure 4-7 shows the atmospheric absorbtion spectra for a 0.3 km path found in the Infrared Handbook [17]. This is one of several sources used to evaluate the interfering species. Generally, the selected regions appeared to be interference free.

Combustion interference was evaluated by comparing the measured optical temperature for conditions where the furnace was serially purged with air and purged with combustion products. The combustion products were introduced using the catalytic combustor. Three such tests were conducted of which two were determined to be unsuccessful. The failed tests resulted from the formation of condensation on the window of the sensor during the combustion purge period. Condensation on the window reduced the signal levels for all wavelengths uniformly and to a much greater degree than could be expected from molecular absorbtion at any wavelength.

Figure 4-8 shows the relative temperature detected for the successful interference test. The bottom four temperature-time traces represent the

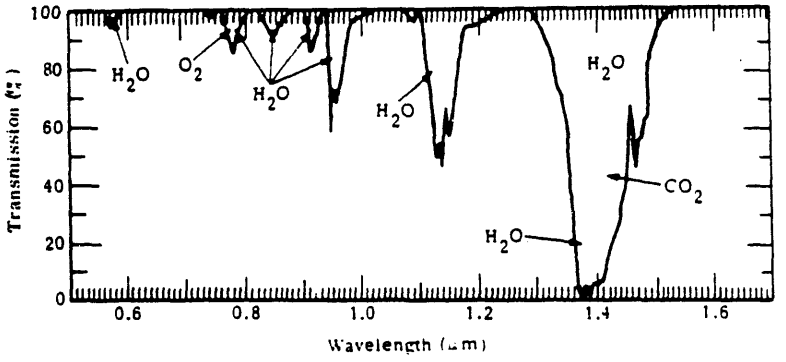

(*a*) 0.5 to 1.7 μm.

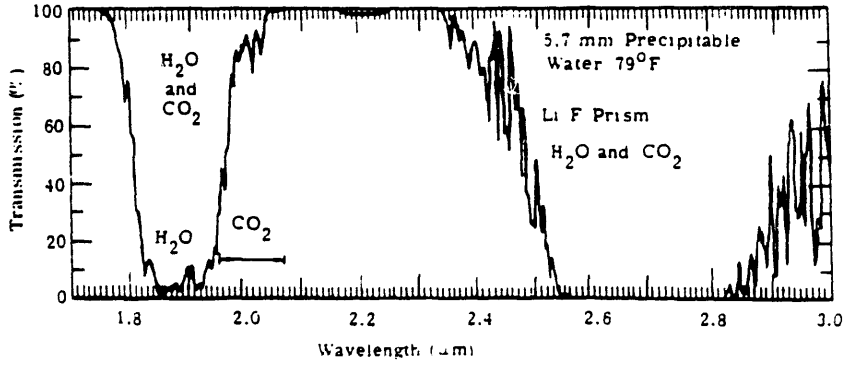

(*b*) 1.7 to 3.0 μm.

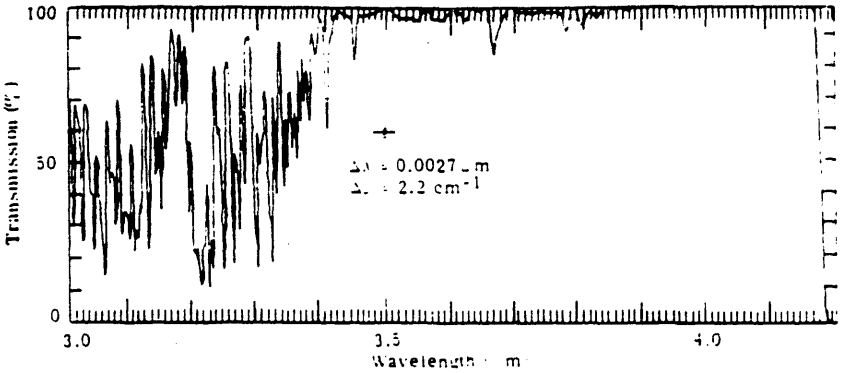

(*c*) 3.0 to 4.2 μm.

Figure 4-7. Atmospheric absorbtion.

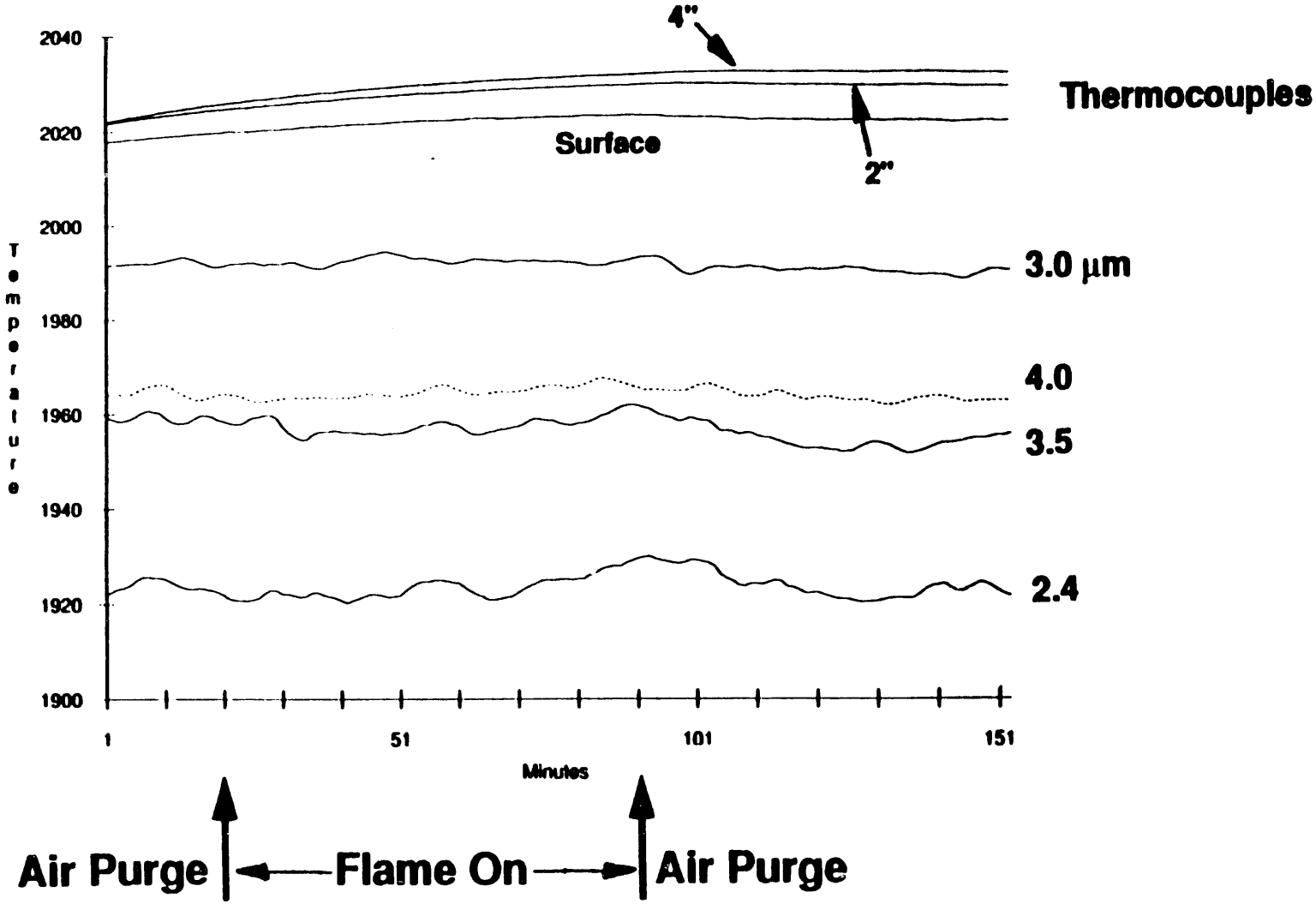

Figure 4-8. Gaseous interference test.

relative temperature detected at the wavelengths 2.4, 3.0, 3.5, and 4.0 micron. The top three traces represent the three output temperatures from the referee tri-plex thermocouples, of which the lowest is the surface temperature. The test was initiated by starting a purge of the furnace with air at 11 SCFH. The purge increased the air circulation in the furnace, causing the glass temperature to increase. At the 20 minute mark the catalytic combustor was ignited to purge the furnace with combustion species. The flame was on for 70 minutes which allowed 12 or more volume changes of gas. Over this period no discernable effect of the combustion gas on signal output was measured. The most strongly affected wavelength would theoretically be the 3.0 micron filter, potentially having no more than a 1.6% drop in signal. Ninety minutes into the test the catalytic combustor was turned off and the air purge was resumed. Again, no measured effect of the purge air change with the exception of a minor drop in the surface temperature caused by the change in purge gas temperature.

The results of this test indicate that there is no gaseous interference at the wavelengths tested and that the method selected for choosing usable wavelengths is sound.

4.3.2 Optical Methods Assessment

Two optical sighting angles were initially studied, normal and Brewsters', to determine which best mitigates signal error due to reflected surface radiation from background sources.

Normal Incident Angle Measurements

The first approach involves collection of the radiant energy from the melt at a normal angle. At wavelengths away from specific absorption bands, four to nine percent of the normal incident light is reflected. Aligning a detector at a normal angle is much simpler than alignment at Brewster's angle (and its polarization filter) as described below. For a low radiant background environment, detector alignment normal to the melt surface offers a means for

enhancing the signal-to-background ratio since normal and near normal surface reflection is lowest.

Background radiation would not be a concern if it were possible to isolate a truly collimated beam of light emanating normal to the glass surface. If the beam were truly collimated and normal to a flat glass surface, then the only source of reflected radiation would be the detector. In reality, however, it is not possible to isolate a perfectly collimated beam. Furthermore, the surface of the glass will rarely be perfectly flat. Nonetheless, there are advantages to making normal incident angle measurements. First of all, it is a much simpler tactic with a greater potential to obtain a higher instrument signal to noise ratio. Secondly, there are many applications such as mold and gob temperature measurement, where background radiation is negligible.

Finally, for materials such as glass melt, reflected background radiation at transparent wavelengths is a small percentage of the total incident radiation. Applying Fresnel's equations at a normal incident angle ($\theta_i = \theta_t = 0°$) the following Reflective ($R_\perp$) and transmission (T_τ) results are obtained:

$$R_\perp = R_{||} = 0.04$$

$$T_\perp = T_{||} = 0.96$$

While this approach does not provide a means for eliminating background radiation, in a low background environment a normal collimated detector will enhance the signal-to-background ratio by as much as a factor of 24 relative to off normal signal collection.

Further reductions in background radiation can be obtained by the judicious design of the sensor. The level of background radiation detected is a function of the surface reflectivity of the glass, the temperature and emissivity of the surface from which the background originates, and the area of the background surface that lies in the field of view of the sensor. Normal angle detection uses a design that mitigates these the latter two effects.

The off-axis parabolic mirror collects and reflects light into a 450 micron diameter optical fiber. The optical radiation acceptance angle of the sensor from off normal radiation is limited to about 0.34°. Though this restricts the amount of radiation detected it also limits the amount of background in the field of view. If the sensor is aligned very nearly normal to the glass surface the background radiation will only originate from a circular area surrounding the rim of the view port. One sensor was designed so as to cool this area of potential background interference. This sensor, called the "Cold Ring" Sensor, was used for the majority of the tests. The sensor design effectiveness was determined, by simulating background radiation from the furnace walls. The experimental test furnace did not allow for creating a strong background environment because of temperature constraints and essentially isothermal operation.

The test was conducted by placing a donut shaped heating element on the furnace roof around the sensor penetration. By operating the furnace at a nominal temperature and progressively heating the element up to 2300°F, a high background environment could be created at the most sensitive location, and hence the sensor designs could be evaluated.

The cold ring sensor used water as a coolant, though design calculations showed that a cold ring temperature to 500°F below that of the glass would be sufficient for background radiation control. Cooling with instrument air in an actual field application is preferred. Three sensor configurations were evaluated for normal angle detection. These normal angle configurations were:

1. Sensor 1, normal angle with cold ring coolant on;

2. Sensor 1, normal angle with cold ring coolant off; and

3. Sensor 2 at normal angle with no cold ring.

Each case was evaluated with the furnace at a 1800°F set point and with the background heating element operated at five different power settings. The background temperatures ranged from 1750°F to 2300°F. The test data was then

analyzed by evaluating the average relative temperature error detected with respect to the referee glass temperature. Figure 4-9 is a bar chart showing five sets of data. The first column of each set is the measured error using sensor 1 with the cold ring on, the second column of each set is the measured error using sensor 1 with the cold ring off, the third column of each set is the measured error of sensor 2. The standard deviation of the average data is about ±3°F.

It is immediately obvious from this data that the cold ring has a very strong effect in suppressing the background radiation and that the cold ring may be essential for applications involving high background radiation. In the actual application in a forehearth the cold ring design may need to be redesigned to allow for air cooling, and a longer detection height

Brewster's Angle Detection Verification

From a theoretical standpoint, the detection methodology of reducing background radiation by taking advantages of unique reflection properties at Brewster's angle is very promising. In reality though, it requires hurdling a number of technical challenges. These challenges arise primarily as a result of making measurements in the mid infrared.

Testing of the Brewster's angle approach was implemented by measuring the glass radiation at angles between 45° and 65° (from the horizontal) with Sensor 2 fitted with an IR polarizing filter. A polarizing filter that works in the infrared region from 2.0 to 5.0 microns, and removes at least 99.0% of the radiation in the unwanted polarization plane is needed. Unfortunately all polarizers that fit this criterion are of ceramic construction and cost in excess of $1,500.00. At this cost the TAS would be significantly more expensive. A less expensive polarizer of polymer construction was selected with a narrower band pass, between 1.0 and 2.0 microns. The test was planned to use two IR filters with wavelengths centered near 2.0 microns for a proof-of principle experiment.

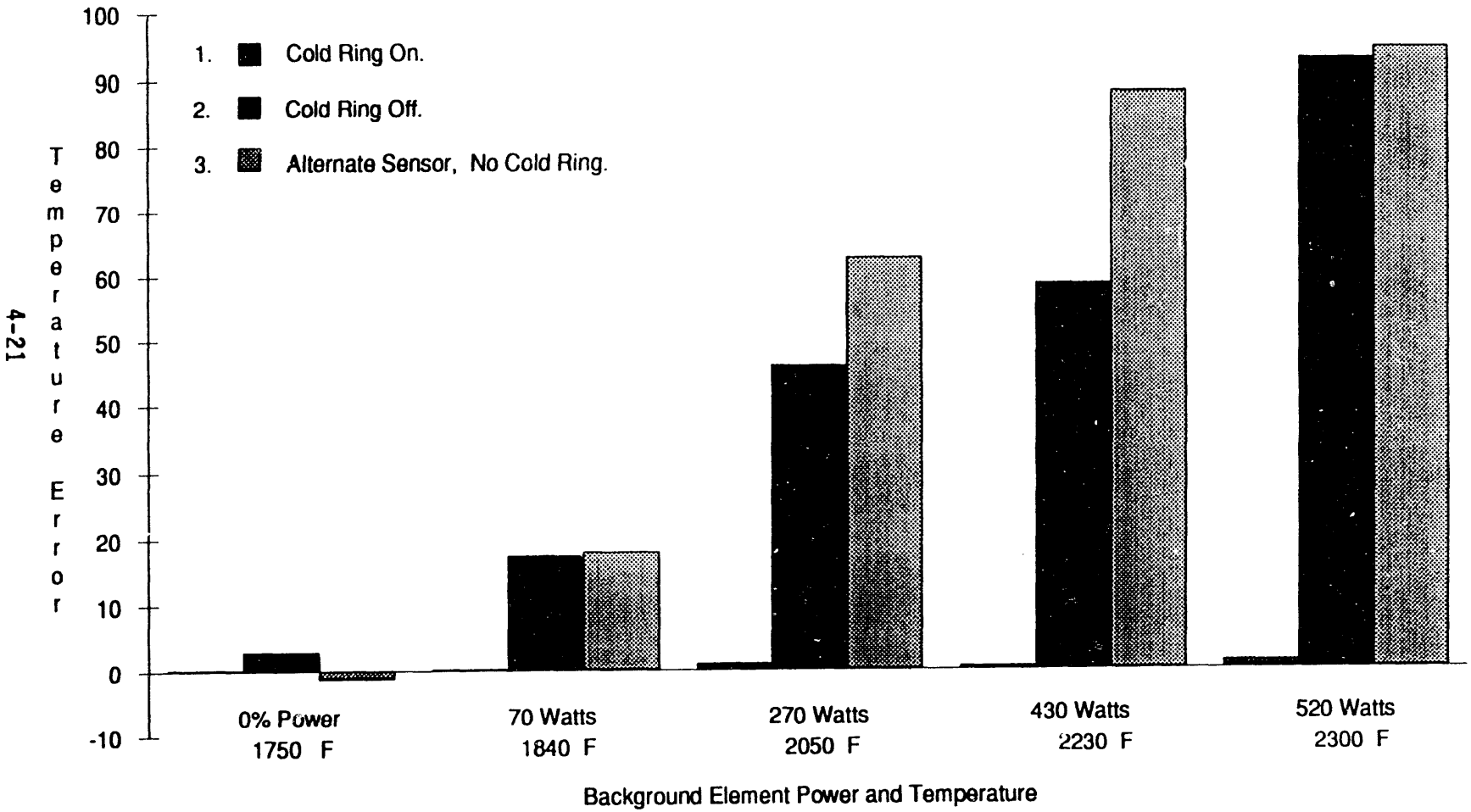

Figure 4-9. Normal angle: relative error due to background radiation.

A series of tests were conducted with sensor 2 collecting data from a calibration source, and from glass at normal, 65°, 55° and 45° angles from the horizontal.

The test series started with a calibration test using the calibration source in the oven followed by four green glass melt tests, each at a different angle. From the onset of the data series, the measured temperatures showed a steady and gradual increase over the referee measurement. At the end of the test series the error, relative to the calibration test, ranged between 200 and 400°F. This steady signal increase is believed to be evidence of the failure of the polarizing filter due to excessive heat. The sensor head was always less than 300°F, which is safe for most optical components. The polarizer, however, behaves differently than most optical components in that in a broad band sense it is predominately a radiative absorber.

The overall transmittance of the filter is less than 20% (over its range of transmission) which means the remaining 80% of the incident radiation is transformed to thermal energy. As a result the filter temperature rose rapidly and eventually melted. The time of filter failure is unknown, although most of the data was determined to be uninterpretable.

A number of issues regarding the theoretical soundness of the Brewster's angle method were raised. The method might be effective in the visible and near-infrared region, however in the mid-infrared glass dielectric properties change considerably and are difficult to evaluate. The Brewster's angle is a function of the glass refractive index. As a rule of thumb, if the glass transmissivity is relatively constant over a spectral range the refractive index is also constant. Typically the glass refractive index will drop sharply in regions where the transmittance falls to near zero. Beyond this point the refractive index is not measurable.

The thermal deconvolution method requires measurements at wavelengths where the glass has distinctly different transmission levels in order to measure temperature profiles. As a consequence the glass will have distinctly different

Brewster's angles of those wavelengths. Additionally, since the refractive index of the glass is not measurable at some of these wavelengths, the dielectric properties contributing to Brewster's angle effects cannot be assured.

In summary, further evaluation of the Brewster's angle method does not seem productive because of indeterminable variations of the dielectric-optical properties of glass at the wavelengths of interest.

4.3.3 Glass Characterization

The deconvolution process requires knowing key physical properties of the glass. Those properties most important to optical measurements are the spectral emissivity, $E(\lambda_i)$ and the spectral absorbtion coefficient $K(\lambda_i)$. Each of these quantities will vary significantly with temperature over the range of interest. The following describes the characterization method and test procedures to develop this data.

Emissivity Characterization

The emissivity is a dimensionless ratio which describes the degree to which the radiation emitted from an object compares with the radiation emitted from an ideal black-body or:

$$\varepsilon_{\lambda T} = \frac{L(\lambda, T)}{L_b(\lambda, T)}$$

The emissivity is required so the radiant energy measurement can be converted to temperature using to the Planck equation of black-body radiation. According to the literature, the glass emissivities for opaque thickness are typically in the range between 0.85 to 0.97 and are primarily a function of the internal surface reflectivity, i.e., the first term of the Viskanta equation:

$$N_\nu^+(0,\mu) = [1-\rho_{1\nu}(\mu)]\,[\frac{n_{0\nu}}{n_\nu}]^2\int_0^L n_\nu^2 N_{b\nu}(y)\,e^{-\tau_\nu(y)}\,\frac{\kappa_\nu}{\mu}\,dy$$

from which the emissivity is given by:

$$\varepsilon_{\lambda T} = [1-\rho_{1\nu}(\mu)]\,.$$

Since there is not a very large data base of spectral emissivities of glasses at different temperatures, it is necessary (and preferred) to measure this property in-situ under identical test conditions. The requirement for measuring the glass melt emissivity is clear when the Viskanta equation is considered for the isothermal limiting case. In this case the equation reduces to

$$N_\nu^+(o,\mu) = \varepsilon_{\lambda T} N_{b\nu}(\mu)$$

Changing this to a more familiar nomenclature where the direction cosine term is dropped and the emitted radiation is notated by radiance resulting in the relation:

$$L(\lambda,T) = \varepsilon_{\lambda T} L_b(\lambda,T)$$

$$where, \qquad L(\lambda,T) = N_\nu^+(0,\mu=1)$$

Therefore by measuring the radiance of an isothermal glass melt of a known temperature the emissivity can be calculated for each wavelength λ and, henceforth, characterized for future deconvolution calculations.

Absorbtion Coefficient Characterization

The absorbtion coefficient (κcm^{-1}) reflects the degree to which radiation is absorbed as it passes through the glass. It is key to determining the optical thickness of glass τ_λ and is described by:

$$\tau_\lambda = \int_0^L e^{\kappa_\lambda l}\,dl$$

where L is the glass total thickness.

In the case of a linear temperature gradient, as shown in Section 3.5.1, the absorbtion coefficient falls out of the exponent. In the limiting case of an optically opaque glass melt the radiative transfer equation has the form:

$$L(\lambda_i, T) = \varepsilon_{\lambda T}[L_b(\lambda_i, T) + \frac{d[L_b(\lambda_i, T)]}{dT}(\frac{a}{\kappa_\lambda})]$$

where the linear temperature gradient is described by

$$T(y) = T_s + ay.$$

It follows that the absorbtion coefficient can be easily measured by creating a glass melt with a linear temperature gradient and the previously calculated emissivity.

Glass Characterization

The test matrix and test procedures were originally selected under the assumption that the characterizations could all be completed in a series of initial tests. After shakedown it was found that the physical properties coefficients required for data analysis could be most accurately measured individually for each test run. The test procedures were revised as follows:

1) Melt glass in crucible and fill to required level. Cold plate must be on.

2) Calibrate sensor on cal source in hot oven, record TAS data and referee TC reading.

3) Absorbtion coefficient measurement; record TAS data and triplex TC output for glass melt on cold plate. Take data for each required furnace set point temperature.

4) Shut off cold plate, allow glass melt to stabilize to an isothermal state.

5) Emissivity characterization; record TAS data and triplex TC output for glass melt in isothermal state. Test at required furnace set point temperatures.

6) Conduct any additional tests.

7) Slowly ramp down furnace temperature to reduce crucible damage.

Emissivity Measurements

These procedures were followed closely, but initial data indicated some variability in the properties of the glass melts. Figure 4-10 shows typical data for an emissivity test. The referee triplex thermocouple (top 3 lines) and the calibrated outputs (lower lines) for each filter wavelength show conflicting trends. These outputs represent the relative color temperature detected by the sensor. To the right of each data line is the calculated mean emissivity value. By dividing the raw data by the emissivity the output should be normalized to the surface temperature.

The emissivity should be uniquely characterized by wavelength and temperature, Figure 4-11. The different symbols indicate emissivity values measured at different wavelengths. Several tests were conducted at the 2025°F region, showing some scatter in the data. This scatter appears to have two sources. The first is instrument drift, which was an occasional problem that is addressed below. The second is that some changes in the glass surface were observed during runs. In particular, the appearance of bubbles or the accumulation of dirt on the surface of the glass appeared to influence emissivity. In a real application, the constant renewal of the surface should avoid these problems.

Absorbtion Coefficient Measurements

Measurements of the glass absorbtion coefficients were derived by establishing an approximate (-10%F/in) linear gradient with the cold plate under

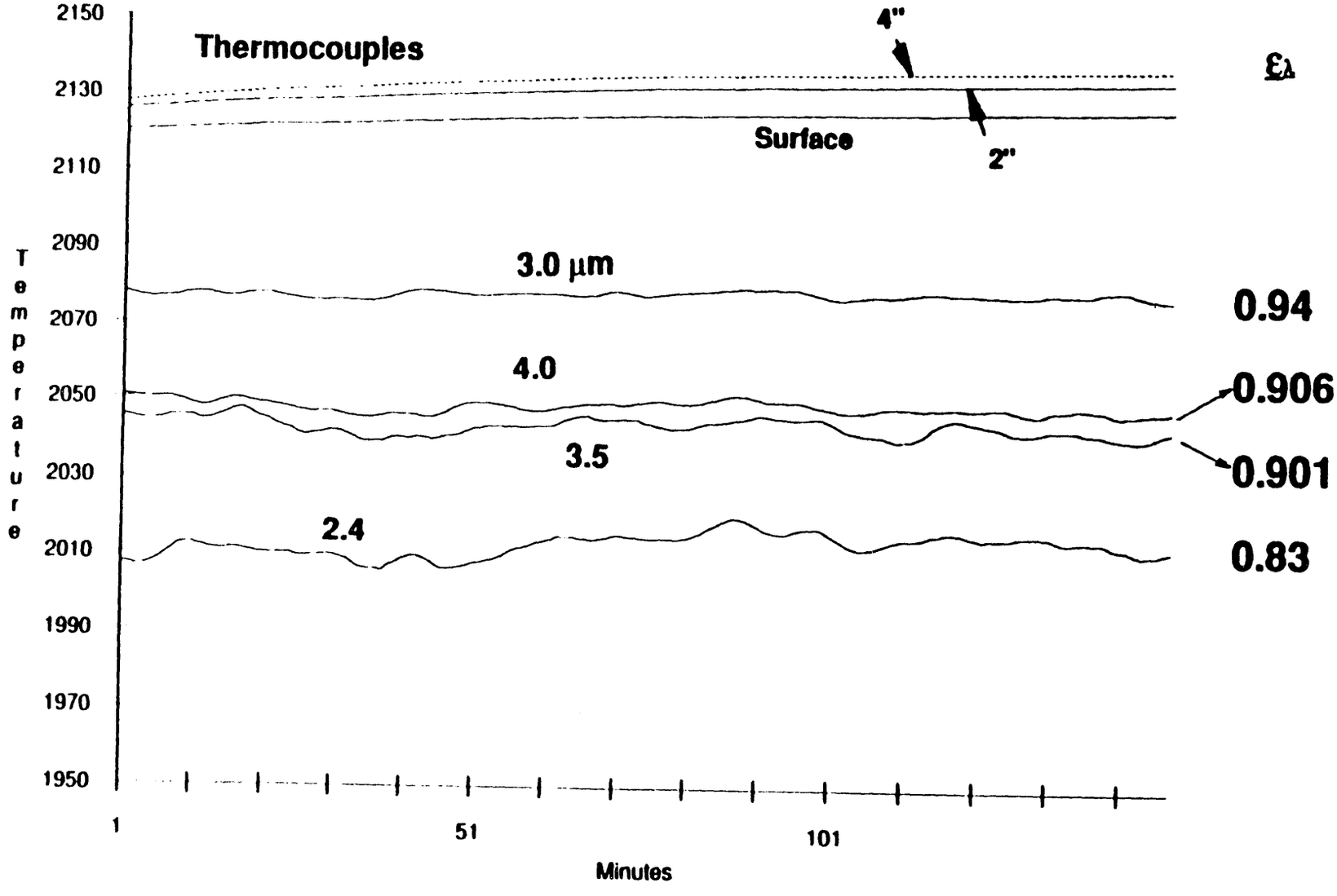

Figure 4-10. Emissivity test data.

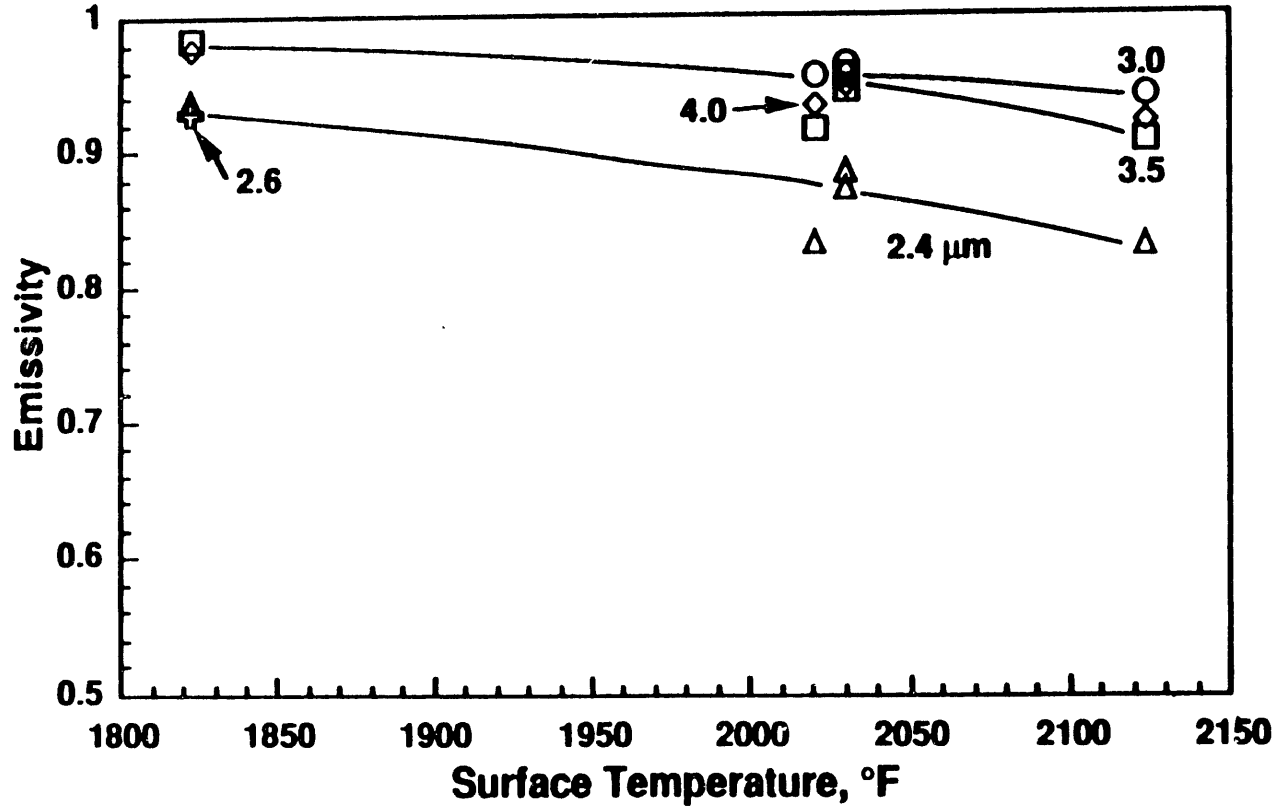

Figure 4-11. Emissivity vs. temperature.

the crucible. This gradient appears to be too small to yield well-resolved data. It was concluded that direct absorption coefficient measurement would be a superior approach. Literature values for absorption coefficient were available for the glass melts used in the present experiments. These were used to resolve the data.

4.3.4 Temperature Profile Deconvolution

Section 3.5.6 described several approaches to deconvoluting a temperature profile from radiance measurement made at different wavelengths. By judicious selection of the spectral wavelength various depths within the glass are accessed. The filter wavelengths chosen were strongly influenced by the constraints of fiber transmission and the gas interference spectra. Figure 4-12 shows the spectral parameters considered in the selection of the IR-visible filter wavelengths. The lowest curve shows the filter wavelengths required for depth resolution, e.g. the depths at which 50% absorbtion occurs for both green glass and flint glass. These absorbtion values are based on generic glass properties from the literature. The middle curves show the 10 m optical fiber transmission attenuation for two types of heavy metal fluoride fibers. The lower of the two curves represents the fiber used in the tests. Absorbtion curves for 10% water and CO_2 are also shown to indicate regions to be avoided. The top curve is the Planck black body radiation for the temperatures of interest. All of the filters selected produce good signal outputs when used in the multiplexer except for the 4.7 micron filter. At this wavelength the attenuation through the optical fiber is too great.

Simplified Approach

Two means of generating thermal gradients were used. Steady-state gradients were formed by using the cold plate to continuously extract heat from the base of the crucible. Transient gradients were formed by changing the temperature setpoint of the furnace and observing the response of the glass to the new thermal environment.

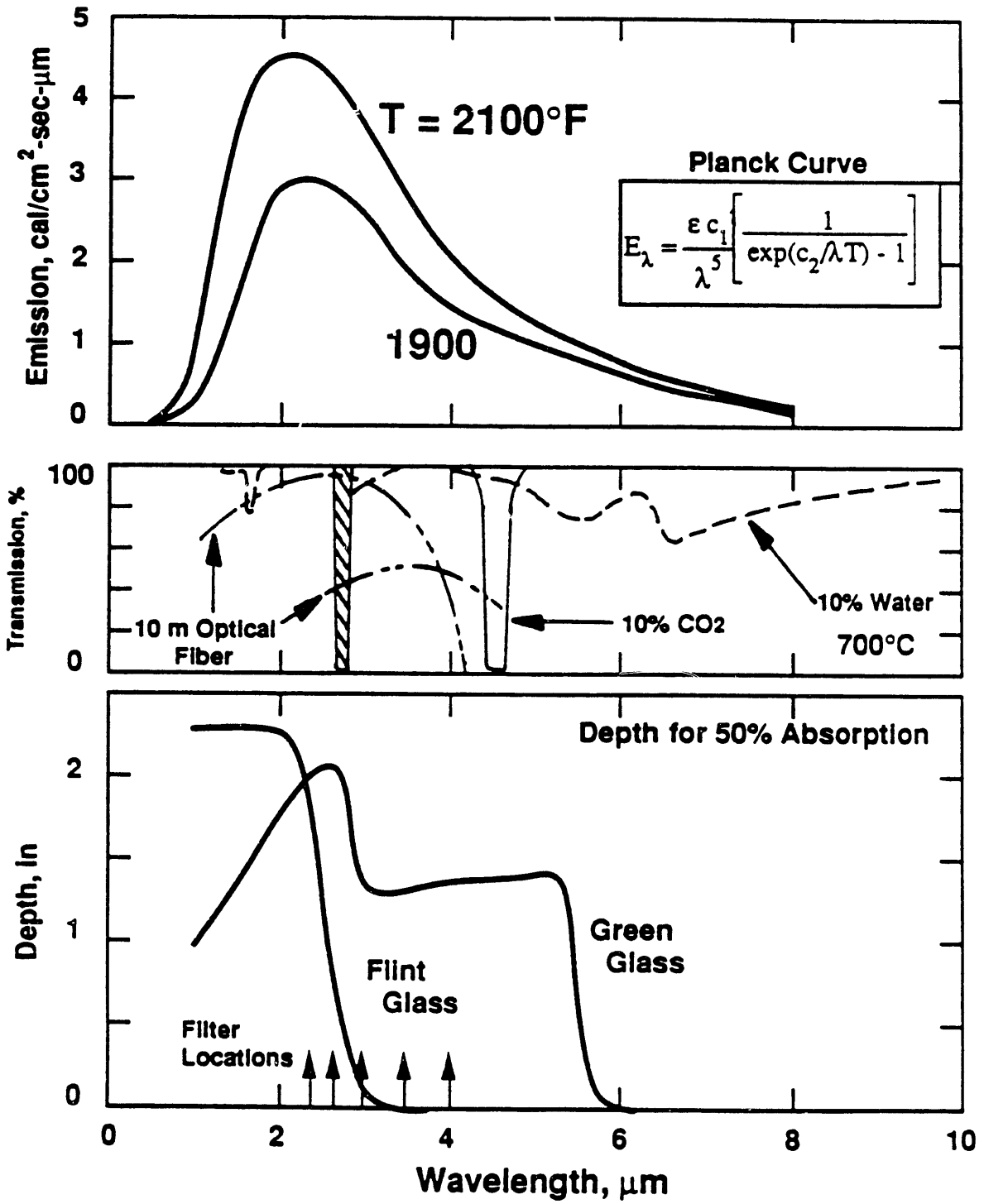

Figure 4-12. Spectral properties of radiation, and absorbtion of glass, fiber, and gases.

The simplified approach was applied to the transient data by assigning a unique depth to each measurement wavelength based upon the absorption coefficient curve for green glass, Figure 4-12. Figure 4-13 is a set of raw data which represents a transient from a 2035°F furnace temperature to a 2125°F furnace set point. The referee thermocouple data are shown along with the measured color temperature at each wavelength. The pyrometer data shown are not corrected for emissivity.

The data for each wavelength were normalized with the emissivity and the resultant temperatures were compared to the referee measured temperature profile at the corresponding assigned depths. The measured referee profiles are plotted with the respective pyrometer depth measurements in Figure 4-14. It is clear from the figure the wavelength selection is not optimized for green glass due to the small separation between the depths measured.

The pyrometer depth measurements appear to correlate quite well to the profile measured by the triplex thermocouples. The statistical error analysis is given in Table 4-2 below.

TABLE 4-2. MEAN ERROR IN DEPTH MEASUREMENT

Depth (in)	Wavelength (μm)	Mean Error (°F)	Maximum Error (°F)
0.90	2.6	1.1	2.7
0.95	2.4	2.6	4.1
1.30	4.0	1.3	1.9
1.45	3.0	1.2	3.5

This data show the TAS system can make accurate measurements of temperature at depth when using the simple approach to deconvolution.

Further validation of the method was pursued by comparing the accuracy of the depth measurements relative to the steepness of the gradient. This was done by calculating the color temperatures for three different gradient profiles. The

- **Plot shows T.C. data and raw color temperature data.**
- **Optical pyrometer is clearly following the increasing temperature. Is the gradient resolvable?**

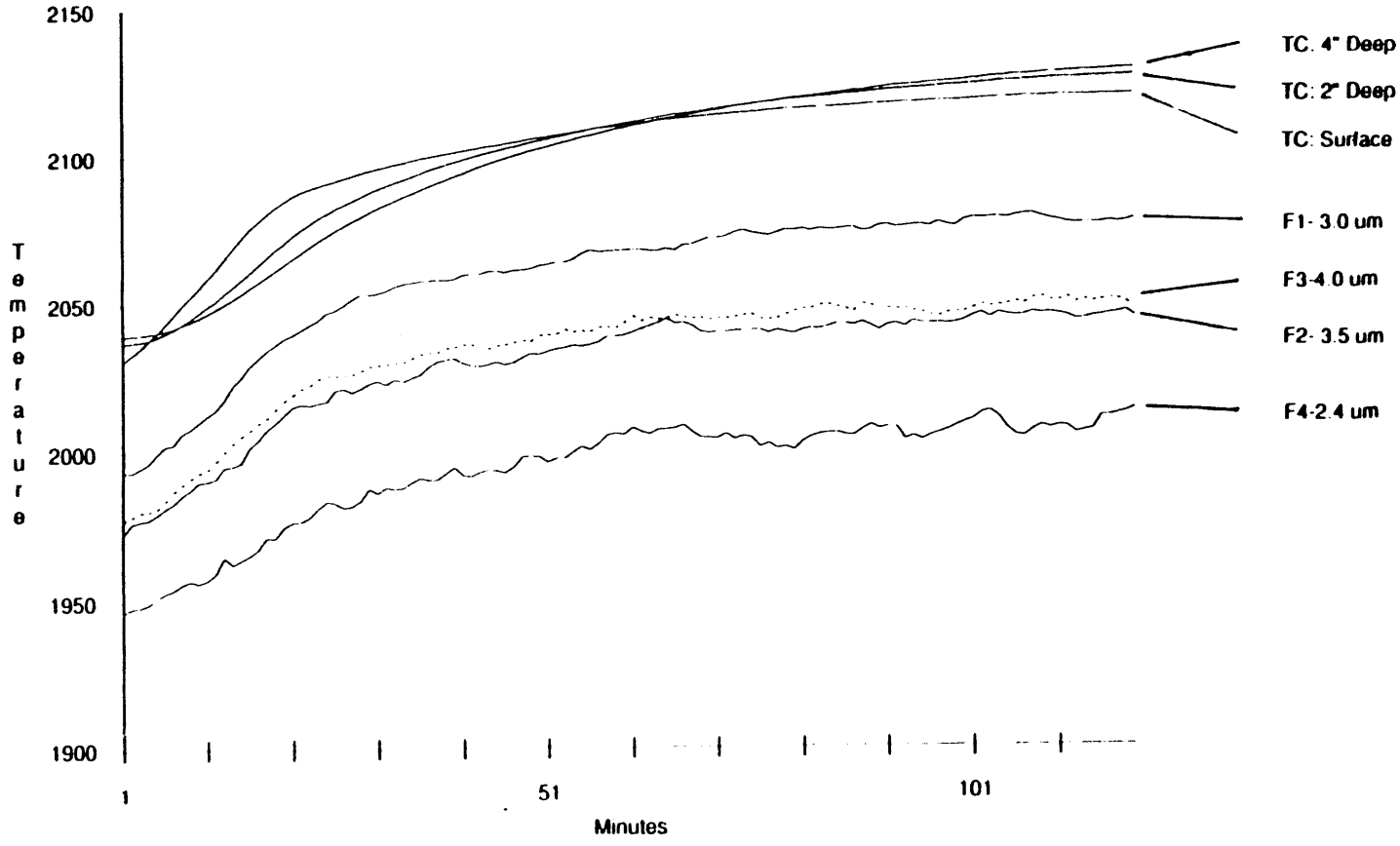

Figure 4-13. Transient gradient data.

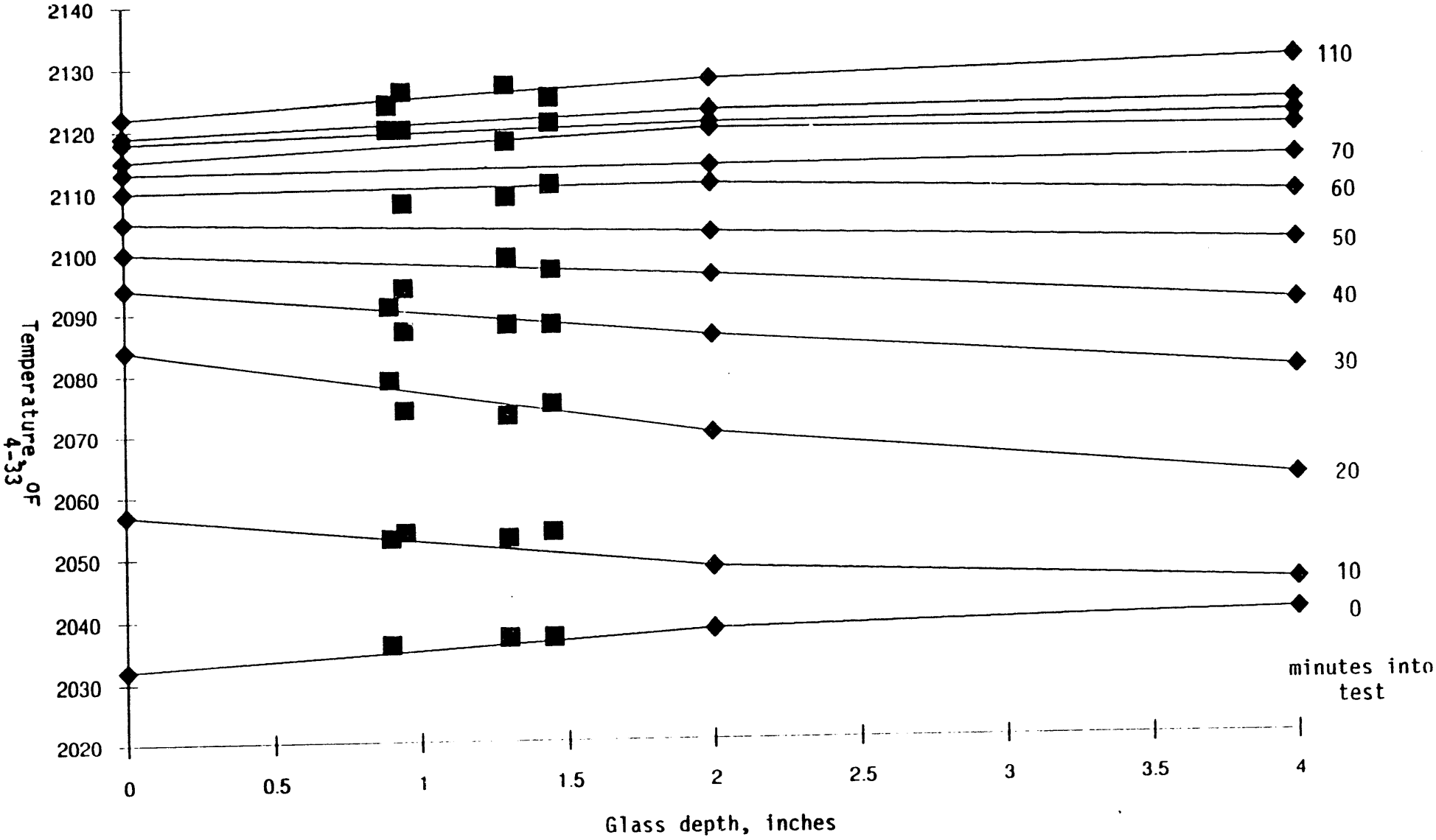

Figure 4-14. Referee temperature profile vs. pyrometric depth measurements.

accuracy of the approach is quantified by how systematically a particular wavelength measures temperature at depth. Figure 4-15 shows a plot of three different negative gradients and the predicted color temperature measurements. It is clear from this analysis that each wavelength measures the same depth to an accuracy of ±.10 in. This suggests that for the wide range in temperature gradients shown in Figure 4-15, very little error is incurred by assigning a unique depth to the color temperature associated with each wavelength.

The most evident drawback of this approach is the relatively shallow depths achieved in the pyrometer measurement. This analysis is based upon literature values of spectral absorption in green glass. A more transparent glass such as flint would have yielded deeper depth measurements given the wavelengths available. A more complex method however may have more power in deconvoluting the measurements to give deeper depth measurements.

General Approach

The General Approach is a more powerful technique. Here, any form of temperature profile can be hypothesized. For example, the temperature can simply be specified at four depths, and a spline routine used to draw a smooth logical curve between the points. An alternative is to assume a specific functionality where the constants in the function specify the profile All that is important to have is some variable means of specifying temperature with depth. The approach is to use the assumed temperature profile in the Viskanta equation to calculate radiance for each wavelength. Then the calculated values are compared to the measure radiance, the error noted, and the temperature profile adjusted for another iteration. This iterative cycle continues until the error between the radiance values is minimized.

As an example, consider the following functionality:

$$T(y) = T_s + a_1 y + a_1 a_2 \exp(-y/a_2)$$

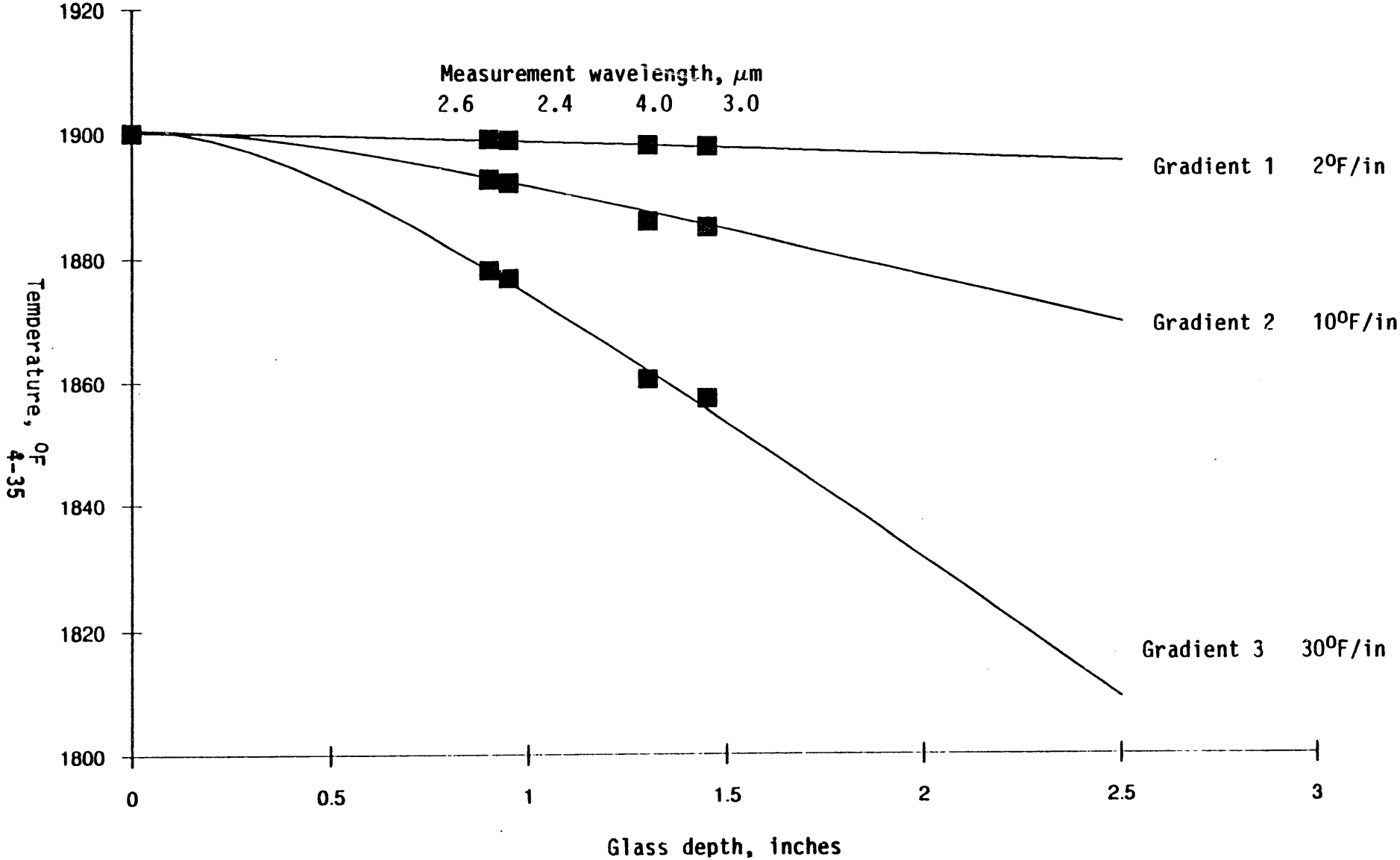

Figure 4-15. Four wavelength depth measurements vs. gradient.

This form provides a good model of glass behavior during the steady gradient experiments. The gradient conditions existing in the glass melts were the result of a steady continuous heat flux created by the extraction of heat from the bottom of the melt. This creates a linear gradient within the interior of the glass. At the surface of the glass there exists two mechanisms of heat transfer, convection and radiation, of which thermal analysis indicated the heat transfer to be radiation dominant. Given the temperatures at which the glass is melted, 80% of the radiant energy emitted from the glass lies between 1.7 and 7.3 microns. Over this spectral range the spectral absorption by the glass will give it a characteristic optical depth over which most of the energy is absorbed.

Within the optical depth at the surface of the glass, heat is able to escape via radiative transfer creating a bi-directional heat transfer situation leveling off the gradient. In the limiting case of the air glass interface the thermal gradient dT/dy is zero. The above model reproduces both the linear gradient at great depth, and the zero gradient condition at the surface. The term T_s represents the projected surface temperature (or y intercept) for the linear profile in the case $a_2 = o$. The slope of the linear portion of the curve is a_1, and a_2 represents the characteristic leveling off of the profile at the surface ($y = o$) which is related to the characteristic optical depth of the glass.

The general approach is an iterative technique by which the above thermal profile form is chosen and the constants (T_s, a_1, a_2) are selectively varied until the theoretical predictions of the four radiance measurements match the actual measurements.

Numerical analysis indicates the constant most strongly influencing the equation is T_s and that which is weakest is a_2. The iteration would be configured to first change T_s until the sum of the errors reaches a minimum. This would push the equation to the color temperature. The calculations would then switch to varying a_1 and then a_2. The iterations would cycle through this process until the sum of the errors (or some other error function) reaches an acceptable minimum. Since a_2 is related to the glass properties, it is possible

it is reasonably constant for all temperatures and only unique to each glass type, thereby simplifying the analysis. There are a number of more sophisticated numerical techniques by which an error function can be minimized by varying constants of an equation, one of which is the method of steepest descents. The key point is that this general approach is equally applicable to any temperature model, not just the one assumed here.

It is felt that the simplified procedure is appropriate for well-behaved temperature profiles, i.e., monotonic profiles that do not vary too much from linear. The iterative approach may be used under more severe conditions.

4.3.5 Bench Scale TAS Operating Characteristics

The bench scale temperature analyzer system designed for the Phase I testing was comprised of a number of individual subsystems and subassemblies which up until now have not performed as an integrated unit. The TAS system is comprised of sensors, optical fibers, multiplexer, and signal processing hardware and software and a Data Acquisition System. The following section will address the operation of the TAS, specifically with respect to the output signal characteristics (noise, stability, optical transmission).

Noise

The data acquisition system was designed to filter noise and condition the signal prior to being recorded on the computer. Data were logged at one minute intervals and it was important for the recorded number to be representative of the signals output over that time interval. The signals were recorded in arbitrary counts which were proportional to the output voltage. Typical output levels for the Mux ranged between 6000 to 16000 counts for sensor 1 and 12000 to 26000 counts for sensor 2 which had a larger aperture. These values were very good considering the signal level used in preliminary engineering design was 10000 counts, i.e.: potentially better signal-to-noise ratio.

The differences in signal level were primarily the result of the differences in optical transmission through the filters and fibers. The typical signal to noise ratio for the recorded data was between 160 and 650. The noise is evident in Figure 4-16 and is clearly much greater than that of the thermocouple data shown. In order to meet the functional specification of ± 1°F the signal to noise ratio will need to be near 1000. The above described noise levels are on a short term basis and translate to a relative precision of ± 2°F to ± 6°F. From the signals shown in Figure 4-16 it is apparent that short term noise is not the predominant factor affecting the performance of the system.

At present, it is felt that the noise arises from a misalignment between the position sensor on the drive motor and the optical elements on the communator wheel. These two elements are connected by a chain drive which appears to develop some play after operation. This will be replaced by a notched belt drive or a direct gear drive during the next design iteration.

Drift

The second area of concern is the drift sometimes noted in the TAS signal output. For many data sets, the average signal outputs stayed constant over runs of several hours. There were instances, however, where the signal of all four wavelengths would inexplicably begin drifting in the middle of an otherwise invariant run. Figure 4-16 indicates that the glass temperature is stable, however the four pyrometric outputs are drifting at about 10°F per hour. An evaluation of a number of data sets showed similar characteristics; but no trends. Changes in glass surface characteristics (emissivity) could potentially contribute to the drift, however drift was also measured during calibration (Fig. 4-17) with a constant emissivity black body source. It is also important to note (Figure 4-17) the abrupt change in the signal which are also probably associated with the source of the drift. There were also data sets with long periods of stability. These were used in the deconvolution analyses.

Although the reasons for the drift have not been fully defined, it is suspected to come from the detector. Specifically, the detector is mounted on

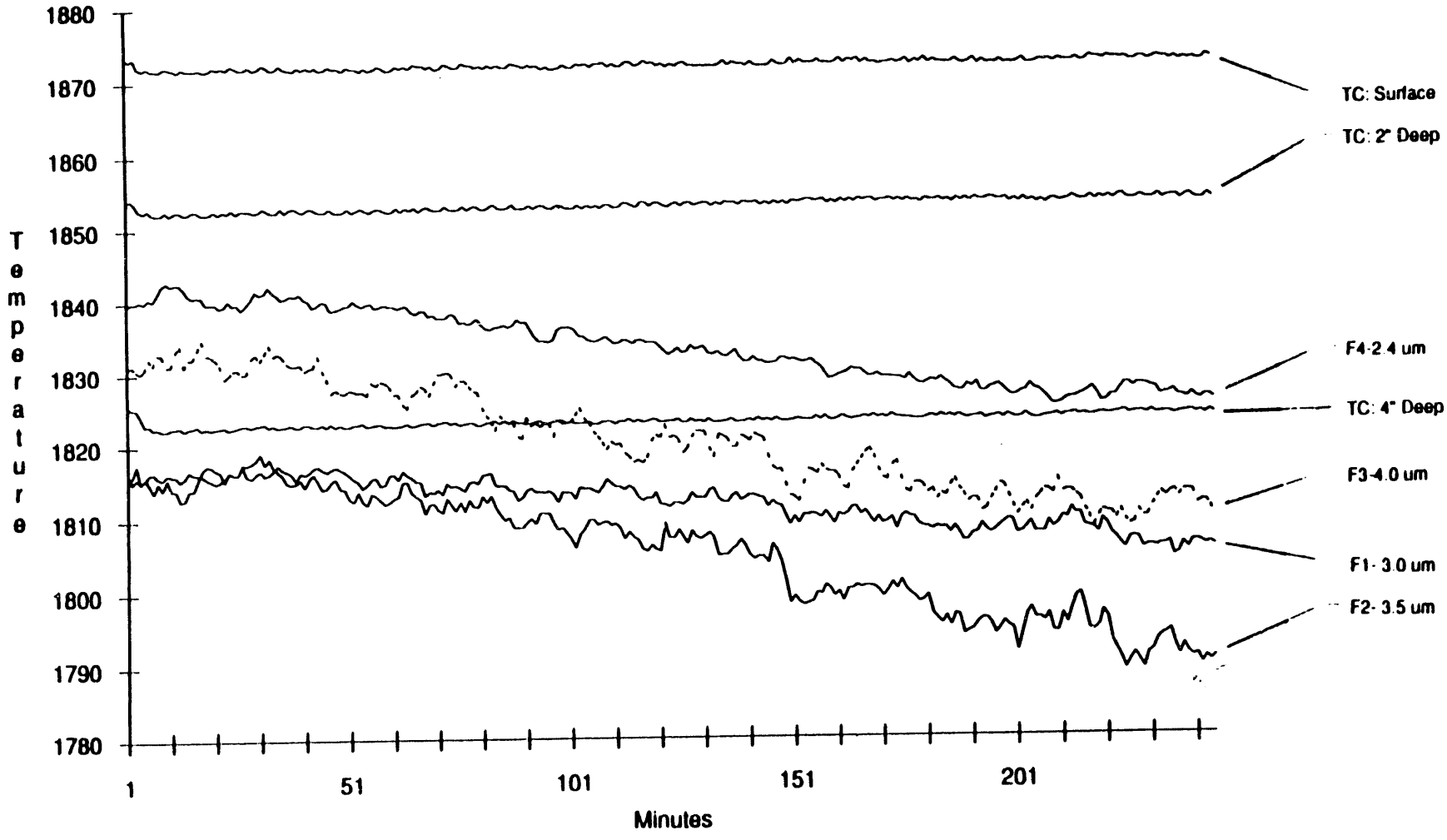

Figure 4-16. Drift and noise (flint glass-negative gradient).

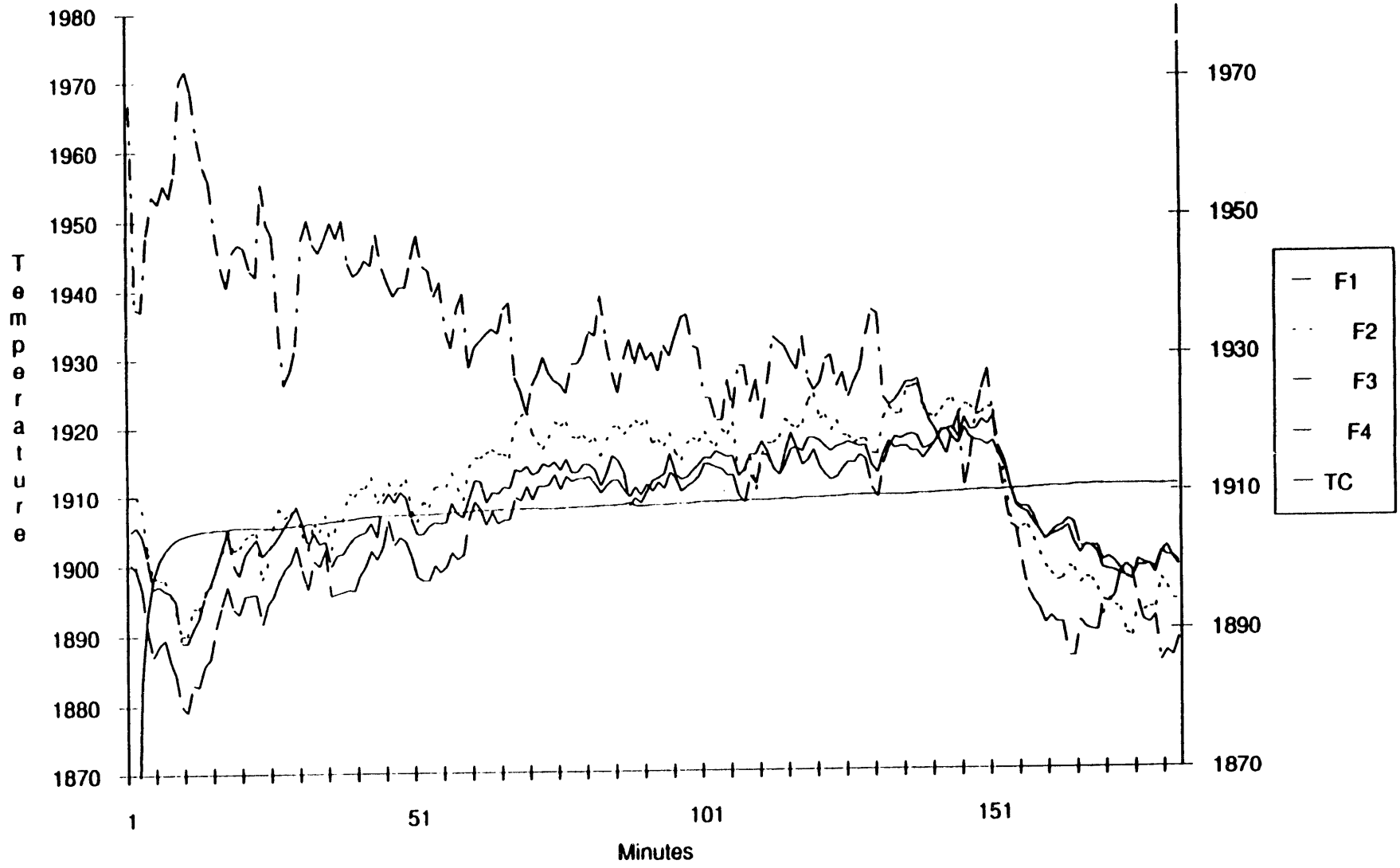

Figure 4-17. Worst case drift (calibration data).

a solid-state thermoelectric cooler that is designed to maintain the detector temperature at a constant value. This is critical because detector response varies strongly with temperature. It is thought that the current design does not provide sufficient contact between the detector and the cooler, due to modifications in the original design that were needed to mount the detector. Under some conditions the detector temperature can drift, yielding the unexpected signal change. This issue will be explored and corrected during the next series of tests.

Fiber Attenuation

The optical fiber is believed to be one of the most restrictive components in the temperature analyzer system. The fiber limited the spectral operating range and the total energy throughput. The very small area of the fiber core limited the energy collection and the attenuation of the fiber reduced the output of the fiber at the mux.

The fiber used was a relatively new (available for about a year now) heavy metal fluoride or ZBLAN fluoride fiber which has good transmission in the 3.5-5.0 micron range. Since one of the detection objectives was to measure the radiance in an opaque spectral range (4-5 micron), it was determined that this fiber would be best.

Tests of the fiber attenuation were conducted by connecting the two 10 meter fiber cables together and comparing the output to that of a single 10 meter cable. The data was taken using sensor 1 (cold ring sensor) which has a small aperture. The 10 meter signal levels ranged from 8500 to 15000 counts and the signal levels with a 20 meter length ranged from 4000 to 8000 counts. The comparison between EER's and the manufacturers' certified attenuation is given in Table 4-3 below.

TABLE 4-3. FIBER ATTENUATION

Wavelength (μm)	Factory Measured Loss (dB/m)	EER Measured Loss (dB/m)
2.4	*	0.65
2.5	0.7	*
3.0	*	0.57
3.5	0.6	0.56
4.0	0.7	0.92
4.5	1.0	*
5.0	1.9	*

It is apparent the measured losses compare well with the factory measured values. At 20 meters the fiber has definitely usable signal levels, although noise would be increased somewhat.

4.4 Recommended Methods

The goal of the Phase I test program was to resolve issues of componentry, optimal designs, assembly configuration, analytical methods, and operational parameter with respect to designing a high temperature glass melt temperature analyzer system which meets the functional specification. These issues were addressed through breadboard and bench scale tests and detailed numerical analysis. This section describes the methods, components, and operational requirements recommended for the Phase II program based upon the work completed to this date.

Sensing Parameters

The recommended sensing configuration is a normal angle approach. The sensor must be aligned with its optical axis normal to the surface of the glass

melt to minimize background radiation interference. Tests showed the sensor should be equipped with a cooled surface (or ring) which blocks reflected radiation from its field of view. This surface needs to be 500°F lower than the glass surface temperature. The sensor standoff and acceptance angle will define the width of the cold ring surface in combination with the requirements for sensor alignment tolerance. Cooling can be implemented with plant air.

The sensor should conform to the following specifications.

SENSOR SPECIFICATION

View port diameter	1" minimum
Aperture diameter	0.45" minimum
Sensing optics	90° off axis parabolic mirror
Optics diameter	1" minimum
Optical materials	Mirrors - Aluminum Windows - Sapphire
Optical coating	Mirrors - Gold Windows - None
Sensor body material	Stainless 316

A larger diameter aperture would allow for larger signal levels and hence longer and smaller diameter optical fibers. A forehearth application will impose no temperature limitations on the above design.

Optical Fiber

The fibers used in the test program worked very well and are recommended for further use. These fibers were a glass clad heavy metal fluoride (ZBLAN) type fiber sold under the name of "sensor grade 2." Due to the high cost of these fibers it is recommended that the fiber lengths are kept to a minimum. At a 10 meter length the fibers transmitted sufficiently and could be used in 20 meter lengths with a 2 fold drop in sensitivity.

RECOMMENDED FIBER SPECIFICATIONS

Fiber type	Heavy Metal Fluoride
Cladding	Glass
Fiber grade	Sensor Grade II
Core diameter	450 micron
Length	10 meter recommended 20 meter maximum

The core diameter is recommended at 450 microns however if the aperture of the sensor is increased the same light could be collected into a smaller fiber. This would yield significant cost benefits. Additionally, improvements in the signal to noise ratio would allow increasing fiber length.

Optical Processing

The EER optical multiplexer consists accepts 8 optical fibers and contains a set of four IR band pass filters and a series of lenses which focus the light onto a lead selenide detector. The multiplexer performs all of the optical processing and was designed specifically for operation in the mid-infrared spectral region for the TAS. This device functionally worked very well though a few improvements appear necessary.

The IR filters are selected to avoid gaseous interference bands in the regions of 2.60 to 2.95 microns and 4.15 to 4.45 microns. Beyond 4.6 microns the optical fiber attenuation is too high. The optical throughput requires the filter bandwidths to be between 0.10 and 0.20 μm.

The combinations of filters must be optimized for each glass type according to unique optical properties. The filters must be selected so that each wavelength measures a region where the glass has distinctly different absorbtion coefficients. For Green glass the filter wavelengths of 2.4 and 2.6 microns both view the same depth and the depth difference between 3.0, 3.5 and 4.0 microns is slight.

Further work is necessary to properly characterize each glass so the filter combinations can be optimized for individual glass types. Such work will hopefully yield accurate definition of absorbtion coefficients and enhance the sensitivity of the instruments.

The multiplexer optical lens components should be fabricated from calcium fluoride (CaF_2) or zinc sulphide (ZnS). These materials have excellent transmission over the 1.0 to 5.0 micron range and worked extremely well in the optical bench. Modifications to the multiplexer drive assembly are recommended to improve the system noise levels. No change in the design wavelength of 3.5 microns is believed necessary.

Calibration

Calibration against a black body is required for accurate system operation. A grey body could be used in place of a black body. However, the emissivity of the grey body would need to be known and must be stable. The calibration temperature should be near the process temperature so that nonlinearities in the detector can be minimized.

Calibration of the system must be performed after any instance where the optical system has been altered because the calibration constants are sensitive to the optical system transmittance and spectral responsivity.

As a result of drift problems, an on-line calibration system is highly recommended. Such a system would greatly improve the accuracy of the instrument. Since the noise and drift sources could not be isolated the true calibration needs are unknown. Further work in developing an on-line calibration method is needed and should be considered prior to or as a part of Phase II. The on-line calibrator need not be a black body but a steady hot thermal source with repeatable output. With such a system, off-line black body calibration would be required on a weekly to monthly basis.

Deconvolution Methods

Two methods of deconvolution are described earlier in Section 4.3.4. The simple approach was tested against Green glass and found to give adequate results at shallow depths. Further work is recommended to confirm the viability of this approach against other glasses and with other filter combinations. It is believed to be a workable method but not the most powerful.

The general approach described earlier is recommended for implementation in the TAS. It has the power to measure the thermal profiles existing in glass melts and is able to predict deeper temperature trends in the glass. Further experimental work is required to optimize the iterative error minimization technique.

5.0 PROVISIONAL ECONOMICS

A provisional cost effectiveness assessment has been performed to confirm that a TAS can be marketed at a competitive price and achieve process benefits consistent with its cost. Only the primary target application, forehearth instrumentation and control is addressed. The assumptions, methodology, and assessment are described below, and are the substantial result of Task 5, Design and Economics, of the project plan.

5.1 Approach

Sensor cost effectiveness is evaluated in an order of magnitude economic study to determine the potential production and energy savings resulting from improved temperature mapping. Typical industrial process data and broad assumptions were made bounding the probable effects of improved temperature control on production. Baseline data are essentially a subjective average of those found in the literature [17, 18, 19] and/or provided by various end users. The Industrial Panel members (Latchford, Kerr Glass and Gallo Glass) reviewed and generally concurred with the operating parameters selected and the assumptions relative to the effectiveness of the technology. Fundamental economic parameters used and the assumptions are detailed in Appendix A, Tables A-1 and A-2 and summarized in Table 5-1. Major operating and process assumptions are:

- pull rates of 150 and 250 tons/day corresponding to melter efficiencies of 6 and 5 M^2BTU/ton and forehearth efficiencies of 0.4 and 0.3 M^2BTU/ton

- a range of post TAS efficiency improvements

High packing efficiencies are associated with state-of-the-art forehearth control such as currently offered by Emhart and BHP. Typically, instrumentation consists of 3 to 9 submerged thermocouples and several optical pyrometers. Low packing efficiencies would be associated with an older forehearth near the end of its campaign, and having limited instrumentation (pyrometers and wall temperature

TABLE 5-1. COST EFFECTIVENESS SENSITIVITY STUDY

Plant Capacity Ton/Day	Existing I&C[1,4]	Saving, $(000) Production[2]	Energy[3]	TAS Cost $(000)	Payback Years
150	Hi	362.3	47.2	145.7	0.4
	Med	189	26.0	145.7	0.8
	Lo	80.3	15.7	145.7	1.8
250	Hi	603.7	65.5	22.3	0.4
	Med	315.0	36.2	22.3	0.7
	Lo	157.9	23.3	22.3	1.4

Notes:

[1]Hi, highly impacted, minimum existing instrumentation and control strategy implementation; Lo, small impact, advanced computer control such as WTA using a combination of submerged triplex thermocouples and pyrometers duplicating the proposed TAS.

[2]Production valued at $300/shipped ton and a 10 percent before tax profit.

[3]Energy priced at fuel oil equivalent, between 2.50 and 3.00 $/m^{2}Btu.

[4]Improvement assumptions

Process Steps and Control Strategy		Hi	Mid	Lo
Increased Pull Rate	%	3	2	1
Temperature Control				
Mold Speed Increase				
Decreased Energy Consumption	%	30	20	15
Refiner				
Forehearth				
Increased Packing Efficiency	%	2	1	1/2
GOB Control				
Mold Control				

TC's, and being operated under substantially manual control. Improvement assumptions (Table 5-1) are:

- Melter pull rate improvement (1 to 3%) which increases unit production and net profitability at higher production rates.

- Improved packing efficiency (1/2 to 2%) which is the most substantial impact since it converts a bad product to a good at no additional cost except for the advanced sensor systems.

- Energy efficiency improvement in the forehearth, nominally in the range of 15 to 30 percent; and indirectly an increased melter fuel efficiency improvement at higher pull rate.

5.2 Cost Savings

Based upon these assumptions it is estimated that for the 250 ton/day median case approximately $315,000 in production savings can be affected, and about $36,000 of energy savings. This results in a total savings of $351,000 a year.

5.3 Capital Costs and Payback

Capital costs for the system were developed assuming 250 and 150 tpd plants with four or two forehearths per melter, each requiring a 12 channel instrument system. The total number of sensors assumed per furnace is 48 and 24, respectively. This would be judged to be a very highly instrumented system by current standards. These sensors are sighted on the surface and into the forehearth melt approximately 4 to 6 inches, and predict temperatures with an accuracy of plus or minus 2°F. Total installed cost for the system was estimated at $219,020 and a cost per point of about $4,563. Payback on this investment for the median case is approximately half a year on the total savings and 1.2 years for the worst case assumptions.

It should be noted that the glass container industry is focusing on several major technologies to become more cost competitive with other container manufacturing processes. Light weighting is a method by which container weight can be reduced some 20 to 30 percent. This requires improved forehearth operations for precision temperature control and gob delivery. Since implementation of this technology requires new mold machines and a special coating, the TAS is but a key component in a more complex system. It is difficult to allocate an incremental improvement to a specific component; therefore, the potential cost benefits of the TAS in this application were not considered, although believed to be substantial.

The capital cost for a TAS has been estimated from a preliminary design activity directed at modifying the basic EER technology, an optical multiplexing, time shared signal processing system, to achieve the performance objectives of the functional specification, Table 2-1. The hardware modifications primarily relate to improved instrument spectral capability:

- Increase the number of measurement wavelengths from two to four or five
- Increase the spectral range from 2.0 to 5.0 μm
- Modify optical sensor to a sight tube containing an off axis focusing mirror configuration

The number of sensors required to implement advanced forehearth control has been variously estimated at nine to twelve. Thermocouple forehearth arrays are typically three per cross section with locations at the front, rear, and nose. Additional locations in the refinery and bowl area might also be beneficial. The larger number was used in the economic study along with the above design changes as reflected in a revised parts list (Table A-1). Multipliers on the two major subsystems have been selected from previous experience in the moisture analyzer development program and rules of thumb in the electronic industry:

- Low complexity optical sensing and transmitting system, X2.

- High complexity electro-optics and electronics, X4.

These markups provide gross profit margins (net of cost to make of 100 percent) and net before tax profit margins of about 35 percent (thru marketing and warranty expenses).

The FOB manufacturers selling price for a 48 sensor forehearth (4) application (250 ton melter) is then:

				Price, $(000)	
		Markup	Quant.	Unit Parts	Total
1	Analyzer Subsystem Chassis	4X	3	7.6	98.8
2	Sensors and Cabling	2X	48	0.9	86.4
3	Total, capital				185.2
	, per point $(000)/sensor				3.8

The parametrically developed savings project simple, before tax payback periods of 0.4 to 1.8 years. This should be well within the acceptable range for the industry. The longer periods reflect already well controlled state-of-the-art systems. As a point of reference the triplex thermocouples' FOB cost is between 3000 and 5000 $/pt. Therefore initial capital costs are similar although life cycle costs for triplex units should be significantly higher because of the need to remove, repair, and replace malfunctioned units. This can easily double the life costs of triplex systems. Optical sensors are substantially passive and require no replacement. In terms of applications requirements and technology constraints, it would appear that the selection of the forehearth and forming

processes have good cost effectiveness relative to both process improvements and the current state-of-the-art systems.

REFERENCES

1. Greene, C. R. and J. M. Torrey. "Glass Industry Scoping Study," EPRI Rept. EM-5912, July 1988.

2. Garrett-Price, B. A., A. G. Fassbender, and G. A. Bruno. "Potential for Energy Conservation in the Glass Industry," Battelle PNL-5640/UC-95 f, June 1986.

3. Private Communication with M. Meese, Gallo Glass Co. and W. Van Saun, Latchford Glass Co., Subject: Refiner and Forehearth Energy Balances.

4. Holmsten, D. 1986. "Precision Infrared On-line Scanning for Process Control." Proceedings of SPIE - The International Society for Optical Engineering. v 581. Publ. by SPIE, Bellingham, WA, USA p 35-46.

5. Hunter, G. B., C. D. Allemand, and T. W. Eagar. 1985. "Improved Method of Multi-wavelength Pyrometry." Proceedings of SPIE - The International Society for Optical Engineering. v 520. Publ. by SPIE, Bellingham, WA, USA p 40-46.

6. Infrared Fiber Syst. Inc., Silver Spring, MD, USA. 1988. "IR Fiber Temperature Sensing System." Proc. SPIE - Int. Soc. Opt. Eng. (USA). vol. 843, pp.: 148-54.

7. Stanley, G. M. and T. F. Ensor. 1981. "Thermocouple Control for Forehearths." Glass Technol., 22[N 2]91-4.

8. Beattie, J. R. 1972. "Application of Pyrometry to Glass Tempering." IEEE Trans. Ind. Appl. v IA-8 n 3 May-June 1972 p 237-239.

9. Gardon, R. "Calculation of Temperature Distributions in Glass Plates Undergoing Heat Treatment." J. Am. Ceram. Soc. 41, 6, 200-209 (1958).

10. Madjid, A. H. 1973. "Spectral Emissivity of Nonisothermal Semi-infinite Slabs of Transparent Materials." Journal of Applied Physics. v 44 n 12 Dec 1973 p 5423-5425.

11. Isard, J. O. 1986. "Emission of Thermal Radiation from Hot Glass: I, Emissivity of Sheets, Spheres, Cylinders, and Tubes." Glass Technol., 27[1]24-31.

12. Viskanta, R. 1974. "Infrared Radiation Techniques for Glass Surface and Temperature Distribution Measurements." IEEE Ind. Appl. Soc., Annu. Meet., 9th, Conf. Rec., Pittsburgh, PA, Oct. 7-10 1974 pt 2, p 1045-1056. Publ. by IEEE (74 CHO 833-41A), New York, NY, 1974.

13. Barron, B. "Application Design Features for Non-Contact Temperature Measurement." Proc. Soc. Photo-Opt. Instrum. Eng. 446 (1983).

14. Viskanta, R. and Xigi Wu. "Effect of Radiation on the Melting of Glass Batch." Glastech. Ber. V56, n 6-7, 1983, p 138-147.

15. Curran, R. L. and J. H. Farag. "Modeling Radiation Pyrometry of Glass During Container-forming Process," Glastech. Ber. 61 (1988).

17. Wolfe, W. L. and G. J. Zissis. Infrared Handbook, Environmental Research Institute of Michigan, 1989.

18. Nixon, S. S. 1982. "Recent Experience with Digital Process Control for a Glass Furnace and Forehearths." American Ceramic Society Bulletin. 61(12): 1290-1291.

19. Douglas, R. J. July 1983. "Improving Glass Container-Manufacturing Productivity." Glass Industry. 64(7). Ashlee Publishing Company, Inc., New York, New York.

20. Edgington, J. H. 1984. "How the Glass Container Industry Can Improve Its Profitability." Glass Industry. 65(4):14-20.

APPENDIX A

COST ESTIMATES

- 250 ton Furnace Savings and TAS Capital Costs
- 150 ton Furnace Savings TAS Capital Costs
- TAS Parts List and Cost

TABLE A-1. ESTIMATED ENERGY AND COST SAVINGS GLASS CONTAINER FORMING 250-TON FURNACE

1.0 ASSUMPTIONS		Estimate[1]		
1.1 Typical Container Mfg		High	Med	Low
Melter Operating Conditions				
Temp	TM °F	-------2800-------		
Pull Rate	tons/day	------- 250-------		
Efficiency	M^2Btu/ton	------- 5-------		
Forehearth				
Efficiency	QFH/P, M^2Btu/ton	------- 0.3-------		
Entrance	°F	-------2300-------		
Spout	°F	-------2000-------		
Production, GOB Temp	TG °F	-------2000-------		
Selling Price	C/P $/ton	------- 300-------		
Packing Efficiency	EFFP %	87-90	92	94
1.2 Process Steps and Control Strategy				
Increased Pull Rate	EFFP %	3	2	1
Temperature Control				
Mold Speed Increase				
Decreased Energy Consumption	%	30	20	15
Refiner				
Forehearth				
Increased Packing Efficiency	%	2	1	1/2
GOB Control				
Mold Control				
1.3 Operating Costs				
Fuel	CF $/$M^2$Btu	3	2.5	2.5
Profits	PBT %	10	10	10

Notes:

1, Estimated saving based upon as found plant efficiency assumptions, highly impacted by outdated control (High) to slightly impacted because of state-of-the-art I&C (Low).

TABLE A-1. ESTIMATED ENERGY AND COST SAVINGS GLASS CONTAINER FORMING 250-TON FURNACE (Continued)

		High	Med	Low
2.0	ESTIMATED SAVINGS		$(000)	
2.1	Productivity Increase, Incremental Profit			
	CP = Pull * EFFPY*C/P t*PBT			
	= 250 t/da*$\begin{Bmatrix}.03^{1}\\.02\\.01\end{Bmatrix}$*300 $/ton *350 da/yr 0.1 =	78.1	52.5	6.7
2.2	Production Efficiency, Incremental			
	CPE = Pull * EFFP * C/P * t			
	= 250 t/da *$\begin{Bmatrix}.005\\.01\\.02\end{Bmatrix}$ * 300 $/ton * 350 da/yr =	525.0 603.7	262.5 315.0	131.2 157.9
2.3	Energy Efficiency Savings			
	2.3.1 Forehearth			
	a) Fuel			
	QFH = -QFH/P * EFFFH			
	= 0.3 m^2Btu/ton x$\begin{Bmatrix}0.3\\0.2\\0.15\end{Bmatrix}$= 0.09			
	b) Cost of Fuel			
	CF = QFH * Pull * C/F*t			
	= $\begin{Bmatrix}.09\\* 3\end{Bmatrix}$ m^2Btu/ton * 250 ton/da $/$m^2$ * 350 day/yr (2.5) =	23.5	13.1	11.7
	2.3.2 Furnace			
	a) Fuel			
	QFF = -5.35 * Pull (see Note 1)			
	= -5.35 *$\begin{Bmatrix}.03\\.02\\.01\end{Bmatrix}$= 0.16			

Notes:

1, based on typical pull vs. efficiency curve

2, $\begin{Bmatrix}x\\x\\x\end{Bmatrix}$ parameter varied, see Table 5-1

TABLE A-1. ESTIMATED ENERGY AND COST SAVINGS GLASS CONTAINER FORMING 250-TON FURNACE (Continued)

			High	Med	Low
	b) Cost of Fuel				
	CF = QFF * Pull * C/F * t				
	= {.16} m²Btu/ton*250 ton/da {* 3} $/m² * 350 da/yr =		42.0	23.1	11.6
2.3.3	Total Fuel Savings		65.5	36.2	23.3
3.0	CAPITAL COSTS (48 SENSING PTS)				
3.1	TAS System (12 Channel/Forehearth, 4 forehearths)				
	Analyzer Chassis			98.8	
	Sensing Heads & Cabling			86.4	
3.2	Engineering				
	Installation Design	15.0			
	Project Engineering	1.5			
	Assembly & Checkout	3.0			
				19.5	
3.3	Installation				
	Mechanical 4 hr/Sensor x 36 x 60 $/hr	8.64			
	Electrical 2 hr/Sensor x 36 x 65 $/hr	4.68			
	Miscellaneous Materials	5.0			
				18.32	
3.4	Installed Selling Price				
	a) Total System			223.0	
	b) Per Pt			4.6	
4.0	PAYBACK		0.4	0.7	1.4

TABLE A-2. ESTIMATED ENERGY SAVINGS GLASS CONTAINER FORMING 150-TON FURNACE

		High	Med	Low
1.0 ASSUMPTIONS				
1.1 Typical Container Mfg				
Melter Operating Conditions				
Temp	°F	-------2800-------		
Pull Rate	tons/day	------- 150-------		
Efficiency	m^2Btu/ton	------- 6-------		
Forehearth, Fuel Savings	%	------- 30-------		
Efficiency	m^2Btu/ton	------- 0.4-------		
Entrance	°F	-------2300-------		
Spout	°F	-------2000-------		
Production, GOB Temp	°F	------- 200-------		
Cost	$/ton	------- 300-------		
Packing Efficiency	%	86	88	90
1.2 Process Steps and Control Strategy				
Increased Pull Rate	%	3	2	1
Temperature Control				
Mold Speed Increase				
Decreased Energy Consumption	%	30	20	15
Refiner				
Forehearth				
Increased Packing Efficiency	%	2	1	1/2
GOB Control				
Mold Control				
1.3 Operating Costs				
Fuel	$/$m^2$Btu	3	2.5	2.5
Profits	%	10	10	10

TABLE A-2. ESTIMATED ENERGY SAVINGS GLASS CONTAINER FORMING 150-TON FURNACE (Continued)

			High	Med	Low
2.0	ESTIMATED SAVINGS			$(000)	
	2.1	Productivity Increase, Incremental Profit			
		CP = Pull * EFFPY (Cost/Production)			
		x Days x Profit			
		= 1.50 t/da * {.03} *300 $/ton			
		* 350 day/yr $0.1 =	47.3	31.5	15.8
	2.2	Packing Efficiency, Incremental			
		CPE = Pull * EFFP * (Cost/Production) * Days	315.0	157.5	78.7
	2.3	Subtotal	362.3	189	80.3
	2.4	Energy Efficiency			
		2.4.1 Forehearth			
		CF = Pull * DEFFFH * 0.3 m^2Btu/ton			
		= {.09} x 150 * 3 $/m^2$Btu 350 da/yr	18.9	10.5	7.9
		2.4.2 Furnace			
		CF = Pull * EFFT * C/Q * Days			
		= 150 ton/day 6 m^2Btu/ton *			
		{3%/100} * 3 $/m^2$Btu * 350 da/yr	28.0	15.5	7.8
		2.4.3 Subtotal	47.2	26.0	15.7
3.0	CAPITAL COSTS (24 SENSING PTS)				
	3.1	TAS System (12 Channels, 2 Forehearths)			
		Analyzer Chassis		76.8	
		Sensing Heads & Cabling		50.2	
	3.2	Engineering			
		Installation Design	5.0		
		Project Engineering	1.5		
		Assembly & Checkout	3.0	9.5	
	3.3	Installation			
		Mechanical 4/hr/Sensor	4.32		
		Electrical 2 hr/Sensor	2.34		
		Miscellaneous Materials	2.5		
				9.2	

TABLE A-2. ESTIMATED ENERGY SAVINGS GLASS CONTAINER FORMING 150-TON FURNACE (Concluded)

		High	Med	Low
			$(000)	
	3.4 Installed Selling Price			
	a) Total System		145.7	
	b) Per Pt		6.1	
4.0	PAYBACK, YRS	0.4	0.8	1.8

END

DATE
FILMED
3/12/92